

INFORMATION TO USERS

This manuscript has been reproduced from the microfilm master. UMI films the text directly from the original or copy submitted. Thus, some thesis and dissertation copies are in typewriter face, while others may be from any type of computer printer.

The quality of this reproduction is dependent upon the quality of the copy submitted. Broken or indistinct print, colored or poor quality illustrations and photographs, print bleedthrough, substandard margins, and improper alignment can adversely affect reproduction.

In the unlikely event that the author did not send UMI a complete manuscript and there are missing pages, these will be noted. Also, if unauthorized copyright material had to be removed, a note will indicate the deletion.

Oversize materials (e.g., maps, drawings, charts) are reproduced by sectioning the original, beginning at the upper left-hand corner and continuing from left to right in equal sections with small overlaps.

Photographs included in the original manuscript have been reproduced xerographically in this copy. Higher quality 6" x 9" black and white photographic prints are available for any photographs or illustrations appearing in this copy for an additional charge. Contact UMI directly to order.

Bell & Howell Information and Learning
300 North Zeeb Road, Ann Arbor, MI 48106-1346 USA
800-521-0600

UMI[®]

University of Alberta

**Triacylglycerol and Carbohydrate Metabolism in Loblolly Pine (*Pinus taeda* L.) Seeds
during Germination and Early Seedling Growth**

by

Sandra Lee Stone ©

**A thesis submitted to the Faculty of Graduate Studies and Research in partial fulfillment
of the requirements for the degree of Doctor of Philosophy**

Department of Biological Sciences

**Edmonton, Alberta
Fall 1999**



National Library
of Canada

Acquisitions and
Bibliographic Services

395 Wellington Street
Ottawa ON K1A 0N4
Canada

Bibliothèque nationale
du Canada

Acquisitions et
services bibliographiques

395, rue Wellington
Ottawa ON K1A 0N4
Canada

Your file *Votre référence*

Our file *Notre référence*

The author has granted a non-exclusive licence allowing the National Library of Canada to reproduce, loan, distribute or sell copies of this thesis in microform, paper or electronic formats.

The author retains ownership of the copyright in this thesis. Neither the thesis nor substantial extracts from it may be printed or otherwise reproduced without the author's permission.

L'auteur a accordé une licence non exclusive permettant à la Bibliothèque nationale du Canada de reproduire, prêter, distribuer ou vendre des copies de cette thèse sous la forme de microfiche/film, de reproduction sur papier ou sur format électronique.

L'auteur conserve la propriété du droit d'auteur qui protège cette thèse. Ni la thèse ni des extraits substantiels de celle-ci ne doivent être imprimés ou autrement reproduits sans son autorisation.

0-612-46925-5

Canada

University of Alberta

Library Release Form

Name of Author: Sandra Lee Stone

Title of Thesis: Triacylglycerol and Carbohydrate Metabolism in Loblolly Pine (*Pinus taeda* L.) Seeds during Germination and Early Seedling Growth

Degree: Doctor of Philosophy

Year this Degree Granted: 1999

Permission is hereby granted to the University of Alberta Library to reproduce single copies of this thesis and to lend or sell such copies for private, scholarly, or scientific research purposes only.

The author reserves all other publication and other rights in association with the copyright in the thesis, and except as hereinbefore provided, neither the thesis nor any substantial portion thereof may be printed or otherwise reproduced in any material form whatever without the author's prior written permission.




Sandra Lee Stone
#104-8640 108 St
Edmonton, AB
T6E 4M4
Canada

Date: July 19, 1999

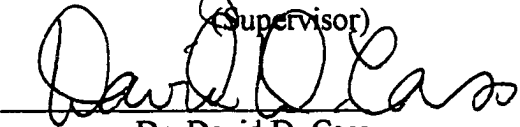
University of Alberta

Faculty of Graduate Studies and Research


The undersigned certify that they have read, and recommend to the Faculty of Graduate Studies and Research for acceptance, a thesis entitled "Triacylglycerol and Carbohydrate Metabolism in Loblolly Pine (*Pinus taeda* L.) Seeds during Germination and Early Seedling Growth" submitted by Sandra Lee Stone in partial fulfillment of the requirements for the degree of Doctor of Philosophy.



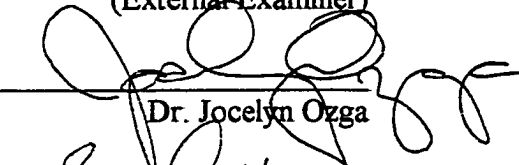
Dr. David J. Gifford
(Supervisor)




Dr. David D. Cass
(Co-supervisor)



Dr. John S. Greenwood
(External Examiner)



Dr. Jocelyn Ozga



Dr. George W. Owttrim



Dr. C. Peter Constabel

Date: July 14, 1999

TO MY FAMILY

Abstract

Mature, desiccated loblolly pine (*Pinus taeda* L.) seeds each contained 3.2 ± 0.9 mg triacylglycerols and 2.1 ± 0.03 mg protein. Approximately 80% of the triacylglycerols and 90% of the proteins were stored in the large haploid megagametophyte that enclosed the diploid embryo. Protein and triacylglycerol reserves were stored throughout the mature embryo. These reserves began to break down during germination (prior to radicle emergence at 30°C) and continued through early seedling growth (after radicle emergence and prior to megagametophyte shedding). The most rapid rate of breakdown occurred in the hypocotyl and radicle. The majority of the seedling's nutrition was provided by the breakdown and metabolism of megagametophytic storage reserves; throughout seed imbibition the seedling maintained a close physical relationship with the megagametophyte through a carbohydrate-positive non-cellular layer. Megagametophyte triacylglycerol reserves were broken down and metabolized to produce carbohydrates that were rapidly exported to the seedling. As this occurred there was little change in megagametophyte carbohydrate levels, while there was a large increase in seedling carbohydrate levels. Sucrose comprised a large proportion of the carbohydrate in both the megagametophyte and seedling which implied that sucrose was exported by the megagametophyte and imported by the seedling. In addition to receiving metabolites from the megagametophyte, cotyledons were capable of producing carbohydrate photosynthetically, as they emerged from the megagametophyte. This was indicated by the early greening, presence of stomata and increase in glycolate oxidase activity during the seedling's early growth. The increasing glycolate oxidase

activity in megagametophytes during the late stages of early seedling growth was likely due to senescence.

The normal metabolism of the megagametophyte was perturbed if the embryo or seedling was removed. The removal of embryos from seeds prior to the start of germination did not interfere greatly with the initial decrease in megagametophyte carbohydrate level. It did, however, cause the accumulation of an unusual non-starch, 80% ethanol-insoluble carbohydrate. Similarly, megagametophytes isolated from seedlings during early seedling growth were capable of exporting carbohydrates into an exudate droplet; however, 24 h after isolation from the seedling the exudate droplet contained invertase activity and high levels of D-glucose and D-fructose.

Table of Contents

Chapter	Page
1. Introduction	1
1.1 Loblolly Pine	1
1.2 Description of the mature seed	1
1.3 Pinaceae Seed Reserves	6
1.3.1 Storage proteins	6
1.3.1.1 Amino acid composition of Pinaceae storage proteins	12
1.3.1.2 Protein storage organelles	14
1.3.1.3 The formation of protein vacuoles during seed development	15
1.3.2 Storage Lipids	18
1.3.2.1 Triacylglycerol (TAG) storage organelles	19
1.3.2.2 The formation of lipid bodies during development	22
1.4 Development of the Pinaceae seed	24
1.4.1 Transcriptional regulation of storage protein synthesis	25
1.5 Preparation of Pinaceae seed for germination	27
1.6 Developmental periods of the study: germination and early seedling growth	30
1.6.1 Storage protein reserves	31
1.6.2 TAG reserves	33
1.6.3 Structural studies of Pinaceae seeds during germination and early seedling growth	33
1.7 The Current Study	35

2. Materials and Methods	37
2.1 Water quality and Chemicals	37
2.2 Seed material	37
2.2.1 Stratification, germination and early seedling growth	37
2.2.1.1 Tissue collection for biochemical analyses	38
2.2.2 Culture of isolated seed parts	39
2.2.3 Culture of isolated intact megagametophytes	39
2.3 Microscopy	40
2.3.1 Tissue Fixation Methods	40
2.3.1.1 Formalin-acetic acid-alcohol (FAA) fixation	40
2.3.1.2 Freeze-substitution fixation	41
2.3.1.3 Glutaraldehyde-Osmium tetroxide (OsO ₄) fixation	42
2.3.2 Histochemical Stains	42
2.4 Biochemical Analyses of Storage Reserves	43
2.4.1 Protein	44
2.4.1.1 Protein Quantification	44
2.4.1.2 Protein Electrophoresis	45
2.4.2 Triacylglycerol (TAG)	45
2.4.3 Carbohydrate	46
2.4.3.1 80% Ethanol-Soluble and -Insoluble Carbohydrate	46
2.4.3.2 Sucrose, D-glucose and D-fructose	47
2.4.3.3 Starch	47
2.5 Enzyme Activities	48
2.5.1 Glycolate oxidase (Glycolate: oxygen oxidoreductase, EC 1.1.3.1)	48

2.5.2 Invertase (β -Fructofuranosidase, EC 3.2.1.26)	49
2.5.2.1 Invertase Extraction and Assay	49
2.5.2.2 Invertase pH Optima	51
2.6 Radiolabel experiments	51
2.6.1 Labeling Experiments	51
2.6.2 Pulse-Chase Experiments	52
2.6.3 Tissue Processing	52
2.6.4 Separation into Basic, Neutral and Acidic Fractions	53
3. Results	54
3.1 Structural changes related to the development of the seedling	54
3.1.1 Cellular organelles in mature, 35 DAI ₂ and 12 DAI ₃₀ seed tissues	54
3.1.2 Xylem formation in the developing seedling	62
3.1.3 Stomatal complex formation in the developing seedling	65
3.1.4 Greening of the seedling	66
3.1.5 Glycolate oxidase (GO) activity	66
3.2 Nutrition of the seedling from reserves laid down during seed development	69
3.2.1 The fate of stored protein reserves during germination and early seedling growth	70
3.2.1.2 Protein vacuole structure	70
3.2.1.3 Megagametophyte protein vacuole distribution and changes during germination and early seedling growth	73
3.2.1.4 Embryo/ seedling cotyledon and hypocotyl protein vacuole distribution and changes during germination and early seedling growth	79
3.2.1.5 Quantitative changes in megagametophyte and embryo/ seedling proteins	83

3.2.2	The fate of stored TAG reserves during germination and early seedling growth	88
3.2.2.1	Quantitative changes in TAG reserves during germination and early seedling growth	88
3.2.3	Carbohydrates in the megagametophyte and seedling during germination and early seedling growth	90
3.2.3.1	Quantitative changes in carbohydrates	90
3.2.3.2	Invertase activities	100
3.3	The relationship between the seedling and megagametophyte	103
3.3.1	The composition of the carbohydrate-positive layer of the inner megagametophyte	103
3.3.2	The rapid transport of substances between the megagametophyte and seedling	107
3.3.2.1	The effect of megagametophyte removal on seedling carbohydrate levels	107
3.3.2.2	The incorporation of [2- ¹⁴ C]sodium acetate into megagametophyte metabolic macromolecules and their subsequent movement into the seedling	109
3.3.3	The role of the seedling in the regulation of megagametophyte metabolism	118
3.3.3.1	The effect of embryo removal on carbohydrate levels of 35 DAI ₂ megagametophytes in culture	118
3.3.3.2	The effect of seedling removal on 9 DAI ₃₀ megagametophytes	120
4.	Discussion	126
4.1	The physical relationship between the seedling and megagametophyte	126
4.2	The transport of metabolites within the seedling	128
4.3	The breakdown and catabolism of stored TAG reserves	129
4.4	The dynamics of reserve breakdown in the seedling	131

4.5 The movement of carbohydrates from the megagametophyte to the seedling	133
4.6 Starch storage	137
4.7 Are Pinaceae seed storage proteins glycosylated?	138
4.8 The development of photosynthetic competence in the seedling	139
4.9 The role of the seedling in the maintenance of megagametophyte metabolism	142
4.10 Senescence of the megagametophyte	144
4.11 Future directions	146
5. Literature Cited	148

List of Figures

	Page
Figure 1. Distribution map of loblolly pine (<i>Pinus taeda</i> L.) growth in south-eastern United States.	2
Figure 9. Glycolate oxidase activity in seedling shoot and root poles following imbibition at 30°C.	67
Figure 10. Glycolate oxidase activity in megagametophytes following imbibition.	68
Figure 17. Quantitative changes in megagametophyte phosphate buffer-soluble and -insoluble proteins following imbibition.	84
Figure 18. Quantitative embryo/ seedling protein changes during imbibition.	85
Figure 20. Quantitative changes in TAGs during imbibition.	89
Figure 21. Quantitative changes in megagametophyte and whole embryo/ seedling 80% ethanol-soluble and insoluble carbohydrate levels during imbibition.	91
Figure 22. Quantitative changes in embryo/ seedling 80% ethanol-soluble and -insoluble carbohydrate levels during imbibition.	93
Figure 23. Quantitative changes in specific carbohydrate levels during imbibition.	94
Figure 26. Invertase incubation buffer pH optima.	101
Figure 27. Megagametophyte invertase activities during imbibition.	102
Figure 28. Embryo/ seedling invertase activities during imbibition.	104
Figure 30. The effect of megagametophyte removal from 35 DAI ₂ seeds, on carbohydrate levels of embryos cultured up to 10 days @ 30°C.	108
Figure 31. Radioactivity incorporated into 80% ethanol-soluble fraction from 10 DAI ₃₀ seed material labeled with [2- ¹⁴ C]sodium acetate up to 120 min.	110
Figure 32. Water-soluble radioactivity from 10 DAI ₃₀ seed material labeled with [2- ¹⁴ C]sodium acetate up to 120 min.	111

Figure 33. Neutral fraction radioactivity from 10 DAI ₃₀ seed material labeled with [2- ¹⁴ C]sodium acetate up to 120 min.	113
Figure 34. Radioactivity in the different water-soluble fractions of the megagametophyte from 10 DAI ₃₀ seed material labeled with [2- ¹⁴ C]sodium acetate up to 120 min.	114
Figure 35. Radioactivity in the different water-soluble fractions of the seedling from 10 DAI ₃₀ seed material labeled with [2- ¹⁴ C]sodium acetate up to 120 min.	116
Figure 36. Radioactivity incorporated into 80% ethanol-soluble fraction from 10 DAI ₃₀ seed material pulsed 30 min with [2- ¹⁴ C]sodium acetate and chased with non-radioactive sodium acetate up to 4 h.	117
Figure 37. The effect of embryo removal from 35 DAI ₂ seeds, on carbohydrate levels of megagametophytes cultured up to 10 days @ 30°C.	119
Figure 38. The effect of embryo removal from 35 DAI ₂ seeds, on starch levels of megagametophytes cultured up to 4 days @ 30°C.	121
Figure 40. The effect of 9 DAI ₃₀ seedling removal on megagametophyte specific carbohydrate levels after 24 h culture @ 30°C.	123
Figure 41. The effect of 9 DAI ₃₀ seedling removal on megagametophyte invertase activities after 24 h culture @ 30°C.	125

List of Plates

	Page
Figure 2. Light micrograph of longitudinal section through a paraffin-embedded mature loblolly pine seed with integuments removed.	4
Figure 3. Light micrographs of mature seed parts.	5
Figure 4. Transmission electron micrographs of 35 DAI ₂ seed material.	56
Figure 5. Transmission electron micrographs of 12 DAI ₃₀ seed material.	57
Figure 6. Transmission electron micrographs of 12 DAI ₃₀ megagametophyte cell organelles.	59
Figure 7. Transmission electron micrographs of 12 DAI ₃₀ seedling organelles.	61
Figure 8A-C. Light micrographs of lignified tracheids in whole seedlings stained with basic fuchsin.	64
Figure 8D-H. Light micrographs of stomatal complex development in seedlings during germination and early seedling growth.	64
Figure 11. Transmission electron micrographs of protein vacuole structure in 35 DAI ₂ seed tissues.	72
Figure 12. Light micrographs of PAS and Aniline Blue Black stained transverse sections through a plastic embedded 35 DAI ₂ stratified seed showing protein vacuole distribution in the three different regions of the megagametophyte.	74
Figure 13. Light micrographs of PAS and Aniline Blue Black stained transverse sections through seeds in the area of a cotyledon and megagametophyte during imbibition at 30°C, showing protein vacuole distribution.	77
Figure 14. Light micrographs of PAS and Aniline Blue Black stained transverse sections through the centre of the megagametophyte middle region during imbibition at 30°C, showing protein vacuole distribution.	78
Figure 15. Light micrographs of PAS and Aniline Blue Black stained transverse sections through the megagametophyte showing the protein vacuole distribution in the single cell layer of the outer region, and part of the middle region, during imbibition at 30°C.	80

Figure 16A-D. Light micrographs of PAS and Aniline Blue Black stained transverse sections through plastic-embedded hypocotyl with surrounding megagametophyte during imbibition at 30°C, showing protein vacuole distribution.	82
Figures 16E-H. Light micrographs of PAS and Aniline Blue Black stained transverse sections through plastic-embedded cotyledons and surrounding megagametophyte during imbibition at 30°C, showing protein vacuole distribution.	82
Figure 19. Coomassie blue stained SDS-PAGE profile of phosphate buffer-insoluble proteins from embryo/ seedling shoot and root poles following imbibition, run under reducing conditions in the presence of 2-mercaptoethanol.	87
Figure 24. Light micrographs of PAS stained 4 DAI₃₀ seed material.	96
Figure 25. Light micrographs of PAS stained sections through the seed transverse to the seedling.	99
Figure 29. Light micrographs of the carbohydrate-positive layer of the inner megagametophyte.	106
Figure 39. Isolated 9 DAI₃₀ megagametophyte with exudate droplet formed after 24 h of culture at 30°C.	122

List of Abbreviations

BSA	bovine serum albumin
μCi	microCurie
CoA	coenzymeA
DAI₂	days after imbibition at 2°C
DAI₃₀	days after imbibition at 30°C
dpm	disintegrations per minute
DTT	dithiothreitol
ER	endoplasmic reticulum
FAA	formalin-acetic acid-alcohol
FW	fresh weight
g	gravity
GO	glycolate oxidase
h	hour
kDa	kiloDalton
min	minute
OsO₄	osmium tetroxide
PAGE	polyacrylamide gel electrophoresis
PAS	periodic acid-Schiff's
pI	isoelectric point
PMSF	phenylmethylsulfonyl fluoride
PVPP	polyvinylpyrrolidone

RER	rough endoplasmic reticulum
RuBisCO	Ribulose 1,5-bisphosphate Carboxylase-Oxygenase
S	Svedberg
SDS	sodium dodecyl sulfate
SER	smooth endoplasmic reticulum
TEM	transmission electron microscope

1. Introduction

1.1 Loblolly Pine

Loblolly pine (*Pinus taeda* L.) is the most important tree grown for timber in the United States, where it is primarily utilized by the pulp and paper industry. Loblolly pine is grown in the south-eastern United States, bounded by Maryland and Delaware in the north, northern Florida to the south, and Texas to the west (Fig. 1, from Fowells, 1965). Because of its importance to the pulp and paper industry, Westvaco and other companies maintain seed orchards to produce high quality loblolly pine seed for reforestation planting. This seed is ideal for studies of important metabolic and physiological changes that occur during germination and early seedling growth, using both biochemical and structural techniques. In order to undertake such a study, it is important to also understand the events that occur in the developing seed that prepares the embryo for germination.

1.2 Description of the mature seed

The mature desiccated seed of pine has three integument layers; the outer two integuments combine to form the hard seed coat. The innermost integument, or endotesta, forms a separate papery layer that covers the entire megagametophyte (Singh and Johri, 1972; Owens and Molder, 1977; Owens *et al.*, 1982). Recently, this has also been described as a layer formed due to the growth of nucellar cells into the endotesta, which was determined by light microscopic observations of mature seeds of *Pinus sylvestris* (Tillman-Sutela and Kauppi, 1995). However, since a developmental study

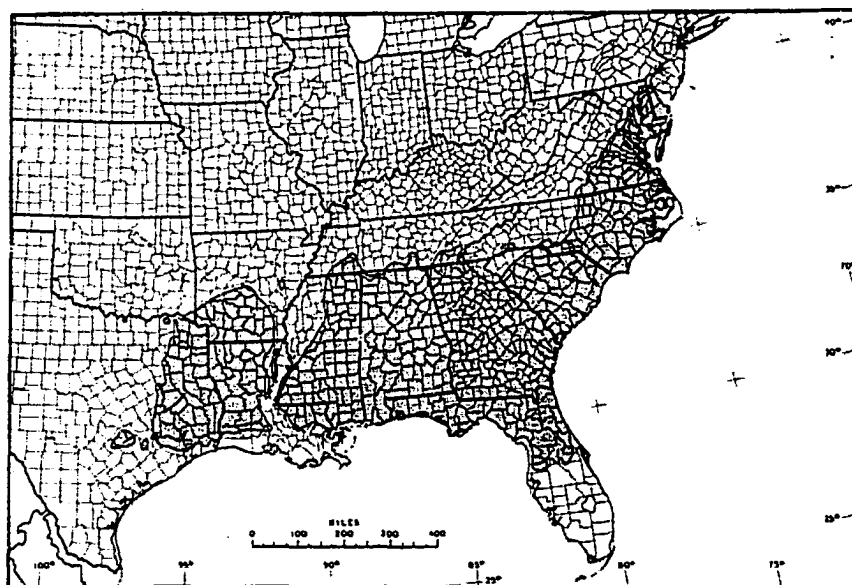


Figure 1. Distribution map of loblolly pine (*Pinus taeda* L.) growth in south-eastern United States. From Fowells (1965). Shaded area indicates loblolly pine's native range.

was not conducted, a change in the terminology of this layer for pines should be viewed with caution. Inside of the papery layer and covering the micropyle area of the megagametophyte (Fig. 2), is a thin, cap-like structure (Fig. 3C), which is generally considered to be the remnant of the nucellus (Singh and Johri, 1972).

The living components of the mature seed are the embryo and the megagametophyte. The diploid embryo typically consists of 6 to 8 cotyledons and an embryonic axis that is enclosed by the large, haploid megagametophyte storage tissue (Fig. 2). The embryonic axis itself is comprised of the shoot apical meristem (Fig. 3A), hypocotyl, and radicle. The radicle is comprised of a subapical root meristem covered by an extensive root cap (Fig. 3B). At the micropylar end of the root cap (Fig. 3C) is the fragmented, flaky remains of what is generally considered to be the crushed embryonic suspensor (Chamberlain, 1957). The main storage reserves in Pinaceae seeds are triacylglycerols and proteins (Misra, 1994). These reserves are found primarily in the megagametophyte; however, the embryo also contains these reserves (Simola, 1974a; Krasowski and Owens, 1993; Owens *et al.*, 1993). Although the embryo is physically close to the megagametophyte storage tissue, these tissues are separated by a space called the corrosion cavity (Singh and Johri, 1972; Hoff, 1987) that arose during embryo development.

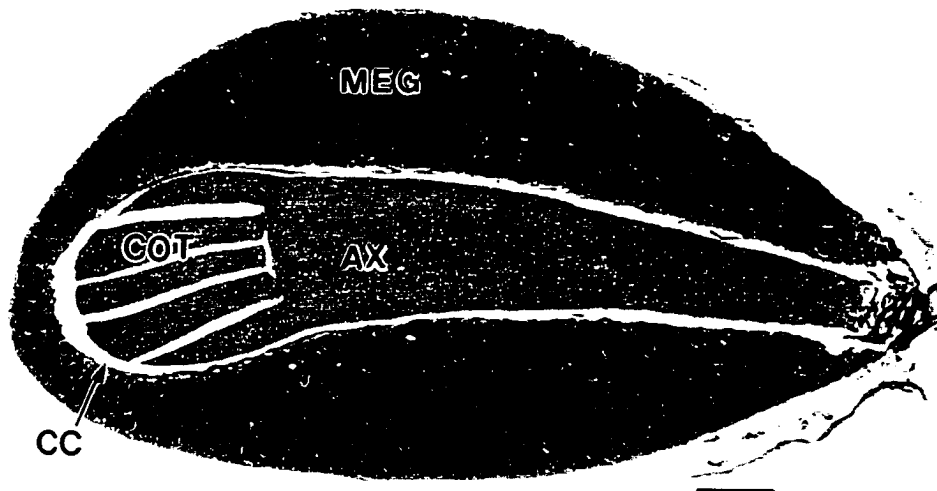


Figure 2. Light micrograph of longitudinal section through a paraffin-embedded mature loblolly pine seed with integuments removed. Megagametophyte (MEG), cotyledons (COT), embryonic axis (AX), and corrosion cavity (CC). Bar = 400 μm .

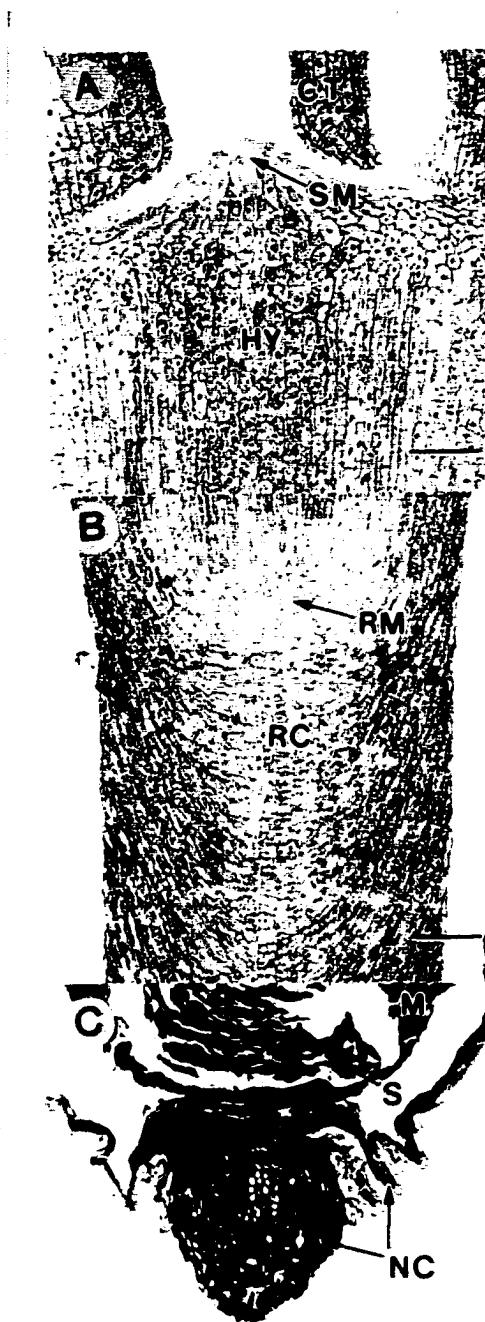


Figure 3. Light micrographs of mature seed parts. Bars = 100 μ m.

A) Shoot apical meristem (SM), cotyledon (CT), and hypocotyl (HY).

B) Components of the radicle. Root subapical meristem (RM) and portion of extensive root cap (RC).

C) Micropylar end of the seed. Nucellar cap (NC), megagametophyte (M), and remnants of the embryonic suspensor (S).

1.3 Pinaceae Seed Reserves

1.3.1 Storage proteins

Seed storage proteins are named as such if they accumulate during seed development, compose at least 5% of the total protein and are rapidly broken down and metabolized during germination and early seedling growth (Derbyshire *et al.*, 1976). These storage proteins are divided into four groups based on solubility (Osborne, 1918). Proteins soluble in aqueous solutions are albumins, while proteins insoluble in water and soluble in salt solutions are globulins. Storage proteins referred to as prolamins are only soluble in aqueous-alcohols. Proteins insoluble in the three previous solutions are glutelins, and these can be solubilized by dilute acid or alkali solutions. Currently, chaotropic agents like sodium dodecyl sulfate (SDS) or urea are used to solubilize glutelins, since they are more effective solubilizing agents (Koie and Nielsen, 1977). In addition to solubilities, storage proteins are further classified based on their ultracentrifugation sedimentation coefficient (S) for their holoprotein; for example 12S legumins and 2S albumins (Derbyshire *et al.*, 1976; Shewry *et al.*, 1995).

Based on sequential extraction, mature loblolly pine seeds contain albumins, globulins and glutelins, but no prolamins (Gifford, unpublished data). Globulins in loblolly pine are partially extractable with low salt solutions, but require high salt solutions with heat in order to extract them fully. Glutelins on the other hand are partially extractable with high salt solutions, but are fully extractable only with chaotropic agents. The solubility overlap between Pinaceae globulins and glutelins means that a salt extraction will not separate them. Instead of trying to separate these

two protein types, many researchers group them together based on their insolubility in aqueous buffer. The buffer-soluble proteins are albumins, and the buffer-insoluble proteins are globulins and glutelins. The insoluble proteins are then solubilized with a buffer containing SDS.

Phosphate-buffer insoluble proteins comprise the majority of storage proteins in the *Pinus* species studied to date, with the exception of *Pinus albicaulis* (Gifford, 1988). Although some globulins are present in this genus, the major seed storage protein in *Pinus* is a group of 51-55 kDa proteins with glutelin-like solubility. Allona *et al.* (1994c) suggests that these glutelin-like proteins are SDS-dissociated subunits that form a hexameric holoprotein *in vivo*. Each of these subunits is composed of a 31 - 34.5 kDa and 21.5 - 22.5 kDa polypeptide joined by disulfide bridges (Gifford, 1988; Lammer and Gifford, 1989; Groome *et al.*, 1991; Jensen and Lixue, 1991; Allona *et al.*, 1992). Nearly all other members of the Pinaceae also store similarly structured 51 - 55 kDa glutelins. Their presence has been demonstrated in species of *Picea* (Gifford and Tolley, 1989; Misra and Green, 1990; Jensen and Lixue, 1991; Allona *et al.*, 1994c), *Larix* (Jensen and Lixue, 1991), *Pseudotsuga menziesii* (Green *et al.*, 1991; Jensen and Lixue, 1991), *Cedrus deodora* (Jensen and Lixue, 1991) and the Cupressaceae (Allona *et al.*, 1994c; Häger and Dank, 1996). However, these glutelins are not present in any studied species of *Abies* (Jensen and Lixue, 1991; Allona *et al.*, 1994c), in *Cedrus atlantica* (Allona *et al.*, 1994c), or in the conifer family Taxodiaceae (Allona *et al.*, 1994c). Although glutelins are not present in *Cedrus atlantica*, a 55 kDa protein composed of 21 and 32 kDa polypeptides joined by disulfide bridges is fully extracted in the salt-soluble globulin fraction (Allona *et al.*, 1994c). The 21 kDa polypeptide of this subunit is

recognized by monospecific polyclonal antibodies raised against the 21 kDa glutelin polypeptide of *Pinus pinaster* (Allona *et al.*, 1994c). Salt extractions usually allow the subunits of the holoprotein to remain associated; however, a larger holoprotein composed of the salt extracted *Cedrus* 55 kDa subunit could not be detected by gel filtration. A salt-soluble 57 kDa subunit has also been described in *Ginkgo biloba* of the Ginkgoaceae (Jensen and Berthold, 1989). This subunit forms a hexameric holoprotein called ginnacin (Arahira and Fukazawa, 1994). The partial deduced amino acid sequence from the 20 kDa peptide has 32 - 49% homology to legumin-like proteins in both angiosperm monocotyledons and dicotyledons (Häger *et al.*, 1992; Häger *et al.*, 1995).

The classification and naming of Pinaceae seed storage proteins that have glutelin-like solubility is complex. Difficulties in classifying these proteins have arisen because they share similarities to several other types of storage proteins in angiosperm seeds. Due to their similarities, researchers have described these proteins as: crystalloids, legumins, legumin-like, globulin-like, glutelins and glutelin-like. The Pinaceae glutelins were initially described as crystalloid proteins because of their similarity to the 11S crystalloid proteins of castor bean seeds (Gifford *et al.*, 1982; Gifford, 1988). Both types of proteins require the addition of SDS or urea for full solubilization and both seeds form protein vacuoles that contain a proteinaceous crystalloid. The castor bean crystalloid is a hexameric holoprotein comprised of homologous subunits of about 50 kDa (Gifford and Bewley, 1983). Each subunit is translated as a single polypeptide that is cleaved to produce a large polypeptide (~30 kDa) that is linked to a small polypeptide (~20 kDa) by disulfide bridges. Under SDS-dissociating conditions, the crystalloid's subunit polypeptides can associate by disulfide

bridging to form a complex that migrates at 100 kDa by SDS-PAGE (Gifford and Bewley, 1984). Similar migrating bands have been observed in the buffer-insoluble, non-reduced fractions of several *Pinus* species (Gifford, 1988) as well as in the Cupressaceae (Häger and Dank, 1996). The castor bean large polypeptide is acidic and the small polypeptide is basic (Gifford and Bewley, 1983); however, both subunit polypeptides are basic in conifers (Hakman *et al.*, 1990; Allona *et al.*, 1992). Leal and Misra (1993b) call the large subunit acidic based on the deduced amino acid sequence of a *Pseudotsuga menziesii* cDNA for a legumin-like precursor protein. However, the authors have not provided any evidence that the actual large polypeptide is acidic under isoelectric focusing conditions. Furthermore, there is no antigenic recognition of *Pinus* glutelin-like proteins by three independently produced sets of castor bean crystalloid antibodies (Gifford, 1988; Migabo, 1995). Antibodies supposedly made to *Picea glauca* crystalloids did react with the crystalloid proteins from castor bean (*Ricinus communis*) (Misra and Green, 1994); however the authors did not appear to understand that the *P. glauca* crystalloids are composed of only the 57 kDa subunit. This misunderstanding led them to produce antibodies to a phosphate buffer-insoluble protein fraction that contained both a 43 kDa protein and the 57 kDa crystalloid subunit (Misra and Green, 1991). These non-specific antibodies not only recognize the crystalloid subunit of *P. glauca*, but they also recognize the buffer-insoluble 43 kDa and a low molecular weight protein (which are both likely globulins), and a buffer-soluble albumin in *P. glauca*. These antibodies also cross-react with glutelin-like as well as non-glutelin-like protein bands in other Pinaceae species, and several angiosperms (Misra and Green, 1994); due to the lack of antibody specificity it is difficult to conclude that these proteins are indeed

related. The Pinaceae glutelin-like proteins are similar to crystalloids in castor bean in terms of solubility and subunit structure; however they are different in terms of the large polypeptide isoelectric point (pI) and their antigenic relatedness.

In several other studies, the Pinaceae 51 - 55 kDa proteins are called 11S legumin-like because of their similarity to 11S storage proteins extensively studied in the family Leguminosae (Derbyshire *et al.*, 1976). The legumins are holoproteins composed of six homologous subunits that interact non-covalently. Similar to castor bean crystalloids, each subunit is translated as a single polypeptide that is cleaved to form a large acidic polypeptide (~40 kDa) and a small basic polypeptide (~20 kDa) that are joined by a single disulfide bridge (Shrewy *et al.*, 1995). *Ginkgo biloba*'s legumin-like storage protein fits the legumin criteria since it is: completely soluble in salt solutions, shares the same subunit and holoprotein structure, as well as similar pIs for the polypeptides (Jensen and Berthold, 1989). Protein vacuoles in the seeds of species in the family Leguminosae do not contain protein crystalloids (Lott, 1980). Deduced amino acid sequences of a *Pseudotsuga menziesii* legumin-like storage protein cDNA show only 29 - 39% identity with legumin cDNAs from several angiosperm species (Leal and Misra, 1993b). However, legumins are soluble in salt-solutions, and are thus globulins. By describing the conifer SDS-soluble proteins as legumin-like there is the implication that these proteins are completely soluble in salt solutions. Jensen and Lixue (1991) studied the 51 - 55 kDa subunits in several species of *Pinus*, *Picea*, *Larix*, *Cedrus*, and *Pseudotsuga*. In most of these species, they found that these storage proteins are not fully extracted with aqueous buffers containing 2% NaCl, but are when extracted with a buffer containing SDS. The only Pinaceae seed from which the 51 - 55 kDa subunit is

completely extracted by a salt solution is *Cedrus atlantica* (Allona *et al.*, 1994c). Mono-specific polyclonal antibodies to the 21 kDa glutelin polypeptide from *Pinus pinaster* seeds recognize 20 - 22 kDa globulin polypeptides from pea and soybean (Allona *et al.*, 1992). Thus the legumins and the Pinaceae glutelin-like proteins share a similar secondary structure and antigenicity; however they share limited amino acid sequence identity, differ in the pIs of their large polypeptide and differ in their solubility characteristics.

Because of their solubility, I have referred to the major Pinaceae storage proteins as glutelin-like. However, the glutelins are also known as a complex family of proteins found in monocotyledonous plants that share similar solubility characteristics, but have a variety of subunit and holoprotein structures. The class of glutelins found in rice are similar to angiosperm legumins both in terms of protein subunit structure, amino acid sequence, and polypeptide pIs (Robert *et al.*, 1985; Takaiwa *et al.*, 1991). Both seeds of the Fabaceae family and rice have protein vacuoles that do not contain protein crystalloids (Lott, 1980). The deduced amino acid sequences from cDNAs for legumin-like storage proteins from *Pseudotsuga menziesii* show only 30% identity to rice glutelin cDNAs (Leal and Misra, 1993b). A *Pinus strobus* 11S globulin-like cDNA deduced amino acid sequence also has only 30% identity (42% homology) to rice glutelin cDNAs (Baker *et al.*, 1996). Although there are sequence similarities between rice glutelin genes and glutelin-like genes from Pinaceae seeds, mono-specific polyclonal antibodies to the 21 kDa glutelin polypeptide from *Pinus pinaster* seeds did not recognize any proteins from the similarly structured rice glutelins (Allona *et al.*, 1992). Thus the Pinaceae glutelins and the rice glutelins have similarities in their solubilities and subunit

structure; however, they have limited deduced amino acid sequence identities, have differences in the large polypeptide pIs and do not appear to be antigenically related.

It seems clear that while these 51-55 kDa Pinaceae proteins share many features with storage proteins from diverse plant taxa, there are also differences in each case. Because of these differences, it is more appropriate to separate them and refer to these proteins as coniferalins. It has been hypothesized that the legumins from angiosperms and *Ginkgo*, the rice glutelins, and the Pinaceae coniferalins have evolved from a common ancestral storage protein (Häger *et al.*, 1995). These proteins have maintained a similar subunit and possibly holoprotein structure, perhaps because it is an efficient and effective structure for protein storage.

1.3.1.1 Amino acid composition of Pinaceae storage proteins

The major amino acids in the combined phosphate buffer-insoluble proteins of fully stratified loblolly pine megagametophytes are arginine and a combined glutamate/glutamine fraction (King and Gifford, 1997). These amino acids comprise 23 and 21 mol% of the buffer-insoluble proteins, respectively. The arginine in these storage proteins is even more important since it contains 46% of the nitrogen in these storage proteins (King and Gifford, 1997). Similar amino acid compositions are found in the total HEPES buffer-insoluble fraction from mature seeds of loblolly pine (Feirer, 1995). In Feirer's (1995) study, a 44 kDa protein was also isolated from this fraction and analyzed. It was found to have a lower (8.5 mol %) arginine content compared to the 19.1 mol% arginine content in the total buffer-insoluble protein fraction of mature loblolly pine seeds (Feirer, 1995). This 44 kDa protein likely corresponds to the 47 kDa

protein described in the phosphate buffer-insoluble fraction of loblolly pine by both Groome *et al.* (1991) and King and Gifford (1997). This protein is a globulin based on solubility (Gifford, unpublished data) and comprises less than 5% of the buffer-insoluble proteins in the megagametophyte (King and Gifford, 1997).

Arginine and glutamate/glutamine are also the major amino acids found in individual proteins or protein fractions from other Pinaceae seeds including *Pinus banksiana* (Durzan and Chalupa, 1968; Ramaiah *et al.*, 1971), *P. strobus* (Feirer, 1995) and *Pseudotsuga menziesii* seeds (Feirer, 1995). These amino acids are also enriched in the storage protein from interior spruce (*Picea glauca/engelmannii*) (Newton *et al.*, 1992), *Pseudotsuga menziesii* (Leal and Misra, 1993b; Chatthai and Misra, 1998), the Cupressaceae family (Häger and Dank, 1996), and in *Ginkgo biloba* of the Ginkgoaceae (Häger *et al.*, 1995) based on the deduced amino acid sequences from storage protein cDNAs. The amino acid content of the different fractions from mature *Pinus pinaster* seeds has been extensively analyzed by Allona *et al.* (1992; 1994a; 1994b). Glutamate /glutamine accounts for 17 - 26 mol% of each fraction, with the highest content in the low molecular weight globulins (Allona *et al.*, 1992; 1994b). Similarly the arginine content also varies in these fractions, with the highest content (24.6 mol%) again in the low molecular weight globulins (Allona *et al.*, 1992; 1994b). The albumins, high molecular weight globulins and the glutelin fractions each contained 6.6, 9.4 and 14.9 mol% arginine, respectively (Allona *et al.*, 1992).

Arginine is relatively abundant in Pinaceae storage proteins, compared to most other seeds (Feirer, 1995). The abundance of this basic amino acid is probably the cause of the basic pI of the glutelin large polypeptide. This high level of arginine indicates that

the Pinaceae seed proteins are highly enriched with nitrogen, since each arginine molecule contains four nitrogen molecules. It has been hypothesized that the nitrogen-rich nature of this amino acid, as well as its abundance, make arginine a possible candidate for a transport compound in Pinaceae seeds (Ramaiah *et al.*, 1971; Feirer, 1995; King and Gifford, 1997).

1.3.1.2 Protein storage organelles

During seed development, protein reserves are sequestered into specialized organelles called protein vacuoles or protein bodies. During germination and early seedling growth, these organelles fuse together as the proteins are hydrolyzed to form the cell's central vacuole (Lott, 1980). For this reason, I have referred to these storage organelles as protein vacuoles. Protein vacuoles are single unit membrane-bound organelles that can vary in size from 0.1 μm to 22 μm in diameter (Lott, 1980). Structural studies of Pinaceae seeds have identified protein vacuoles in both the megagametophyte and embryo (Simola, 1974a, 1974b, 1976; De Carli *et al.*, 1987; Misra and Green, 1990; Krasowski and Owens, 1993; Owens *et al.*, 1993). The protein vacuole appearance can vary greatly due to the protein and non-protein substances stored within them. They can be composed entirely of an amorphous proteinaceous matrix, or they can also include one or more non-membrane bound, electron-dense protein crystalloids. Protein vacuoles can also contain an electron-translucent globoid, that sometimes contains electron-dense inclusions called globoid crystals (Lott, 1980). Much smaller (80 - 300 nm diameter) globoid crystals have also been demonstrated in other parts of the protein vacuole, such as in the proteinaceous matrix in soybean

cotyledons and sunflower cotyledons (Lott and Buttrose, 1978). Phytin, which is a cation salt of myo-inositol hexaphosphoric acid, is usually concentrated in the globoid crystal. However very small phytin deposits can also be found outside the globoid, in other areas of the protein vacuole (Lott, 1980). Less frequently, one or more druse or rosette shaped crystals of calcium oxalate may also be embedded in the proteinaceous matrix (Lott, 1980). These protein vacuoles can be the same throughout the seed, or they may differ in protein content and appearance within the same cell, within the same tissue, or between seed tissues (Shrewry *et al.*, 1995). Observations using the transmission electron microscope (TEM) have been made for a limited number of mature seeds from Pinaceae species. Protein vacuoles with protein crystalloids and globoids embedded in a proteinaceous matrix have been described in *Pinus banksiana* cotyledons (Durzan *et al.*, 1971), *P. pinea* megagametophytes (Gori, 1979), and megagametophytes and embryonic organs of *P. sylvestris* (Simola, 1974a), *Picea abies* (Simola, 1976), *P. excelsa* (De Carli *et al.*, 1987), *P. glauca* (Misra and Green, 1990; Krasowski and Owens, 1993) and *Pseudotsuga menziesii* (Owens *et al.*, 1993).

1.3.1.3 The formation of protein vacuoles during seed development

Most storage protein mRNAs are translated on the RER (Higgins, 1984; Casey *et al.*, 1986). For example, pulse-chase experiments using radiolabelled amino acids demonstrated the synthesis of legumin storage proteins on the RER in pea (Chrispeels *et al.*, 1982a, 1982b). Immunocytochemical evidence is available supporting the synthesis of specific storage proteins on the RER of different species such as castor bean crystalloids (Brown and Greenwood, 1990) and wheat gliadins and glutenins (Stenram *et*

al., 1991). Pinaceae storage proteins are thought to be translated on the RER based on the presence of signal peptide sequences from cDNAs of a 7S globulin from interior spruce (Newton *et al.*, 1992) and an 11S legumin-like protein and 2S protein from *Pseudotsuga menziesii* (Leal and Misra, 1993b; Chatthai and Misra, 1998). In addition, deduced amino acid sequences from cDNAs coding for a legumin from *Ginkgo biloba* of the Ginkgoaceae (Arahira and Fukazawa, 1994) and a legumin with glutelin-like solubility from *Calocedrus decurrens* of the Cupressaceae (Häger and Dank, 1996) also contain signal peptide sequences.

There are two main routes for protein vacuole formation during seed development. They can form from fragmentation of an existing vacuole, or by budding off the ER membrane (Lott, 1980; Shewry *et al.*, 1995). Protein vacuole formation from the ER appears to be associated with the storage of prolamins in some species. Prolamins in rice (Krishnan *et al.*, 1986), maize starchy endosperm (Kyle and Styles, 1977; Larkins and Hurkman, 1978) and sorghum starchy endosperm (Taylor *et al.*, 1985) accumulate within ER lumen, causing its distention and budding to form protein bodies. However, not all prolamins are retained by ER. For example in wheat, it was shown through immunolocalization with antibodies to gliadins (a prolamins) that these prolamins are not retained by the ER, but are transported to dictyosome vesicles (Kim *et al.*, 1988; Stenram *et al.*, 1991).

The Golgi apparatus is the term used to describe interassociated dictyosomes functioning synchronously (Mollenhauer and Morré, 1980); this apparatus is often associated with the trafficking of non-prolamins storage proteins. Based on ultrastructural observations, storage proteins are transported via the Golgi apparatus to

the fragmenting vacuole in pea (Craig, 1988), beech (Collada *et al.*, 1993) and *Cercis siliquastrum* (Baldan *et al.*, 1995). Immunological studies using antibodies to 11S crystalloids of castor bean (Brown and Greenwood, 1990) and the 42 kDa globulin of *Picea abies* (Hakman, 1993b) have also shown the involvement of the Golgi apparatus in the deposition of storage protein to the fragmenting central vacuole.

Unlike the case of *P. abies*, few dictyosomes are observed during stages of maximum protein accumulation in *P. glauca* (Krasowski and Owens, 1993) and *Pseudotsuga menziesii* (Owens *et al.*, 1993), leading the authors to hypothesize that the Golgi apparatus is not involved in storage protein deposition at these stages. During the early stages of protein deposition in *Picea glauca* megagametophytes, the deposition may occur by more than one mechanism (Krasowski and Owens, 1993). In addition to the deposition of protein into the tonoplast of fragmenting vacuoles, two other distinct mechanisms have been described. Membranous vesicles containing electron dense globules are found inside large vacuoles, adhering to the tonoplast. The identity of the globule is unknown, and the mechanism of the vesicle's transport into the vacuole is also unknown. However, the authors speculate that it could be caused by invagination of the tonoplast membrane. Proteinaceous material accumulate on both the tonoplast membrane, as well as around the intravacuolar membrane. No vesicular transport is noted in the cytoplasm at this time, and the RER is in close proximity to the tonoplast. Additionally, no budding of RER is observed. These findings lead to speculation that protein translocation without vesicles may occur across the tonoplast during early stages of development. An additional way protein storage organelles formed is by the enlargement of *de novo* formed protein bodies by fusion with cytoplasmic vesicles. This

de novo formation of protein organelles from vesicle fusion is also noted in cowpea cotyledons (Harris and Boulter, 1976) and in wheat endosperm (Kim *et al.*, 1988; Stenram *et al.*, 1991). The transport of protein containing vesicles to the tonoplast of fragmenting vacuoles is observed in later stages during *Picea glauca* seed development (Krasowski and Owens, 1993).

In the variety of angiosperm seeds studied thus far, protein vacuole formation appears to be quite complex and can vary greatly depending on the storage protein, timing, tissue and species studied. It should not be surprising that a consensus has not been reached concerning protein vacuole formation in Pinaceae seeds, considering the limited number of developmental studies done. It is possible that in the Pinaceae, differences in storage protein trafficking may be observed with time, tissue, storage protein type, as well as species. Clearly more ultrastructural studies of the development of Pinaceae seeds need to be undertaken using antibodies to specific storage proteins in order to identify the deposition route or routes of individual storage proteins.

1.3.2 Storage Lipids

Lipids are a heterogeneous group of compounds that share the similar properties of insolubility in water, and solubility in non-polar solvents like chloroform, hydrocarbons or alcohols (Gurr and Harwood, 1991). Lipids contain more than twice the energy of starch or protein on a per weight basis (Huang, 1992). Perhaps because of this, lipids are commonly stored as reserves in seeds (Huang, 1992). Triacylglycerol (TAG) is the predominant form of lipid stored in most seeds, although jojoba seeds store wax esters instead (Huang, 1992).

The main storage reserve stored in Pinaceae seeds is TAG (Ching, 1966; Kovac and Vardjan, 1981; Hammer and Murphy, 1994). A TAG molecule is composed of three fatty acids esterified to a glycerol backbone. Conifer seed TAGs have been extensively studied for taxonomic purposes (Imbs and Pham, 1996; Wolff *et al.*, 1996, 1997a, 1997c, 1998). These studies have demonstrated that 90 - 95% of the fatty acids stored in TAGs are unsaturated (Janick *et al.*, 1991; Wolff *et al.*, 1997c). In addition to linoleic (18:2) and oleic (18:1) acids that are common in angiosperm seeds, all conifer seeds contain 18 and 20 carbon fatty acids with a Δ^5 ethylenic bond arranged without methylene interruptions. These fatty acids are called Δ^5 -olefinic acids which are quite rare in other plant species (Attree *et al.*, 1992; Wolff, 1997). There are six different Δ^5 -olefinic acids found in conifer seed fatty acids (Wolff *et al.*, 1997a); 79 - 94% of these unique fatty acids are esterified to the sn-3 position of TAG molecules in the Pinaceae, Taxaceae, Taxodiaceae, and Cupressaceae (Wolff *et al.*, 1997b). Not only conifer families, but also the genera within families, can be differentiated on the basis of the presence and proportions of specific Δ^5 -olefinic acids, as well as other fatty acids (Wolff *et al.*, 1997c). In *Pinus* species the main fatty acid is linoleic acid (44 - 57%) and either oleic acid (13 - 25%) or the Δ^5 -olefinic type pinolenic acid (18:3 $\Delta^5,9,12$) (1.5 - 25.2%) is the next most abundant fatty acid (Janick *et al.*, 1991; Imbs and Pham, 1996; Wolff *et al.*, 1997a).

1.3.2.1 Triacylglycerol (TAG) storage organelles

TAG is stored in organelles called lipid bodies. Because plant TAG is liquid at room temperature, these storage organelles are sometimes referred to as oil bodies. The

diameters of lipid bodies have been measured from several angiosperm crop species using TEM serial sections. Based on this data, the average diameter of lipid bodies is 0.6 - 2 μm (Tzen *et al.*, 1993). Pinaceae seed lipid bodies have not been measured using this technique. Lipid bodies of Pinaceae seeds, like most others, are comprised of three main constituents: TAGs, oleosins, and phospholipids. TAGs comprise the majority of the lipid body volume (Lee *et al.*, 1994).

In angiosperm seeds, fatty acid biosynthesis takes place in the proplastid (Stumpf, 1980). The assembly of the fatty acids to form TAGs occurs in the ER, primarily through the glycerol phosphate pathway (Gurr, 1980). Glycerol-3-phosphate from the glycolytic or pentose phosphate pathways or by phosphorylation of glycerol by glycerol kinase, forms the backbone of the TAG molecule. Fatty acids are esterified to the sn-1 and sn-2 positions of the glycerol-3-phosphate in two separate reactions, which are catalyzed by two different acyltransferase enzymes. Esterification of a fatty acid to the sn-3 position is accomplished by diacylglycerol acyltransferase. This is the only enzyme of this pathway that is unique to TAG synthesis, and it has been localized to the rough endoplasmic reticulum in maize, soyabeans, groundnuts, and castor bean (Cao and Huang, 1986). Little is known about TAG biosynthesis in Pinaceae seeds.

TAGs make up a spherical mass that is surrounded by a monolayer of phospholipid embedded by oleosin proteins (Tzen *et al.*, 1993). Recently it has been demonstrated that the phospholipid monolayer in sesame seed is predominantly composed of phosphatidylcholine (Peng and Tzen, 1998). Oleosins are a family of low molecular weight alkaline proteins (15-26 kDa) and usually only a few isoforms are present within the seed (Huang, 1992). Two oleosins (15 kDa and 10 kDa) were

identified in both mature megagametophyte and embryo lipid bodies of *Pinus ponderosa* (Lee *et al.*, 1994). Only the cDNA encoding the 15 kDa oleosin in the megagametophyte was isolated. The predicted amino acid sequence from this cDNA is similar to other oleosins found in angiosperm seeds (Lee *et al.*, 1994). All oleosins have three distinct domains. There is a relatively polar C-terminal region, a central hydrophobic region, and an amphipathic N-terminal region. Two hypotheses have been proposed as to how oleosins are inserted into lipid bodies. Both theories have the C-terminal and N-terminal regions on the outer surface of the lipid body and the central hydrophobic region inserted through the phospholipid monolayer, lying within the TAG matrix. However, the extent to which the central region is inserted into the TAG matrix is open to debate. Huang (1992) favors the theory that the central portion is structured as an anti-parallel β -strand stabilized by a triple-proline turn which is embedded deep within the lipid body. Murphy (1993) speculates that the central portion is also an anti-parallel β -strand. This region is also proline stabilized but is embedded less deeply within the TAG matrix, and instead lays against the underside of the phospholipid monolayer. Because this central portion is highly conserved among deduced amino acid sequences from angiosperm and gymnosperm oleosin cDNAs (Lee *et al.*, 1994) it is thought that it might be important for the targeting of oleosins to the lipid body or for the function of oleosins. It has since been shown by deletion analysis that both the N-terminal and central portion are necessary for *Arabidopsis thaliana* oleosin targeting to *Brassica napus* lipid bodies (van Rooijen and Moloney, 1995).

Oleosins have isoelectric points of 5.7 - 6.6, making the surfaces of lipid bodies negatively charged at a physiological pH (Tzen *et al.*, 1993). This negative charge has

led to the speculation that the role of oleosins in the surfaces of lipid bodies is to maintain their integrity as they become packed close together during seed maturation desiccation. Cummins *et al.* (1993) have shown that lipid bodies from developing rapeseed embryos have little oleosin associated with them, and lipid body preparations from this tissue coalesced forming large oil globules together when desiccated. Recently, evidence has been provided supporting another function of oleosins in the stabilization of lipid bodies during imbibition. A comparative study of desiccation-tolerant and -intolerant oil seeds was completed using a low-temperature scanning electron microscope. It was found that the desiccation-intolerant species had less than 5% of the oleosin content of desiccation-tolerant species (Leprince *et al.*, 1998). Both during and after desiccation there was little change in lipid body sizes in both seed types; however, when desiccation-intolerant seeds were imbibed after desiccation, oil bodies coalesced and germination was inhibited (Leprince *et al.*, 1998). This study provides evidence that oleosin may have a role in the maintenance of lipid body stability, not only during maturation drying, but during the subsequent imbibition of the seed.

1.3.2.2 The formation of lipid bodies during development

There are two different hypotheses to explain the formation of lipid bodies during seed development (Huang, 1992; Murphy, 1993). One hypothesis, originally proposed on the basis of ultrastructural studies, is that complete lipid bodies form by budding of the ER. In support of this theory is the biochemical localization of enzymes involved in the synthesis of TAGs, phospholipids, and oleosins to the ER (Huang, 1992). The biosynthesis of TAGs is thought to occur between the ER lipid bilayer leaflets, where the

TAG can accumulate and form a lipid droplet due to its hydrophobic nature. Oleosin mRNAs have been shown to associate with the ER (Qu *et al.*, 1986) but do not encode for a typical cleavable N-terminal signal peptide (Huang, 1992). It is thought that the oleosin mRNAs are translated on ER associated ribosomes but are not inserted into the ER lumen due to the absence of a signal peptide. Instead the highly hydrophobic central portion of the oleosin is inserted into the ER membrane outer leaflet, and migrates to the area of accumulating TAGs. The association of TAG which are highly hydrophobic, with oleosins will stabilize the central oleosin domain. The accumulation of TAG eventually forces the lipid bilayer apart and the lipid body enclosed by a monolayer of phospholipid from the ER membrane's outer leaflet, embedded with oleosin proteins, buds off (Huang, 1992). This particular model works best if the oleosin structure has the central region embedded deep inside the lipid body, as proposed by Huang (1992). Based on ultrastructural observations, lipid bodies appear to be secreted by the smooth ER (SER) in *Picea glauca* megagametophytes (Krasowski and Owens, 1993). However, lipid body budding from RER is more commonly observed in endosperms and cotyledons of several angiosperms (Frey-Wyssling *et al.*, 1963; Wanner and Theimer, 1978; Wanner *et al.*, 1981; Fernandez and Staehelin, 1987; Briggs, 1993). The different types of ER involved in lipid body budding could be due to differences in tissue fixation that affected ribosome stability. The RER and SER are thought to be part of a continuous ER membrane system within the cell (Chrispeels, 1980). It is possible that the biosynthesis of TAG and oleosin occurs in the RER membrane, but is transported to an area of the SER where accumulation and budding of the lipid body occurs. Another

possibility is that lipid bodies in *Picea glauca* are budded from the ER without oleosins, that are inserted later.

The second hypothesis is also based on ultrastructural studies in which no swelling of the ER was observed (Harwood *et al.*, 1971; Rest and Vaughan, 1972; Smith, 1974; Bergfeld *et al.*, 1978). Based on these studies, it is thought that “naked” TAG droplets arise by condensation in the cytoplasm, then are surrounded by a half-unit membrane of phospholipids and oleosins (as reviewed by Huang, 1992 and Murphy, 1993). Supporting this theory are two studies in which the majority of oleosin accumulates in lipid bodies after the storage TAG has reached its maximum level in embryos of *Brassica napus* (Murphy and Cummins, 1989; Cummins *et al.*, 1993). However, another study of *Brassica napus* development shows that TAGs and oleosins accumulate at the same time (Tzen *et al.*, 1993).

1.4 Development of the Pinaceae seed

Few studies have examined the deposition of storage materials in Pinaceae seeds throughout development using histochemical, biochemical, or molecular tools. This is likely due to the difficulty of collecting large amounts of material from early stages of seed development. Structural studies have noted that the megagametophyte is fully developed prior to fertilization (Chamberlain, 1957; Owens and Molder, 1977; Owens *et al.*, 1982). During fertilization and proembryonic stages, starch is the only storage reserve found in the megagametophyte of *Pseudotsuga menziesii* (Owens *et al.*, 1993). Most of the starch is found in the central portion of the megagametophyte, the area into which the embryo eventually grows (Trenin, 1985; Hakman, 1993a; Owens *et al.*, 1993).

As the embryo grows and develops, these starch containing megagametophytic cells around the embryo degenerate, presumably to create space for and to feed, the growing embryo. The fluid-filled space that forms by the breakdown of megagametophyte cells is called the corrosion cavity (Chamberlain, 1957; Singh and Johri, 1972).

Storage protein genes are not transcribed prior to fertilization in the megagametophytes of *Pinus strobus* (Baker *et al.*, 1996) and *Pseudotsuga menziesii* (Chatthai and Misra, 1998). Lipid body and protein vacuole formation begin in the megagametophyte before it begins in the embryo of *P. menziesii* (Owens *et al.*, 1993). The majority of lipid and protein deposition to lipid bodies and protein vacuoles occurs in the megagametophyte after the embryo became club-shaped and continues until the formation of early-organs. In contrast, this process occurs during cotyledon development in the embryos of *Picea abies* (Hakman, 1993a; Krasowski and Owens, 1993) and *Pseudotsuga menziesii* (Owens *et al.*, 1993). TAGs are detected in *Picea abies* and loblolly pine megagametophytes before cotyledon development. TAG is also detected in *P. abies* embryos at this stage, but is not detected in loblolly pine embryos until the cotyledon primordia are observed (Feirer *et al.*, 1989). TAG levels increase during development in both the megagametophyte and embryo, with the highest rate of accumulation occurring after the embryos had well-defined cotyledons and continued until the mature seed had formed.

1.4.1 Transcriptional regulation of storage protein synthesis

Similar to the formation of protein vacuoles, Pinaceae storage protein transcripts are detected in the megagametophyte before they are detected in the embryo. The

megagametophyte storage protein gene transcripts are detected by northern blotting a few days after fertilization for *Picea glauca* crystalloid protein (Leal and Misra, 1993a) and *Pseudotsuga menziesii* 2S protein (Chatthai and Misra, 1998), and a few weeks after fertilization for *P. menziesii* legumin-like storage protein (Leal and Misra, 1993b). In the embryo of interior spruce, transcripts for 11S legumin, 7S vicilin and 2S albumin are detected later, during early cotyledon development (Flinn *et al.*, 1993). Legumin-like storage protein gene transcripts are also detected in *P. glauca* embryos at the early cotyledonary stage. However, the occurrence of transcripts in earlier stages in this tissue were not examined (Leal and Misra, 1993a, Leal *et al.*, 1995).

In Pinaceae seeds, the similar timing of the appearance of storage protein transcripts and of storage proteins suggests that storage protein genes are transcriptionally regulated. Storage proteins in the megagametophyte are detected by SDS-PAGE a few days after fertilization in both *Picea abies* (Hakman, 1993a) and *P. glauca* (Misra and Green, 1991). In contrast, they are detected by SDS-PAGE one month after fertilization, during early organ formation stages in embryos of *P. glauca* (Misra and Green, 1991) and interior spruce (Flinn *et al.*, 1991). Correlated with the onset of storage protein translation in the megagametophyte, the level of free amino acids rises dramatically in whole ovules of *Pinus strobus* after fertilization (Feirer, 1995). Glutamine and asparagine are the predominant free amino acids, sometimes comprising over 50% of the free amino acid pool. These amides are thought to be important transportable compounds or intermediates of nitrogen metabolism, making them important during the anabolism of storage proteins (Lea and Mifflin, 1980). Arginine, an

important component of storage proteins, also increases dramatically during this time period.

Not only is the timing of storage protein gene expression regulated with regards to tissue type, but there is also preliminary evidence to suggest that the genes expressing individual storage proteins are regulated differently (Misra, 1994). It has been shown that the 57 kDa protein accumulates before a 42 kDa protein in the phosphate buffer-insoluble fractions of megagametophytes and embryos of *Picea glauca* (Misra and Green, 1991), and 33-35 kDa and 22-24 kDa high salt soluble globulins accumulate before a 41 kDa albumin in the embryo of interior spruce (Flinn *et al.*, 1991). The 57 kDa protein in *Picea glauca* and the high salt soluble globulins in interior spruce are probably a coniferalin subunit and coniferalin polypeptides, respectively. Transcript levels for the high salt globulin and albumin genes in interior spruce also indicate that the high salt globulin transcript level peaks in the embryo earlier than transcripts for the albumin (Flinn *et al.*, 1993). Unlike storage protein appearance in *P. glauca* and interior spruce, four unidentified storage proteins appeared at about the same time during development of megagametophytes in *P. abies* (Hakman, 1993a). This observation may be an artifact of extracting the storage proteins with a salt solution, since coniferalins are not fully solubilized under these conditions and may not have been extracted if present in low levels in the early megagametophyte stages.

1.5 Preparation of Pinaceae seed for germination

Mature, desiccated Pinaceae seeds often have a low rate of germination when imbibed at a given germination temperature; for example only 19% of mature, desiccated

loblolly pine seeds germinate when imbibed at their optimal germination temperature of 30°C (Schneider and Gifford, 1994). However, mature Pinaceae seed embryos are non-dormant, since the embryos can germinate after the removal of all or some of the surrounding seed tissues (Kao and Rowan, 1970; Baron, 1978; Carpita *et al.*, 1983; Downie and Bewley, 1996; Bianco *et al.*, 1997; King, 1998). The inhibition of seed germination by tissues surrounding the embryo is termed coat-imposed dormancy (Bewley and Black, 1994). This type of dormancy may inhibit the embryo's germination in a number of ways including: interference with water uptake and/or gas exchange, mechanical restraint of the embryo, prevention of the exit of inhibitors from the embryo and the possible supply of inhibitors to the embryo (Bewley and Black, 1994). The coat-imposed dormancy is broken in Pinaceae seeds by a period of moist chilling, called stratification. In loblolly pine, the increase in germination with stratification time is correlated with an increase in seed water content (Schneider, 1993), while the levels of total lipid, buffer-insoluble protein, total DNA and total RNA did not change (Schneider and Gifford, 1994; Mullen *et al.*, 1996). However, an increase in 80% ethanol-soluble carbohydrate content is observed in both the megagametophyte and embryo during this time period (Gifford, unpublished results). Similarly, Kao and Rowan (1970) found an increase in sucrose, organic acid, organic phosphate and high energy phosphate (likely ATP) levels during stratification of *Pinus radiata* seeds. ATP levels also increase during stratification in both the megagametophyte and embryos of *P. lambertiana* (Noland and Murphy, 1984). Although lipase activity (Kao and Rowan, 1970) does not increase during stratification, and no change in total lipid levels (Kao and Rowan, 1970; Schneider and Gifford, 1994; Mullen *et al.*, 1996) has been noted, activity of the

glyoxylate cycle enzyme isocitrate lyase (Noland and Murphy, 1984) increases in both the megagametophyte and embryo; however, the increase was minor relative to the increase in activity following germination. These observations may indicate that a very limited number of free fatty acids are metabolized to produce carbohydrates. Sucrose hydrolysis through increased sucrose synthase activity (Murphy and Hammer, 1988), but not invertase activity (Kao and Rowan, 1970; Murphy and Hammer, 1988), may release glucose that is used to produce ATP (Kao and Rowan, 1970; Noland and Murphy, 1984). A relatively high ATP level may be required by the embryo, once it is placed at a germination temperature, to use for energy to grow through the seed tissues to germinate.

During stratification in loblolly pine embryos and megagametophytes, a population of mRNAs (Mullen *et al.*, 1996), and a population of proteins (Schneider and Gifford, 1994), decreased. These proteins may have a role in maintaining the dormancy of loblolly pine seeds; their disappearance during the period of time in which the greatest increase in percent germination occurs supports this hypothesis. Similar to the disappearance of proteins, there is also synthesis of a new population of mRNAs (Mullen *et al.*, 1996) and proteins during stratification (Schneider and Gifford, 1994). The newly translated proteins may also be involved in the breaking of loblolly pine dormancy. It is unknown what the role(s) of these proteins is (are); perhaps they are involved with the initial, low level metabolism of fatty acids required to produce carbohydrates, organic acids and ATP.

It is unknown whether the changes noted during stratification help to eliminate the seed coat dormancy effect or if they are a result of its elimination. In any case, in

order to study germination and early seedling growth in Pinaceae seeds, a period of stratification is often necessary to break coat-imposed dormancy and to increase the uniformity of germination. The coat-imposed dormancy of loblolly pine seeds (Carpita *et al.*, 1983; King, 1998) is broken by a 35 day stratification period at 2°C.

1.6 Developmental periods of the study: germination and early seedling growth

Once dormancy is broken, Pinaceae seeds are ready to germinate and to then enter the growth phase referred to as early seedling growth. Germination begins after the seed is imbibed and placed at a germination temperature. During this period the cells of the radicle grow primarily by expansion (Bewley and Black, 1994). Germination is completed when the radicle emerges from the seed coat. Early seedling growth is defined as the growth period that takes place after radicle emergence from the seed coat and before the megagametophyte is shed from the seedling; it is epigeal. The seedling grows out of the seed primarily by the growth of the radicle and hypocotyl, leaving the cotyledons in contact with the megagametophyte. It is during early seedling growth that the majority of the stored reserves in the seed are broken down and metabolized (Ching, 1966). The seedling uses these metabolites as energy, carbon and nitrogen sources as it develops and becomes photosynthetically autonomous (Sasaki and Kozlowski, 1969; De Carli *et al.*, 1987). Eventually the cotyledons expand further and the megagametophyte is shed, which completes the period of early seedling growth.

1.6.1 Storage protein reserves

Since the majority of storage proteins are stored in the megagametophyte, they have to be broken down (Guitton, 1964; Durzan and Chalupa, 1968; Ramaiah *et al.*, 1971; Lammer and Gifford, 1989; King and Gifford, 1997) to peptides and free amino acids which are then transported to the developing seedling. Based on observations of increased activity in megagametophyte cell-free extracts during germination and early seedling growth, it is hypothesized that Pinaceae storage protein reserves are broken down by the concerted activity of aminopeptidases, endopeptidases and carboxypeptidases (Salmia and Mikola, 1975, 1976a, 1976b; Salmia *et al.*, 1978; Salmia, 1981; Pitel *et al.*, 1984; Gifford *et al.*, 1989; Gifford and Tolley, 1989; Kovac and Kregar, 1989). It should be noted that these peptidase activities have only been demonstrated using artificial substrates, and the site(s) of their activity have not been determined. The transport of peptides and free amino acids between the megagametophyte and developing seedling in the Pinaceae has yet to be demonstrated. In germinated barley seedlings the transport of small peptides from the endosperm to the scutellum of germinating barley seedlings has been demonstrated (Higgins and Payne, 1977; Saponen, 1979). In *Pinus*, it has been suggested that arginine released from storage proteins is transported as arginine (Guitton, 1964 as discussed by Cánovas *et al.*, 1998; Ramaiah *et al.*, 1971) to the cotyledons of the seedling (King and Gifford, 1997), where it is assimilated by the activity of arginase (King and Gifford, 1997). Arginase catalyzes the production of urea and ornithine from arginine and is an enzyme of the urea cycle (Thompson, 1980). Arginine transport without prior conversion to glutamine or asparagine, makes Pinaceae seeds different from most angiosperm seeds that store their

reserves in a living endosperm or in the cotyledons (Lea and Miflin, 1980; Bewley and Black, 1994). In these types of seeds, the majority of amino acids transported to or within the seedling are first converted to glutamine, as in castor bean endosperm (Stewart and Beevers, 1967) and pumpkin cotyledons (Chou and Splittstoesser, 1972), or asparagine, as in mung bean cotyledons (Kern and Chrispeels, 1978). Cell-free extract activities of alanine and aspartate aminotransferases increase during early seedling growth in megagametophytes and seedlings of *Pinus banksiana* (Pitel and Cheliak, 1988). In other seed systems, the amino group released by transaminase reactions with alanine and aspartate is shuttled into glutamate (Mazelis, 1980). Glutamine synthetase catalyzes the formation of glutamine from glutamate and ammonia (Lea and Joy, 1982). The activity of this enzyme increases in seedlings of *Pinus pinaster* during early seedling growth (Cánovas *et al.*, 1991); however glutamine synthetase activity in the megagametophyte has not been examined. Based on the high levels of glutamine and asparagine in free amino acid pools in the megagametophyte and seedling during the time of storage protein breakdown compared to the amino acid complement of the mature megagametophyte storage proteins, it is thought that some of the amino acids are converted to glutamine and asparagine in the megagametophyte prior to transport to the seedling (Ramaiah *et al.*, 1971; King and Gifford, 1997). In castor bean endosperm, specific amino acids such as aspartate, glutamate, alanine, glycine, serine and leucine are converted to sucrose which is then transported to the developing seedling (Stewart and Beevers, 1967). It is not presently known whether amino acids released in megagametophytes of germinated Pinaceae seeds undergo any similar conversions.

1.6.2 TAG reserves

During germination and early seedling growth in Pinaceae seeds, megagametophyte lipid reserves (Ching, 1966; Kao, 1973; Kovac and Vardjan, 1981; Groome *et al.*, 1991; Hammer and Murphy, 1994), are broken down and metabolized to provide carbon and energy for the growing seedling. It is hypothesized that free fatty acids are released from Pinaceae megagametophyte TAGs by lipases (Ching, 1968; Kovac and Wrischer, 1984; Hammer and Murphy, 1994). Glycerol is further catabolized to sugars in the cytosol and free fatty acids are catabolized in glyoxysomes by the β -oxidation pathway (Gifford, unpublished data) and the glyoxylate cycle to generate succinate (Firenzuoli *et al.*, 1968; Ching, 1970; Lopez-Perez *et al.*, 1974; Noland and Murphy, 1984; Pinzauti *et al.*, 1986; Mullen and Gifford, 1995a, 1995b, 1997). Succinate is transported to mitochondria where it enters Kreb's cycle and malate is produced. The malate is shuttled to the cytoplasm where it is converted via gluconeogenesis into carbohydrates that are transported to the seedling (Ching, 1966). It is presently unknown whether these metabolic pathways and cycles also occur in Pinaceae seedlings.

1.6.3 Structural studies of Pinaceae seeds during germination and early seedling growth

In addition to the biochemical information available for storage reserve metabolism in Pinaceae seeds, structural changes related to the breakdown of seed storage reserves have also been described. For the most part, these studies have focused on subcellular changes occurring in specific tissues. For example, in megagametophyte

cells of *Pinus sylvestris* (Simola, 1974a), *P. pinea* (Gori, 1979) and *Picea abies* (Simola, 1976) a decrease in protein vacuole and lipid body number occurs primarily after germination is completed. Correlated with this depletion of storage organelle contents in the megagametophyte cells is an increase in the number of microbodies, which are likely glyoxysomes. In contrast, a decrease in seedling protein vacuole and lipid body number begins during germination and progresses into early seedling growth in *Pinus banksiana* cotyledons (Durzan *et al.*, 1971), *P. sylvestris* cotyledons and radicles (Simola, 1974a), *Picea abies* cotyledons and radicles (Simola, 1974b, 1976), and *P. excelsa* cotyledons and hypocotyl (De Carli *et al.*, 1987). Both megagametophyte and seedling cell changes are accompanied by an increase in numbers of organelles such as endoplasmic reticulum, dictyosomes, mitochondria, and plastids.

Other studies have compared the relative timing of structural events in the different tissues of conifer seeds during germination and early seedling growth. For example, protein vacuole changes are initiated before lipid body changes in megagametophyte, radicle and cotyledon tissues in *Picea abies* (Simola, 1974b, 1976), *P. excelsa* (De Carli *et al.*, 1987) and *Pinus sylvestris* (Simola, 1974a). Protein vacuole hydrolysis is also more rapid in the radicle than in either the cotyledon or megagametophyte, for all three seeds. In *Araucaria araucana*, amyloplast and protein vacuole disappearance occurs first in the radicle, and later in the cotyledons and megagametophyte (Cardemil and Reinero, 1982).

In only a few studies have structural changes been correlated with biochemical changes that occur during germination and early seedling growth. In cotyledonary cells of *Pinus banksiana*, a decrease in the level of total buffer-soluble protein is correlated

with the occurrence of protein vacuole cavities (Durzan *et al.*, 1971). A decrease in amyloplast number in *Araucaria araucana* radicles during the first 12 h of germination correlates with the majority of seedling amylase activity being localized in the radicle (Cardemil and Reinerio, 1982). Amyloplast degradation in the hypocotyl and cotyledons occurs later, and correlates with the seedling's period of peak amylase activity, peak soluble carbohydrate level, and decrease in starch level. Megagametophytic amyloplasts are mobilized much slower than embryonic amyloplasts, and megagametophytes have lower amylase activities and soluble carbohydrate levels compared to seedlings. In *Picea excelsa* seedlings, the cotyledon region that has emerged from the megagametophyte contains highly vacuolated cells and highly differentiated chloroplasts, while the cotyledon region that still remains inside the megagametophyte contains less vacuolated cells with less differentiated chloroplasts. Associated with the more highly differentiated cotyledon region is a higher level of O₂ release and a higher level of chlorophyll *a* and *b* content (De Carli *et al.*, 1987).

1.7 The Current Study

It is apparent that only a limited number of studies on Pinaceae seeds during the critical periods of germination and early seedling growth have been published. Loblolly pine is one of many Pinaceae seeds for which no structural observations have been published during these periods. There is a need to understand the biology of loblolly pine during germination and early seedling growth, so that it can be related to biochemical information presently known about the seed. The most information can be learned from a subject if it is approached at a number of levels, using a variety of

techniques. For this reason a study of loblolly pine seed has been undertaken, that uses both structural techniques to understand the biology of the seed, and biochemical techniques to study the cycles and pathways involved in the nutrition of the seedling during germination and early seedling growth.

Throughout germination and early seedling growth the loblolly pine seedling is dependent on the megagametophyte for most of its nutrition and therefore maintains close contact with this storage tissue. This close contact not only facilitates the transport of metabolites from the megagametophyte to the seedling, but may also allow the seedling to send signals to the megagametophyte and vice-versa. Thus, any study of the seedling must also include an examination of the relationship between the seedling and the megagametophyte. The first part of my thesis will investigate some of the structural and enzymatic changes that occur as the seedling grows and develops to become photosynthetically independent. A second part, and the majority of my thesis, deals with the nutrition of the seedling from reserves in the seed. Using both biochemical and structural techniques I have examined the reserves stored in both the megagametophyte and seedling, and the fate of some of those reserves. The third part of my thesis will explore the dynamic relationship between the seedling and its megagametophyte.

2. Materials and Methods

2.1 Water quality and Chemicals

Distilled, deionized Milli-Q water (resistance 18 megohm.cm) from a Milli-Q Filtration Water System (Millipore Corporation, Bedford, MA, USA) was used for all aqueous solutions, unless otherwise stated.

Fine chemicals were purchased from Fisher Scientific (Nepean, ON), Sigma Chemical Co. (St. Louis, MO, USA), BDH (Toronto, ON), VWR (Mississauga, ON), Bio-Rad Laboratories Ltd. (Mississauga, ON), and Marivac Ltd. (Halifax, NS). Biological stains were purchased from Eastman Kodak Co. (Rochester, NY, USA), Fisher Scientific (Nepean, ON), Sigma Chemical Co. (St. Louis, MO, USA) and Matheson Coleman and Bell Manufacturing Chemists (Norwood, Ohio, USA). Bacto-agar for tissue culture was purchased from Difco Laboratories (Detroit, MI, USA). [2-¹⁴C]acetic acid, sodium salt and Aqueous Counting Scintillant was purchased from Amersham Canada Ltd. (Oakville, ON). Enzyme kits were purchased from Boehringer Mannheim Canada (Laval, PQ). Molecular weight markers for protein gel electrophoresis were purchased from Bio-Rad Laboratories Ltd. (Mississauga, ON).

2.2 Seed material

2.2.1 Stratification, germination and early seedling growth

Half-sibling loblolly pine seeds were a gift from Westvaco (Summerville, SC, USA; Clone 11-9, open pollinated and collected in the fall of 1992). All seeds were surface sterilized with Tween 20 (Bio-Rad) and 1% NaOCl according to Groome *et al.*

(1991). To break dormancy, seeds were placed between layers of moist sterile Kimpak (Seedburo Equipment Co., Chicago, IL, USA) for 35 days at 2°C (DAI₂) in complete darkness (Schneider and Gifford, 1994). Seeds were again surface sterilized with 1% NaOCl (Groome *et al.*, 1991), then transferred to freshly autoclaved Kimpak-lined germination trays. The trays were placed in a germinator (Controlled Environments Ltd., Winnipeg, MB) with continuous fluorescent light (19 $\mu\text{mol m}^{-2} \text{s}^{-1}$) at 30°C for up to 12 days. Germination was completed, as indicated by radicle emergence from the seed coat, 4 days after imbibition at 30°C (DAI₃₀). Early seedling growth is defined as the period after radicle emergence, but before the shedding of the megagametophyte. Seedling growth was staged according to radicle size classes, as described in Mullen *et al.* (1996). Embryo is the term used to describe the sporophyte at maturity and during the period of dormancy-breaking at 2°C (stratification). After the seeds were placed at 30°C, the sporophyte was termed a seedling.

2.2.1.1 Tissue collection for biochemical analyses

At different stages of development, harvested seed tissues were separated into megagametophytes and whole embryos/ seedlings. The embryos/ seedlings were kept intact, or were separated into hypocotyls and radicles (root poles), and cotyledons and epicotyls (shoot poles). For most biochemical and enzymatic analyses, 10 megagametophytes were collected per tissue replicate. Because of the seedling's growth during germination and early seedling growth, the number of seed parts collected per embryo/ seedling, shoot pole, and root pole replicate varied for different stages. Unless otherwise stated, mature to 5 DAI₃₀ sporophytic parts were collected in replicates of

twenty, 6 - 9 DAI₃₀ in replicates of ten, and 10 - 12 DAI₃₀ in replicates of five. Tissues were quick-frozen with liquid N₂ and stored at -75°C before biochemical analyses, unless otherwise stated.

2.2.2 Culture of isolated seed parts

Isolated intact embryos or megagametophyte halves from 35 DAI₂ seeds were cultured at 30°C for up to 10 days on 3% (w/v) Bacto-agar (Difco) containing 15 µg/mL rifampicin (Sigma) and 2.5 µg/mL amphotericin B (Sigma). Corresponding tissues from intact seeds cultured under the same conditions with the hard seed coat, thin papery layer, and nucellar cap removed were used as controls. After the appropriate number of days in culture, seed parts were quick-frozen with liquid N₂ and stored at -75°C.

2.2.3 Culture of isolated intact megagametophytes

Under sterile conditions, 9 DAI₃₀ megagametophytes were carefully removed from their seedlings. After removal of nucellar caps, the undamaged megagametophytes with their micropylar ends oriented upwards were partially embedded into 0.5% Bacto-agar, 15 µg/mL rifampicin, and 2.5 µg/mL amphotericin B for support. After 24 h in the 30°C germinator, the drop of liquid (exudate droplet) that had formed in each megagametophyte corrosion cavity was collected and pooled for the experiment. Megagametophytes isolated for 24 h were then collected. Nine DAI₃₀ megagametophytes cultured with seedlings (hard seed coat and papery layer removed) were used as a control for isolated megagametophytes. Invertase activity was analyzed from freshly collected pooled exudate and megagametophytes (section 2.5.2.1). Pooled

exudate (in 0.5 mL microfuge tubes) and megagametophytes were quick-frozen with liquid N₂ and stored at -75°C until analyzed for specific carbohydrates (section 2.4.3.2). Photographs of exudate droplets produced by isolated megagametophytes were taken with an M3 stereomicroscope (Wild Heerbrugg Ltd., Heerbrugg, Switzerland) with an MPS 51S photoautomat attachment (Wild Heerbrugg Ltd.).

2.3 Microscopy

2.3.1 Tissue Fixation Methods

2.3.1.1 Formalin-acetic acid-alcohol (FAA) fixation

The hard seed coat and thin papery layer were removed from mature desiccated seeds, leaving the nucellar cap attached to the megagametophyte. Longitudinal slices (~1 mm thick) through the nucellar cap, megagametophyte and embryo were fixed with formalin-acetic acid-alcohol according to the method of Jensen (1962), dehydrated with an ethanol series and embedded in paraffin. After paraffin blocks were softened in Gifford's solution 1 (Gifford, 1950) for seven days, 10 µm sections were cut with an 820 Spencer microtome (American Optical Corporation, Buffalo, NY, USA) and stained with methyl violet 2B (Eastman Kodak Co.) and erythrosin (Matheson Coleman and Bell Manufacturing Chemists) (Jensen, 1962) for observations of the mature seed structure. Photomicrographs were taken with a Stemi SV11 dissecting photomicroscope (Carl Zeiss, Oberkochen, West Germany) with an EOS Rebel X camera attachment (Canon Canada Inc., Calgary, AB).

2.3.1.2 Freeze-substitution fixation

After the removal of the hard seed coat, thin papery layer and nucellar cap, 1 - 2 mm thick sections through the seed were cut and fixed by freeze-substitution (Jensen, 1962). Because of their brittle nature, mature desiccated seeds were surface-sterilized and imbibed for 24 h at 2°C prior to integument removal and freeze substitution. The seed tissues were plunged into 12% methyl-cyclohexane (Matheson Coleman and Bell Manufacturing Chemists) in 2-methylbutane (Fisher) cooled by liquid nitrogen, then transferred to a vial containing 100% methanol previously cooled in a dry ice/ acetone bath. Sample vials were stored at -75°C for six days, and during this time the methanol was changed three times. After six days, the vials were slowly brought to room temperature over a period of three hours. Methanol was replaced with propylene oxide and specimens were embedded in Spurr's resin (Marivac) (Spurr, 1969). Sections were cut 1.5 µm thick with an OM U 2 ultramicrotome (C. Reichert Optische Werke A. G., Hernalser Hauptstr, Austria) using glass knives made with an 7800B knifemaker (LKB, Stockholm, Sweden). Sections were dried onto gelatin-coated slides (Jensen, 1962), then histochemically stained (section 2.4.2). Photographs were taken with a photomicroscope II (Carl Zeiss) with an MC 63 photomicrographic camera (Carl Zeiss), and a BX40 microscope (Olympus America Inc., Lake Success, NY USA) with a C-35DA-2 photomicrographic camera (Olympus America Inc.).

2.3.1.3 Glutaraldehyde-Osmium tetroxide (OsO₄) fixation

Small tissue pieces were fixed for two hours at room temperature with 4% glutaraldehyde (Marivac) in 0.1 M sodium cacodylate buffer (pH 7.2) (Marivac), 0.5 M sucrose (BDH). Tissues were then post-fixed with 2% OsO₄ (Marivac) in 0.1 M sodium cacodylate buffer (pH 7.2), 0.25 M sucrose for 1.5 - 4 h at room temperature for younger tissues or 4°C for older tissues. After dehydration in an ethanol series followed by a propylene oxide series, tissues were embedded in Spurr's resin (Marivac) (Spurr, 1969). Sections for light microscopy were cut as described for freeze-substituted material (section 2.3.1.2). For transmission electron microscopy (TEM), ultrathin sections of gold thickness were cut using an Ultracut E ultramicrotome (Reichert-Jung, Wien, Austria) equipped with a 45° diamond knife (Diatome Ltd., Bienne, Switzerland). Sections supported on 100 mesh copper grids (Marivac) were stained with 4% aqueous uranyl acetate (Marivac) for 1 h followed by lead citrate (Fisher) (Reynolds, 1963) for 2 min and examined with a Philips 201 transmission electron microscope at 60 kV.

2.3.2 Histochemical Stains

Water-insoluble carbohydrates were stained with a modification of Jensen's (1962) periodic acid-Schiff's (PAS) reaction. Freeze-substituted 1.5 µm sections were treated with 0.5% periodic acid (BDH) for 40 minutes and washed with running water for 10 minutes. Sections were then stained with Schiff's reagent (Fisher) for 3 h, washed with running water 10 min, mounted in water, and observed. Control sections were not incubated with periodic acid. Water-insoluble carbohydrates were stained pink.

Deparaffinized 10 μm tissue sections were stained for cellulose using the IKI- H_2SO_4 method of Johansen (1940). Cellulose was stained blue.

Whole seedlings with and without megagametophytes at different stages were investigated for the presence of xylem. The tissues were cleared and stained with basic fuchsin (Fisher) to show lignified elements using Method 1 of Fuchs (1963). Seedlings were lightly counter-stained with 0.1% fast green FCF (Fisher) in absolute ethanol, then mounted in Permount (Fisher). Lignified tissues were stained red. Root caps were removed before processing so that root interiors were not masked.

Proteins were visualized using a modification of the Aniline Blue Black method outlined by O'Brien and McCully (1981). 1.5 μm freeze-substituted sections were stained with Aniline Blue Black (Matheson Coleman and Bell Manufacturing Chemists) at 50°C for 10 minutes, washed with 7% acetic acid, dried with cold air, then mounted with glycerol in 7% acetic acid for observation. Aniline Blue Black was also used as a counter-stain for PAS stained sections. In both cases, protein was stained blue.

1.5 μm sections from glutaraldehyde- OsO_4 fixed tissues were stained with Sudan black B (Fisher), using the method of Bronner (1975). Sections were incubated for 1 h at 60°C in the saturated Sudan black B solution and then were destained for 1 min in 70% EtOH. Lipids were stained black. Freeze-substituted sections were used as controls.

2.4 Biochemical Analyses of Storage Reserves

All biochemical assays were measured with a DU-65 spectrophotometer (Beckman Instruments Inc., Fullerton, CA, USA).

2.4.1 Protein

2.4.1.1 Protein Quantification

Proteins were extracted from megagametophytes, whole seedlings, and shoot and root poles, using a modification of the method of Gifford *et al.* (1982). Tissue samples (section 2.2.1.1) were homogenized with a mortar and pestle with 1 mL of 0.05 M sodium phosphate buffer (pH 7.5) and centrifuged at 14,000 *g* for 20 min at 4°C. Supernatants contained the buffer-soluble protein fraction. The pellets were resuspended and washed three times with 1 mL of the phosphate buffer and were centrifuged at 14,000 *g* for 15 min at 4°C. Buffer-insoluble proteins contained in the pellets were solubilized by resuspending the pellets with 1 mL Laemmli buffer (Laemmli, 1970) and boiling for 5 min. After centrifuging at 20,000 *g* for 20 min at 22°C, the supernatant containing the buffer-insoluble proteins was retained. Proteins were quantified from each fraction using the method of Lowry *et al.* (1951), with bovine serum albumin (BSA) (Sigma) as standard.

To determine the protein content of mature seed tissues, ten megagametophytes were ground in a total of 5 mL of 0.05 M sodium phosphate buffer (pH 7.5), centrifuged at 20,000 *g* at 4°C for 20 minutes. The pooled supernatants were assayed for buffer-soluble proteins. The pellet was then re-extracted in a total of 7 mL of Laemmli buffer with 5 minutes of boiling and centrifuged at 20,000 *g* at room temperature for 20 minutes. Supernatants were pooled and assayed for buffer-insoluble proteins. A similar procedure was used to determine the protein content of 20 mature whole embryos, using 3 mL 0.05 M sodium phosphate buffer (pH 7.5), and 3 mL Laemmli buffer.

2.4.1.2 Protein Electrophoresis

SDS-PAGE and sample preparation were carried out as described by Laemmli (1970) using a mini-PROTEAN II electrophoresis system (Bio-Rad), with a 0.75 mm 12% slab gel at 200 V. Following electrophoresis, proteins were stained with Coomassie blue R (Sigma) (Burk *et al.*, 1983). Molecular mass markers included: phosphorylase b, 97.4 kDa; bovine serum albumin, 66.2 kDa; ovalbumin, 45 kDa; carbonic anhydrase, 31 kDa; soybean trypsin inhibitor, 21.5 kDa; and lysozyme, 14.4 kDa (Bio-Rad).

2.4.2 Triacylglycerol (TAG)

TAG was extracted from megagametophytes, whole seedlings, and shoot and root poles using a modification of the method of Feirer *et al.* (1989). All glassware used was acid-washed with Chromerge (Fisher) and thoroughly rinsed with distilled water to remove any lipid contaminants. Tissue samples (section 2.2.1.1) were homogenized with 1.25 mL isopropanol (anhydrous, Fisher HPLC grade). Samples were gently mixed for 15 min, centrifuged at 20,000 *g* for 15 min, and supernatants collected. The pellets were re-extracted once with 1.25 mL isopropanol, and the supernatants pooled. An 800 μ L aliquot of the pooled supernatant was added to test tubes containing 0.8 g alumina (Activity Grade I, Sigma) and 1.8 mL isopropanol. Tubes were capped, gently mixed for 15 min, and then centrifuged at 1,240 *g* for 20 min in a GLC-1 general laboratory centrifuge (Ivan Sorvall Inc., Norwalk, CT, USA). Free glycerol, monoacylglycerol, and diacylglycerol were trapped in the alumina, while TAG remained in the supernatant. The alumina pellet was washed twice with 2.6 mL isopropanol and all supernatants were pooled. The TAG concentration in the pooled supernatants was colorimetrically

determined by the method of Feirer *et al.* (1989). TAG was hydrolyzed with KOH, and the resulting glycerol was oxidized with sodium *m*-periodate (Fisher) to produce formaldehyde. After reaction with acetylacetone (Sigma) and ammonium acetate (Sigma), diacetyldihydrolutidine was produced and its absorbance was measured at 410 nm. Triolein (Sigma) was used as standard.

2.4.3 Carbohydrate

2.4.3.1 80% Ethanol-Soluble and -Insoluble Carbohydrate

The 80% ethanol-soluble and -insoluble carbohydrates were extracted from megagametophytes, whole seedlings, and shoot and root poles using a modification of the method of Joy *et al.* (1991). The tissue sample (section 2.2.1.1) was homogenized with 1 mL 80% (v/v) ethanol and gently mixed for 1 h. The homogenate was centrifuged at 20,000 g for 15 min at 22°C, and the supernatant collected. The pellet was re-extracted twice with 1 mL 80% ethanol and 15 min incubations. Pooled supernatants contained the 80% ethanol-soluble carbohydrates. The 80% ethanol-insoluble carbohydrates were extracted by suspending the above pellet in 1 mL cold H₂O and 1.5 mL 52% perchloric acid (Fisher), and incubating on ice for 20 min. After incubation, 2.5 mL cold H₂O was added to the sample prior to centrifugation at 17,400 g for 30 min at 4°C. The supernatant was collected and filtered through Whatman #1 filter paper. Pellets were re-extracted once by the same procedure and the supernatants pooled. Soluble and insoluble carbohydrates were determined spectrophotometrically using the phenol-sulfuric acid method of Dubois *et al.* (1956) as described by Joy *et al.* (1991); anhydrous D-glucose (BDH) was used as a standard.

2.4.3.2 Sucrose, D-glucose and D-fructose

Sucrose, D-glucose, and D-fructose were extracted from megagametophytes and seedlings. The tissue sample (section 2.2.1.1) was homogenized with 1 mL 100 mM HEPES (Sigma) buffer (pH 7.5), 3 mM magnesium acetate (Sigma) and 20 mg polyvinylpolypyrrolidone (PVPP) (Sigma). The sample was centrifuged at 14,000 *g* for 20 min at 4°C, and the supernatant collected. To 0.6 mL of pooled supernatant, 75 µL Carrez I solution (3.6% w/v $K_4Fe(CN)_6 \cdot 3 H_2O$) (Fisher), 75 µL Carrez II solution (7.2% w/v $ZnSO_4 \cdot 7 H_2O$) (Fisher) and 150 µL 0.1 M NaOH were added, vortexing after each addition. The resulting solution was centrifuged at 20,000 *g* for 20 min at 4°C and the supernatant collected. D-glucose in the presence of hexokinase and glucose-6-phosphate dehydrogenase activity resulted in the stoichiometric production of NADPH, measured using a Boehringer Mannheim kit (# 716 260). Sucrose was determined by the difference in D-glucose before and after sucrose hydrolysis by β -fructosidase (invertase). D-fructose was determined by the difference in D-glucose before and after addition of phosphoglucose isomerase.

2.4.3.3 Starch

Starch was extracted from megagametophyte (50 seed parts) and whole seedling (40 seed parts for 11 DAI₃₀, 80 seed parts for other stages) tissues by homogenization with 0.1 g PVPP (Sigma) and 10 mL 80% ethanol. The homogenate was centrifuged at 31,000 *g* for 20 min at 22°C and the supernatant was discarded. The pellet was washed twice with 10 mL 80% ethanol. The final pellet was allowed to air dry, and transferred to a 25 mL Erlenmeyer flask with 5 mL dimethyl sulfoxide (Fisher) and 1.25 mL 8 M

HCl. The flask was covered with Parafilm "M" (American National Can, Chicago, IL, USA) and incubated in a 60°C shaking water bath for 30 min. After cooling to 22°C, 1.25 mL 8 M NaOH and 15 mL 112 mM citrate buffer (pH 4.0) (citric acid (BDH)/sodium citrate (Fisher)) were added in order, stirring vigorously after each addition. After rinsing the flask with 2 mL of citrate buffer, the slurry was centrifuged at 31,000 *g* for 20 min at room temperature. The supernatant was filtered through Whatman #1 filter paper and made up to a final volume of 25 mL with citrate buffer. Native starch from this supernatant was quantified enzymatically using a Boehringer Mannheim kit (# 207 748) as follows: starch was hydrolyzed by amyloglucosidase to yield D-glucose units, and NADPH produced by the actions of hexokinase and glucose-6-phosphate dehydrogenase was measured at 340 nm. Starch was expressed in terms of D-glucose units.

2.5 Enzyme Activities

All enzyme assays were measured with a DU-65 spectrophotometer (Beckman Instruments Inc.).

2.5.1 Glycolate oxidase (Glycolate: oxygen oxidoreductase, EC 1.1.3.1)

Glycolate oxidase activity was examined in megagametophyte, and shoot and root pole tissues. Megagametophytes (150 - 300 mg FW) and shoot and root poles (50 - 150 mg) were collected (section 2.2.1.1). Tissue samples were homogenized with 1 mL 0.05 M sodium phosphate buffer (pH 7.5). The homogenates were centrifuged at 14,000 *g* for 20 minutes at 4°C. Supernatants were filtered through glass wool and

assayed for glycolate oxidase activity and buffer-soluble protein. Glycolate oxidase activity was assayed essentially by the method of Murray *et al.* (1973) by measuring the rate of production of glyoxylate phenylhydrazone at 324 nm after a 7.5 min lag period. The 100 mM Tris-HCl (Sigma) assay buffer (pH 7.8) was adjusted to pH 7.5 in order to obtain the highest glycolate oxidase activity for loblolly pine. Controls consisted of the assay mixture without addition of the substrate, glycolate (Sigma). One unit of glycolate oxidase activity was defined as that amount of enzyme that yielded 1 nmol of glyoxylate phenylhydrazone in 1 minute at 22°C. Protein was quantified using the method of Lowry *et al.* (1951) using BSA (Sigma) as standard.

2.5.2 Invertase (β -Fructofuranosidase, EC 3.2.1.26)

2.5.2.1 Invertase Extraction and Assay

Fresh megagametophytes and whole seedlings (section 2.2.1.1) were homogenized with 1 mL of extraction buffer (100mM HEPES buffer (pH 7.5) (Sigma), 3 mM magnesium acetate (Sigma)), 20 mg PVPP (Sigma), 5 μ L 1 M DTT (Sigma), and 10 μ L 10 mM PMSF (Sigma). Homogenates were centrifuged at 14,000 g for 20 min at 4°C. The supernatant was collected and 0.4 mL aliquots (or pooled exudate from section 2.2.3) were loaded onto 1 mL Bio-Gel P-6DG (Bio-Rad) spin columns, and centrifuged at 1,240 g to remove approximately 60% of the background carbohydrates. The spin-through fraction was collected for assay of soluble acidic and neutral invertases. The protein content was determined at this step using a Bio-Rad protein assay kit based on the method of Bradford (1976), using BSA (Sigma) as standard. The pellet was resuspended twice with 1 mL of extraction buffer, and 4 times with 1 mL of H₂O,

centrifuging after each extraction for 15 min at 4°C and discarding the supernatant washes. The washed pellet was resuspended with 1 mL of extraction buffer and used to assay for cell wall-associated invertases.

Invertase activity was determined by the production of reducing sugars from sucrose, using a modification of the method of Nelson (1944). D-glucose (BDH) was used as a standard. Nelson's alkaline copper reagent was made fresh daily by mixing Copper reagent A (2.5% NaCO₃ (anhydrous, BDH), 2.5% C₄H₄KNO₆·4H₂O (Sigma), 2% NaHCO₃ (BDH), 20% Na₂SO₄ (anhydrous, BDH) in H₂O) and Copper reagent B (15% CuSO₄·5H₂O (Fisher) in H₂O) in a 25:1 ratio (Nelson, 1944). Because of different pH optima, two different incubation buffers were used. For assay of soluble acidic and cell wall associated invertases, 100 mM sodium acetate (pH 4.25) (Fisher), 20 mM sucrose (BDH) was used. Neutral invertase activity was assayed with 100 mM sodium phosphate (pH 7.5), 20 mM sucrose. A maximum of 20 µL of sample was aliquoted into assay tubes, mixed with 180 µL of appropriate incubation buffer and incubated for 10 min at 37°C. After incubation, 1 mL of freshly prepared Nelson's alkaline copper reagent was mixed with each assay tube to stop invertase activity. A separate series of blanks were run for every sample, with the sample added to the copper reagent for immediate inactivation. Tubes were covered with marbles, and boiled for 20 minutes. After the tubes were cooled to 22°C, 1 mL of arsenomolybdate color reagent (Nelson, 1944) was added and mixed thoroughly, and incubated for 10 min. Assay tubes were centrifuged at 1,240 g for 4 min to precipitate denatured protein and other insoluble materials. Supernatants were collected and absorbances read at 525 nm.

2.5.2.2 Invertase pH Optima

The incubation buffer pH optima for invertases from buffer-soluble and insoluble extracts were determined using fresh 11 DAI₃₀ megagametophytes and seedlings. 100 mM sodium acetate, 20 mM sucrose was adjusted from pH 3.0 to 5.5 using acetic acid. 100 mM sodium phosphate, 20 mM sucrose was adjusted from pH 6.0 to 8.0 by varying the proportions of monobasic (BDH) and dibasic (Fisher) sodium phosphate.

2.6 Radiolabel experiments

In order to study the movement of carbohydrates from megagametophytes to seedlings, radiolabeling experiments were conducted.

2.6.1 Labeling Experiments

Seed coats and thin papery layers were removed from 10 DAI₃₀ seedlings with megagametophytes. Along the micropylar-chalazal axis, the megagametophyte is asymmetrical. It is thicker on one side of the axis, with the thickest portion in the centre. Using a razor blade, a small portion of the thickest area of the megagametophyte was cut and peeled. Five prepared megagametophytes with seedlings were placed in a 9 cm Petri dish lined with 9 cm diameter Whatman #1 filter paper wet with 1 mL of H₂O. To limit the possibility of radiolabel leaching out of the megagametophyte, treated megagametophytes were propped on 1.5 mL microfuge tube lids. A 2 µL (0.4 µCi) drop of [2-¹⁴C]acetic acid, sodium salt (Amersham) was carefully applied to the cut surface of each megagametophyte. Two Petri dishes without lids were placed on grids above 220 mL H₂O (to help maintain humidity) in larger culture trays. A separate uncovered

Petri dish containing 10 mL of 1 N NaOH was included in each culture tray to trap released $^{14}\text{CO}_2$. Sealed culture trays were placed in the 30°C seed germinator for a maximum of 120 min. Two replicate Petri dishes were used for each labeling time period. At the end of the label period, the megagametophytes with seedlings were removed and the megagametophytes were carefully washed with non-radioactive 3.6 mM sodium acetate (Fisher) so that the wash stream did not contact the junction between the megagametophyte and seedling.

2.6.2 Pulse-Chase Experiments

The 10 DAI₃₀ megagametophytes with seedlings were prepared as described in section 2.6.1. Cut megagametophyte surfaces were labeled for 30 min at 30°C, and megagametophytes were carefully washed with non-radioactive 3.6 mM sodium acetate, blotted dry, and placed on a new Petri dish identical to the labeling dish. A 2 µL drop of 3.6 mM sodium acetate was applied to each megagametophyte cut surface. Culture trays were incubated at 30°C for up to 4 h. After every hour during the chase period, a 2 µL drop of unlabeled sodium acetate was applied to the original chase drop. At the end of the chase period, cut surfaces of megagametophytes were blotted dry.

2.6.3 Tissue Processing

Megagametophytes and seedlings were homogenized separately with 1 mL 80% ethanol, centrifuged at 20,000 g at 22°C for 15 min, and supernatants collected. Supernatant aliquots of 10 µL were mixed with 10 mL Aqueous Counting Scintillant (Amersham) and counted 2 min for [^{14}C] in a LS 6000TA liquid scintillation counter

(Beckman Instruments Inc.) to determine the 80% ethanol-soluble radioactivity in each tissue sample. The remaining supernatant was placed into round bottomed glass flasks, dried under N_2 in a $40^\circ C$ water bath for 30 min. Dried samples were washed twice with 5 mL anhydrous ether (BDH) and the supernatants were discarded. Residual ether was removed with air, then samples were resuspended with 3 mL H_2O .

2.6.4 Separation into Basic, Neutral and Acidic Fractions

Separation of the water-soluble samples into different fractions was based on ion exchange chromatography. Columns (5 mL volume) of Dowex 50WX8-400 strongly acidic cation exchanger resin (Sigma) or Dowex 1X8-200 strongly basic anion exchanger resin (Sigma) were used. Resuspended samples in H_2O were loaded onto Dowex 50 columns, then 40 mL H_2O was applied to the column. Neutral and acidic fractions were collected in the eluant. The eluant was dried under N_2 in a $40^\circ C$ water bath. The basic fraction, bound to the Dowex 50 column, was eluted with 70 mL 1N HCl.

The neutral and acidic mixture was dissolved in 3 mL H_2O and loaded onto the Dowex 1 column, and 40 mL H_2O was added to the column. The neutral fraction collected in the eluant. The acidic fraction, bound to the Dowex 1 column, was eluted with 70 mL 1N HCl. The fraction radioactivity was determined by the addition of 1 mL aliquots with 10 mL of Aqueous Counting Scintillant (Amersham) and counting 2 min for [^{14}C] in a LS 6000TA liquid scintillation counter (Beckman Instruments Inc.).

3. Results¹

3.1 Structural changes related to the development of the seedling

3.1.1 Cellular organelles in mature, 35 DAI₂ and 12 DAI₃₀ seed tissues

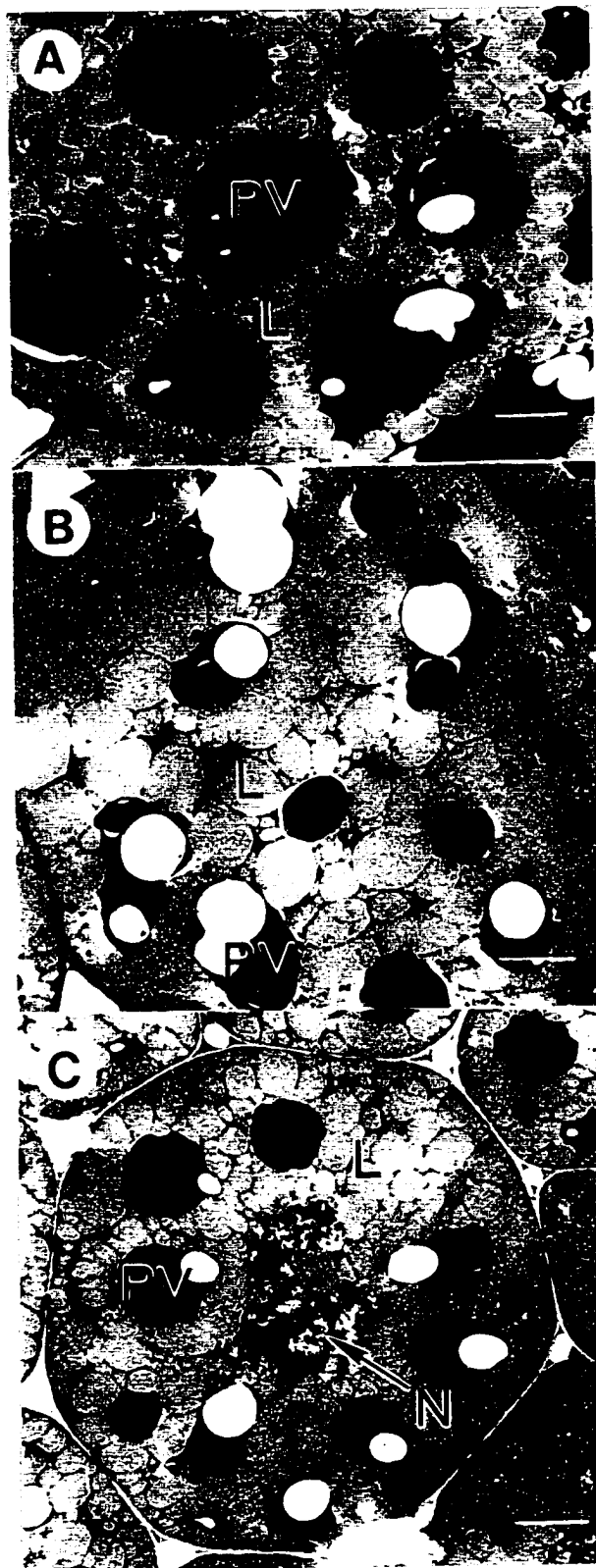
During the development of the Pinaceae seed, protein and TAG reserves were deposited in protein vacuoles and lipid bodies, respectively (Krasowski and Owens, 1993; Owens *et al.*, 1993). It was observed in mature, desiccated seeds and 35 DAI₂ seeds of loblolly pine, that these organelles filled the cytoplasm of nucleated storage parenchyma cells in megagametophytes (Fig. 4A), cotyledons (Fig. 4B) and hypocotyls (Fig. 4C). The appearance of these storage parenchyma cells was typical of other Pinaceae seeds (Durzan *et al.*, 1971; Simola, 1974a, 1976; Gori, 1979; De Carli *et al.*, 1987; Owens *et al.*, 1993).

At 12 DAI₃₀, protein vacuoles and lipid bodies in both the megagametophyte and seedling were reduced in number, and other organelles were observed (Figs. 5A-C). Protein vacuoles were much larger due to protein vacuole fusion, while the lipid bodies were similar in size to those in 35 DAI₂ seeds.

Megagametophyte cells at 12 DAI₃₀ still contained several lipid bodies as well as a few large protein vacuoles that contained electron-dense material, usually on the tonoplast membrane (Figs. 5A; 6A). The nucleus of the cell was relatively large (Fig. 6A). Single membrane bound microbodies, likely specialized peroxisomes called

¹ A version of this chapter has been published. Stone SL, DJ Gifford 1997 *Int J Plant Sci* 158: 727-737. Stone SL, DJ Gifford 1999 *Int J Plant Sci* (accepted).

Figure 4. Transmission electron micrographs of 35 DAI₂ seed material. Lipid body (L), protein vacuole (PV), nucleus (N). Bars = 3 μm. A) megagametophyte cell, B) cotyledon cell, C) hypocotyl cell.



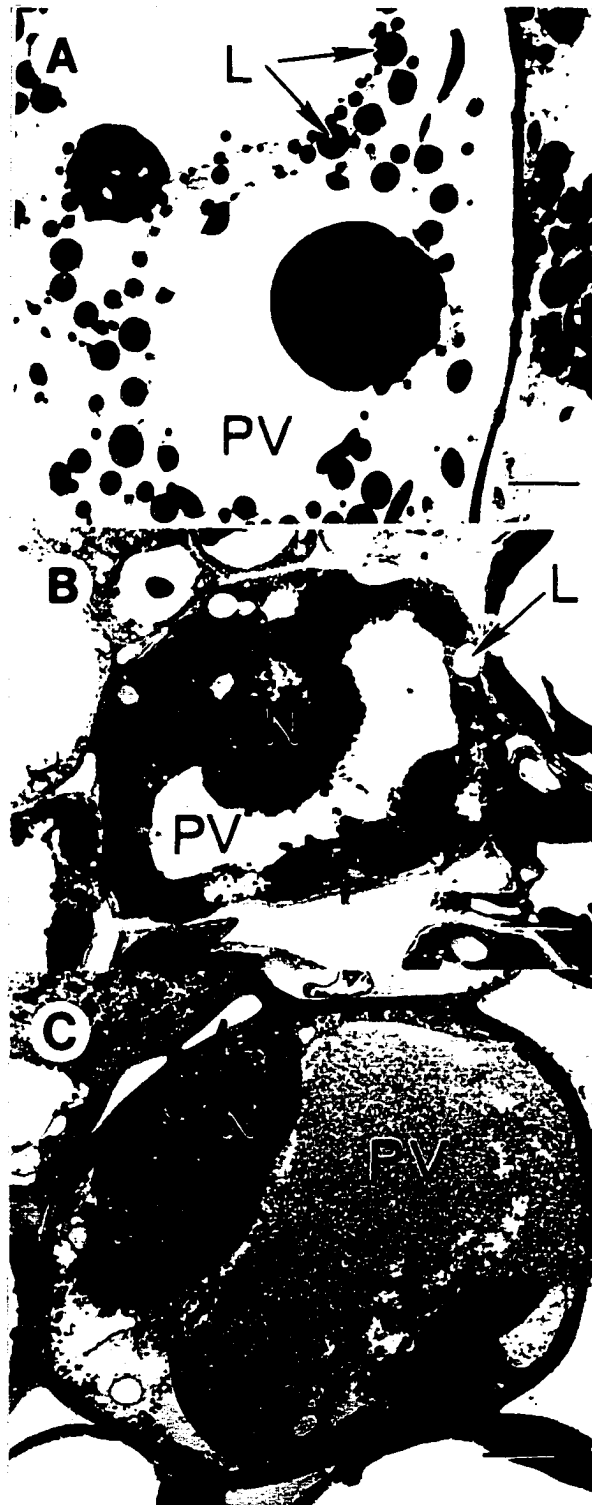


Figure 5. Transmission electron micrographs of 12 DAI₃₀ seed material. Lipid body (L), remnants of coalesced protein vacuoles (PV), nucleus (N). Bars = 3 μ m. A) megagametophyte cell B) cotyledon mesophyll cell C) hypocotyl cortical cell.

Figure 6. Transmission electron micrographs of 12 DAI₃₀ megagametophyte cell organelles.

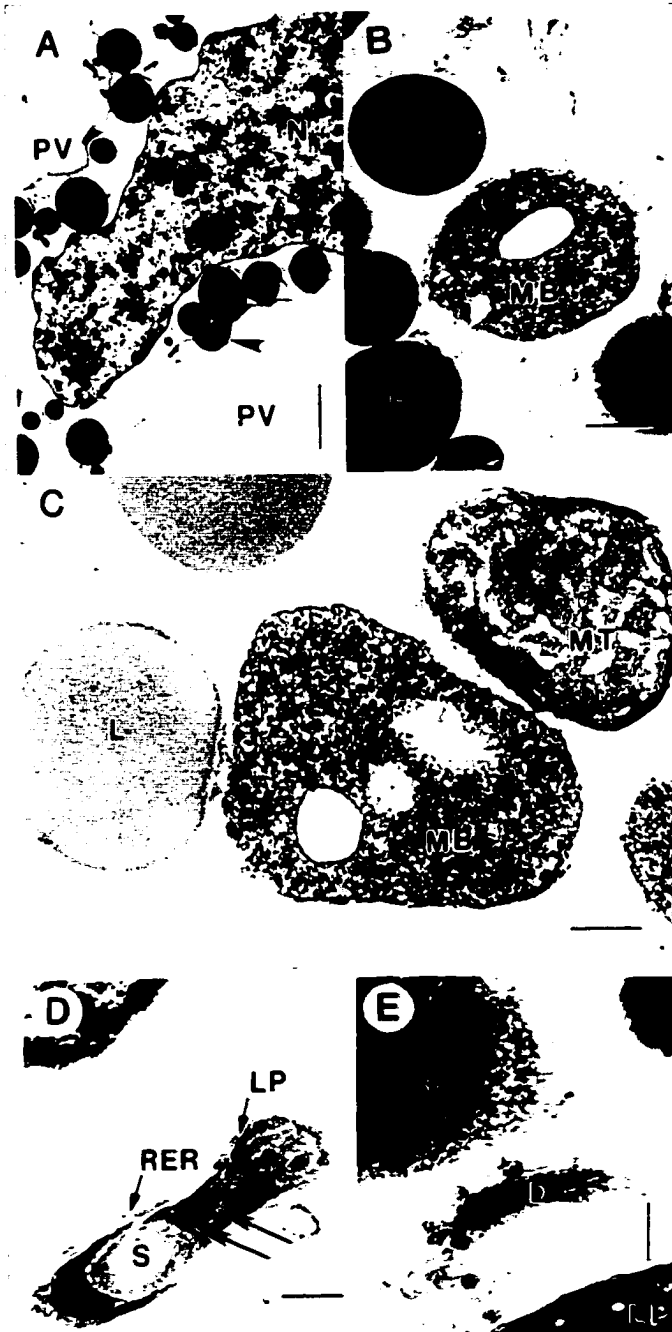
A) Lipid bodies (L)s in the cytoplasm between a portion of the nucleus (N) and portions of two large protein vacuoles (PV)s. Electron-dense deposit on tonoplast (arrowhead). Bar = 2 μ m.

B) A typical microbody (MB) containing a cytoplasmic inclusion. Bar = 500 nm.

C) A microbody in close contact with a lipid body and mitochondrion (MT). Bar = 300 nm.

D) A leucoplast (LP) containing plastoglobuli (arrows) and a starch grain (S). Rough endoplasmic reticulum (RER) was also observed. Bar = 300 nm.

E) A dictyosome (D) between a portion of a leucoplast and a portion of an unknown, non-membrane bound electron-dense sphere (*). Bar = 200 nm.



glyoxysomes, were prevalent in the cytoplasm. Microbodies were approximately 1.5 μm in diameter and were non-spherical, as they often appeared to have one or more cytoplasmic inclusions (Figs. 6B, C). Electron-dense crystals are often, but not always, present in peroxisomes (Gunning and Steer, 1975; Huang *et al.*, 1983); no crystals were observed in loblolly pine megagametophyte microbodies. These microbodies were often closely associated with lipid bodies and mitochondria (Fig. 6C). Dictyosomes were often observed (Fig. 6E). Small leucoplasts (approximately 2 μm in length) sometimes contained single starch grains as well as plastoglobuli (Fig. 6D) but had little internal membrane differentiation. Megagametophyte cell cytoplasm at this stage was not densely stained and little RER was observed (Fig. 6D). Occasionally electron-dense, granular non-membrane bound spheres of unknown origin varying in size from 1.5 - 5 μm in diameter, were observed in 12 DAI₃₀ megagametophyte cells (Fig. 6E).

Protein vacuoles in mature hypocotyl cortex cells often became single central vacuoles containing flocculent material, 12 DAI₃₀ (Fig. 5C). Lipid bodies were usually not observed at this stage. A large nucleus was present in each cell (Fig. 5C) and sometimes nuclear pores were observed on the nuclear envelope (Fig. 7C). In addition, chloroplasts were often present, usually in close association with mitochondria and microbodies (Fig. 7A). Chloroplasts (approximately 4-6 μm in length) contained thylakoid membranes as well as granular stroma and were larger than megagametophyte leucoplasts. Cristae were observed within mitochondria that were approximately 0.7 μm in diameter (Figs. 7A, B). Microbodies, likely specialized leaf-type peroxisomes, did not contain crystals. The shape of microbodies was not as convoluted as in the megagametophyte, as it was rare to find microbodies containing cytoplasmic inclusions.



Figure 7. Transmission electron micrographs of 12 DAI₃₀ seedling organelles.

A) Portion of a hypocotyl cortical cell showing a chloroplast (CP) in close association with a mitochondrion (MT) and microbody (MB) near the cell wall (*). Two large vacuoles (V) containing flocculent material are also present. Bar = 700 nm.

B) Portion of a hypocotyl cell showing a mitochondrion next to the vacuole and rough endoplasmic reticulum (RER). Bar = 200 nm.

C) Portion of a hypocotyl cell near plasma membrane. Vesicles secreted by rough endoplasmic reticulum and dictyosome (D) were observed (small arrows). Occasionally a vesicle was fused with the plasma membrane (arrowhead). A portion of the nucleus (N) with nuclear pores (hollow arrows) was also observed. Bar = 300 nm.

D) Portion of a cotyledon mesophyll cell with two amyloplasts (AP) containing many starch grains (S). The vacuole (V) does not contain any electron-dense material. Bar = 650 nm.

Dictyosomes were abundant, and were often observed, along with RER, secreting vesicles in the vicinity of the plasma membrane (Fig. 7C).

At 12 DAI₃₀, cotyledon mesophyll cells typically contained a large central vacuole with only minor amounts of electron dense deposits at the edge of the tonoplast (Fig. 5B). Unlike the hypocotyl cells, a few lipid bodies were observed within each cell. The vacuole surrounded a central nucleus that contained heterochromatin. Similar to the hypocotyl, the cytoplasm around the edge of the cells usually contained chloroplasts (Fig. 5B), microbodies, and mitochondria. In some mesophyll cells, amyloplasts were observed storing several starch grains (Fig. 7D).

3.1.2 Xylem formation in the developing seedling

Lignified xylem elements were first observed in the seedling 5 DAI₃₀ (Fig. 8A) in the cotyledons and hypocotyl. At this stage, the tracheids stained lightly for lignin. Each cotyledon contained a single xylem trace. Typically the tracheids from two cotyledons anastomosed, forming a single tracheid bundle at the junction of the hypocotyl and cotyledons. Although tracheids were also observed in the hypocotyl close to the radicle, they did not stain for lignin, and thus were not fully differentiated. Lignified tracheids formed a continuous connection between the cotyledons and radicle, 6 DAI₃₀. As the seedling continued to grow and develop, additional tracheids (Fig. 8C) developed in association with the pre-existing xylem bundles (Fig. 8B). All tracheids observed had helical wall thickenings (Fig. 8C).

Figure 8A-C. Light micrographs of lignified tracheids in whole seedlings stained with basic fuchsin.

A) Portion of the cotyledons (COT) and hypocotyl (HYP) of a 5 DAI₃₀ seedling. Bar = 200 μ m.

B) Cotyledons and a portion of the hypocotyl of an 11 DAI₃₀ seedling. Bar = 4 mm.

C) A bundle of tracheids from a 7 DAI₃₀ seedling hypocotyl. Bar = 30 μ m.

Figure 8D-H. Light micrographs of stomatal complex development in seedlings during germination and early seedling growth.

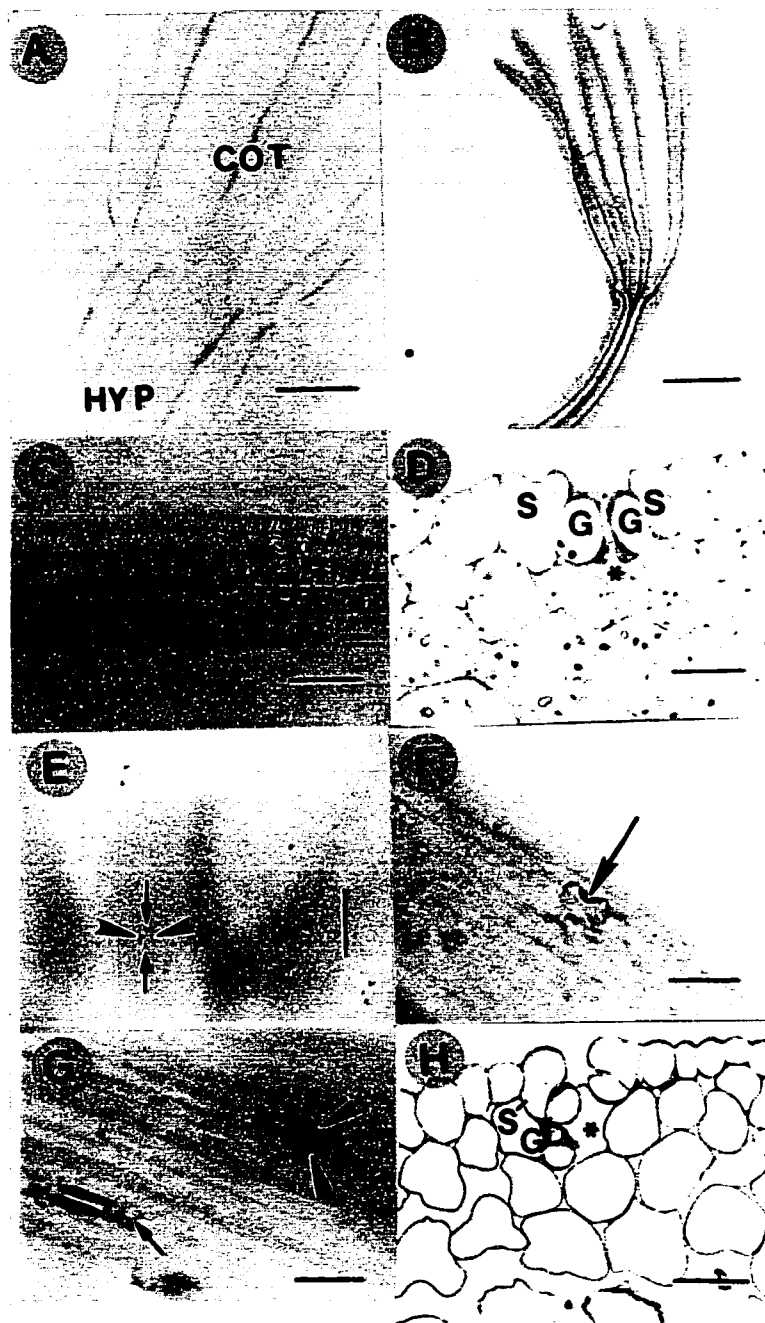
D) Transverse section through a 4 DAI₃₀ hypocotyl stomatal complex stained for water-insoluble carbohydrate with PAS. Notice the cell wall thickenings of the guard cells (G)s. A small substomatal chamber (*) is present beneath the stomatal aperture. Subsidiary cells (S)s next to the guard cells. Bar = 20 μ m.

E) The junction between the cotyledons and hypocotyl of a 6 DAI₃₀ whole seedling stained for lignin with basic fuchsin. The two guard cells are lignified at the ends of their longitudinal axes (small arrows) as well as along their longitudinal axes (arrowheads). Anastomosing tracheids are out of focus in the background. Bar = 100 μ m.

F) A single raised stomatal complex on the 7 DAI₃₀ whole seedling hypocotyl stained with basic fuchsin. Stomatal aperture (large arrow). Bar = 50 μ m.

G) Stomatal complexes on 11 DAI₃₀ basic fuchsin stained seedling hypocotyl. Lignified ends of guard cells (small arrow). Relatively large areas of the guard cells along their longitudinal axes are stained for lignin (arrowheads). Bar = 50 μ m.

H) Transverse section through a 12 DAI₃₀ hypocotyl stomatal complex stained with PAS. Guard cell (G) walls are thickened around the stoma aperture and next to the subsidiary cells (S)s. A substomatal chamber (*) is present beneath the stomatal aperture. Bar = 30 μ m.



3.1.3 Stomatal complex formation in the developing seedling

Stomatal complexes were first observed on seedling hypocotyls 4 DAI₃₀, while this tissue remained inside the megagametophyte (Fig. 8D). The stomatal complex was composed of two guard cells and at least two subsidiary cells parallel to the longitudinal axes of the guard cells. Guard cells at this stage contained cell wall thickenings except next to the subsidiary cells. The wall thickenings were not observed in 4 DAI₃₀ whole seedlings stained for lignin. A small substomatal chamber had formed by this stage. At 6 DAI₃₀, only 6-8 mm of the root and hypocotyl had emerged from the seed coat, yet stomatal complexes with lignin stained areas were observed on cotyledons and at the cotyledon/ hypocotyl junction (Fig. 8E), in addition to the hypocotyl. Observations of the cellular organization of the stomatal complex was difficult with basic fuchsin stained material, since the non-lignified cell walls of the subsidiary cells were not easily visible. Only two subsidiary cells were observed along the longitudinal axis of the stomatal complex in whole mounts of loblolly pine hypocotyls. However it has been observed by Florin (1951; Florin 1931 as described by Foster and Gifford, 1959) that Pinaceae guard cells are usually bordered by four subsidiary cells. Two subsidiary cells neighbor the guard cells parallel to their longitudinal axes and two subsidiary cells neighbor the guard cells where their ends meet. Further investigations using epidermal peels are necessary to see if this is also the case for loblolly pine. However, the two guard cells appeared to be lignified where they met at the ends of their longitudinal axes (Figs. 8E) as well as along their longitudinal axes, bordering the stomatal aperture (Fig. 8E). The lignified area of the guard cells around the stomatal aperture stained more intensely as the cells of the stomatal complex elongated during early seedling growth (Fig. 8G). At 7 DAI₃₀

stomatal complexes were observed in rows along the longitudinal axis of the hypocotyl, and were raised in profile (Fig. 8F), possibly due to the further development and expansion of the subsidiary cells. By 12 DAI₃₀, the stomatal aperture was slightly sunken due to the expansion of the subsidiary cells over the guard cells in both the hypocotyl (Figs. 8H; 25C) and cotyledons (Fig. 25B). At this stage the thickened guard cell walls were easily observed. It was difficult to clearly differentiate guard cell walls from subsidiary cell walls where they met and it is possible that the subsidiary cell walls may also be thickened. Use of the TEM may be necessary to visually separate the walls. A light microscopic study using paraffin sectioned material and a lignin specific stain such as phloroglucinin will be necessary to identify the exact location of the lignin areas.

3.1.4 Greening of the seedling

Loblolly pine embryos were pale yellow to white at maturity. The seedling turned a pale green in the hypocotyl region at 3 DAI₃₀. At 5 DAI₃₀, the base of the cotyledons began to green, and the hypocotyl was a red/purple color, probably due to the production of anthocyanins. The cotyledons were completely green by 8 DAI₃₀. The cotyledons remained pale green while inside the megagametophyte, and became darker green after emergence.

3.1.5 Glycolate oxidase (GO) activity

Glycolate oxidase (GO) is localized to the peroxisome, and is a key enzyme of photorespiration (Huang *et al.*, 1983). Its activity was measured in cell-free extracts of seedling shoot and root poles (Figs. 9A, B) and megagametophytes (Figs. 10A, B)

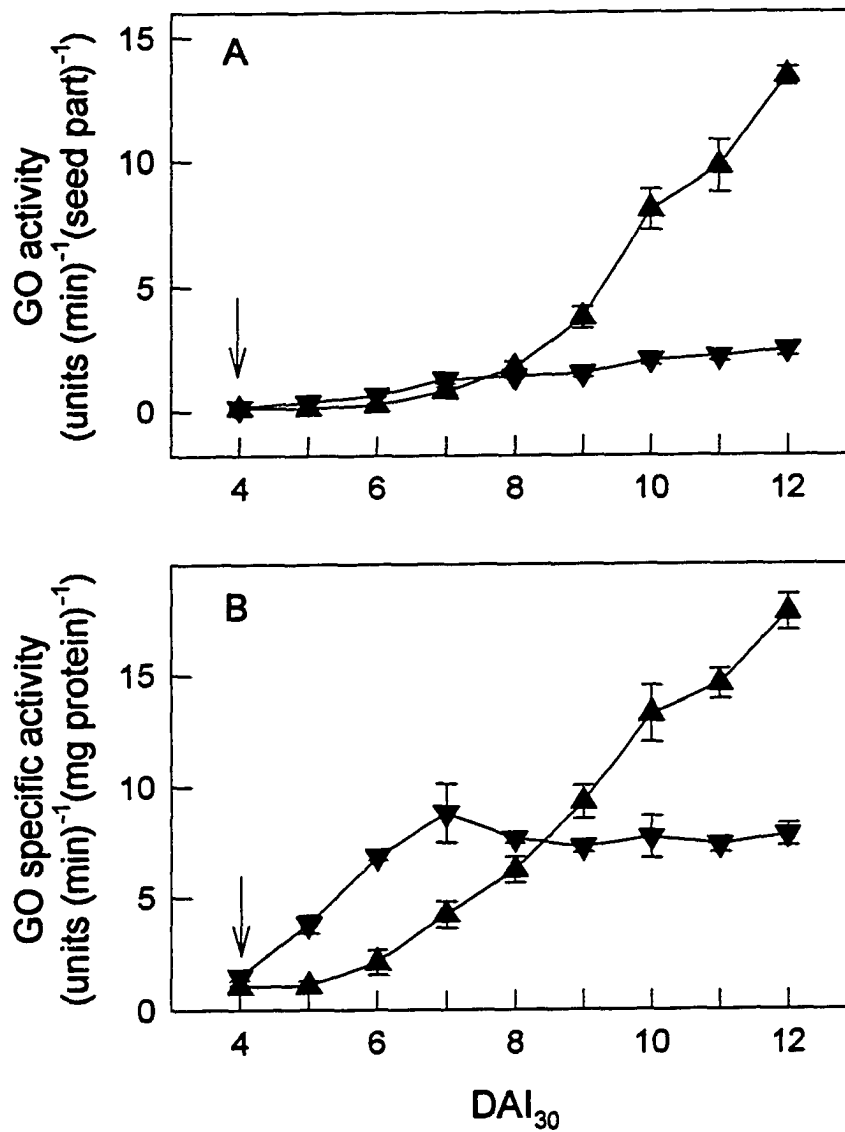


Figure 9. Glycolate oxidase activity in seedling shoot (▲) and root (▼) poles following imbibition at 30°C. A) Activity per seed part. B) Specific activity. Arrow indicates the completion of germination by radicle emergence from the seed coat. Each data point is the mean of three biological replicates each assayed in triplicate \pm SE of the mean.

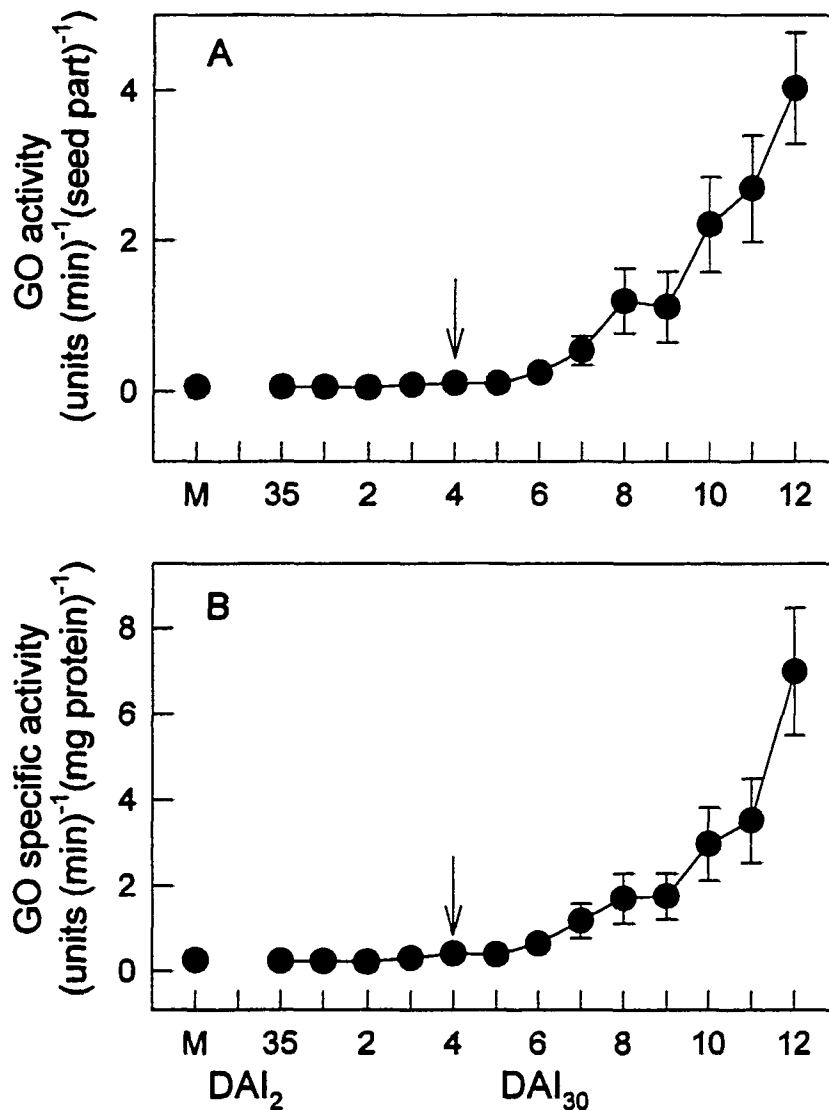


Figure 10. Glycolate oxidase activity in megagametophytes following imbibition. A) Activity per seed part. B) Specific activity. X-axis shows mature seed (M), fully stratified seed (35 DAI₂), and seed imbibed for up to 12 DAI₃₀. Arrow indicates the completion of germination by radicle emergence from the seed coat. Each data point is the mean of three biological replicates each assayed in triplicate \pm SE of the mean.

during germination and early seedling growth. After the completion of germination at 4 DAI₃₀, GO activity was low in both the seedling shoot and root poles (Figs. 9A, B). Correlated with emergence of the radicle and hypocotyl from the megagametophyte and seed coat, root pole GO specific activity increased between 4 and 7 DAI₃₀, then remained constant (Fig. 9B), although no increase in GO activity was measured on a per seed part basis (Fig. 9A). Shoot pole GO specific activity began to rise following 6 DAI₃₀, and continued to rise until 12 DAI₃₀ (Fig. 9B). An increase in shoot pole GO activity per seed part was observed following 8 DAI₃₀ (Fig. 9A).

GO activity was also observed in the non-photosynthetic megagametophyte during early seedling growth (Figs. 10A, B). GO activity per seed part increased following 7 DAI₃₀, and continued to increase to 12 DAI₃₀ (Fig. 10A). GO specific activity increased following 9 DAI₃₀, with the largest increase occurring between 11 and 12 DAI₃₀ (Fig. 10B). Although GO specific activity was relatively high in megagametophytes, its maximum level was only 27% of that found in whole seedlings.

3.2 Nutrition of the seedling from reserves laid down during seed development

Storage TAGs and proteins laid down during the development of loblolly pine seeds are thought to be the primary source of carbon, nitrogen and energy for developing seedlings during germination and early seedling growth (Misra, 1994). For this reason, the timing of storage organelle changes, as well as changes in the levels of storage reserves and their metabolites were investigated.

3.2.1 The fate of stored protein reserves during germination and early seedling growth

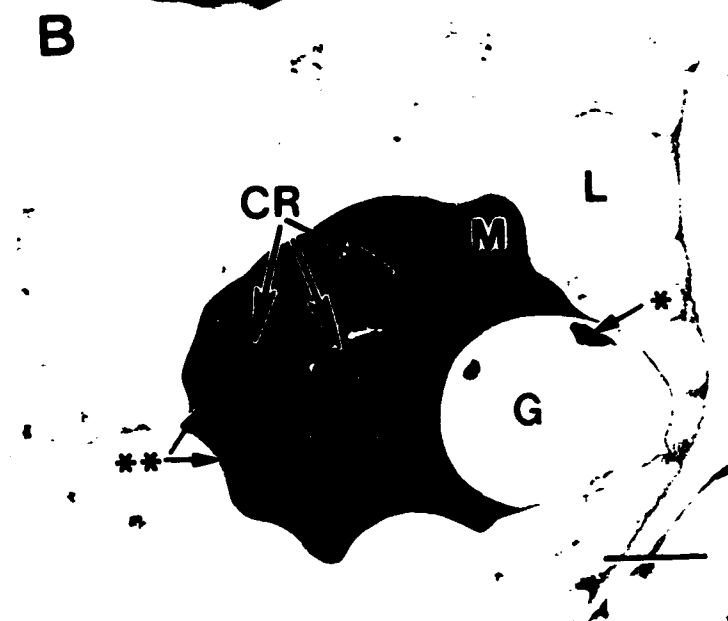
3.2.1.2 Protein vacuole structure

Although protein vacuoles varied in size within each tissue, they were typically larger in the megagametophyte than in the embryo of 35 DAI₂ seeds (Figs. 4A, B, C; 12A); this was also observed in *Picea glauca* (Krasowski and Owens, 1993), *Pseudotsuga menziesii* (Owens *et al.*, 1993), *Pinus sylvestris* (Simola, 1974a). Despite their size difference, protein vacuoles in the megagametophyte and embryo were similar in general structure. In both tissues protein vacuoles contained at least one prominent protein crystalloid embedded in a protein matrix (Figs. 11A, B). However, in the megagametophyte there usually was only one protein crystalloid observed (Fig. 11A), while two to three small protein crystalloids per protein vacuole were typically observed in both the cotyledon (Fig. 11B) and hypocotyl. Multiple protein crystalloids have also been noted in mature cotyledon protein vacuoles of *Pinus banksiana* (Durzan *et al.*, 1971), and in mature megagametophytes of *Picea glauca* (Misra and Green, 1990) and *Pseudotsuga menziesii* (Green *et al.*, 1991). Striations in megagametophyte protein crystalloids were artifacts caused by tissue compression during sectioning (Fig. 11A). It was unknown whether the uneven staining of the megagametophyte protein crystalloid represented different types of storage proteins, or was an artifact due to fixation or staining. Protein vacuoles in both the megagametophyte and embryo usually contained one or two electron-translucent globoids (Figs. 11A, B), as has been observed for *Pinus banksiana* (Durzan *et al.*, 1971), *P. sylvestris* (Simola, 1974a), *Picea excelsa* (De Carli

Figure 11. Transmission electron micrographs of protein vacuole structure in 35 DAI₂ seed tissues. Protein vacuoles contain one or more protein crystalloids (CR)s embedded in a protein matrix (M). One or more globoids (G)s, sometimes containing electron-dense globoid crystals (*), were also embedded in the protein matrix. Lipid bodies (L)s surrounded the protein vacuoles. Bars = 1 μm.

A) A small protein vacuole from a megagametophyte cell. The folded appearance of the single large protein crystalloid was an artifact caused by sectioning. It is unknown whether the dark areas within the protein crystalloid are different from the light areas, or if they are also an artifact.

B) Protein vacuole from a cotyledon cell. In addition to the globoid crystals sometimes seen in the globoid, smaller electron-dense globoid crystal deposits () were also observed outside the globoid, in the protein matrix.**



et al., 1987), *P. glauca* (Misra and Green, 1990) and *Pseudotsuga menziesii* (Green *et al.*, 1991; Owens *et al.*, 1993). The cotyledon protein vacuoles (Fig. 4B) typically contained larger globoids than hypocotyl protein vacuoles (Fig. 4C). Infrequently, electron-dense globoid crystals were observed within a globoid (Fig. 11B). Smaller electron-dense globoid crystals were often observed in the protein matrix of embryonic protein vacuoles (Fig. 11B), but were not observed in the megagametophyte protein vacuoles. The surface contour of the protein vacuoles in both the megagametophyte and embryo was determined by the lipid bodies surrounding them.

3.2.1.3 Megagametophyte protein vacuole distribution and changes during germination and early seedling growth

Protein vacuoles were observed in all megagametophyte cells in mature and 35 DAI₂ seeds. At the light microscope level, tissues of mature desiccated and fully stratified seeds were very similar in appearance. For descriptive purposes, the megagametophyte was divided into three regions; an inner, a middle and an outer region (Fig. 12A). The inner region, proximate to the corrosion cavity, varied between one and three cells in thickness (Fig. 12B). Cells in this region often contained incomplete cell walls, were sometimes polynucleate, and appeared flattened or squashed in transverse section. Projecting into the corrosion cavity from the inner region was a carbohydrate-positive layer of variable thickness (Fig. 12B). In the mature desiccated seed, this layer appeared to be composed of several flaky sheets, while in the stratified seed it was more mucilaginous and malleable. In most areas of the stratified seed, the hydrated carbohydrate-layer filled much of the corrosion cavity space between the embryo and

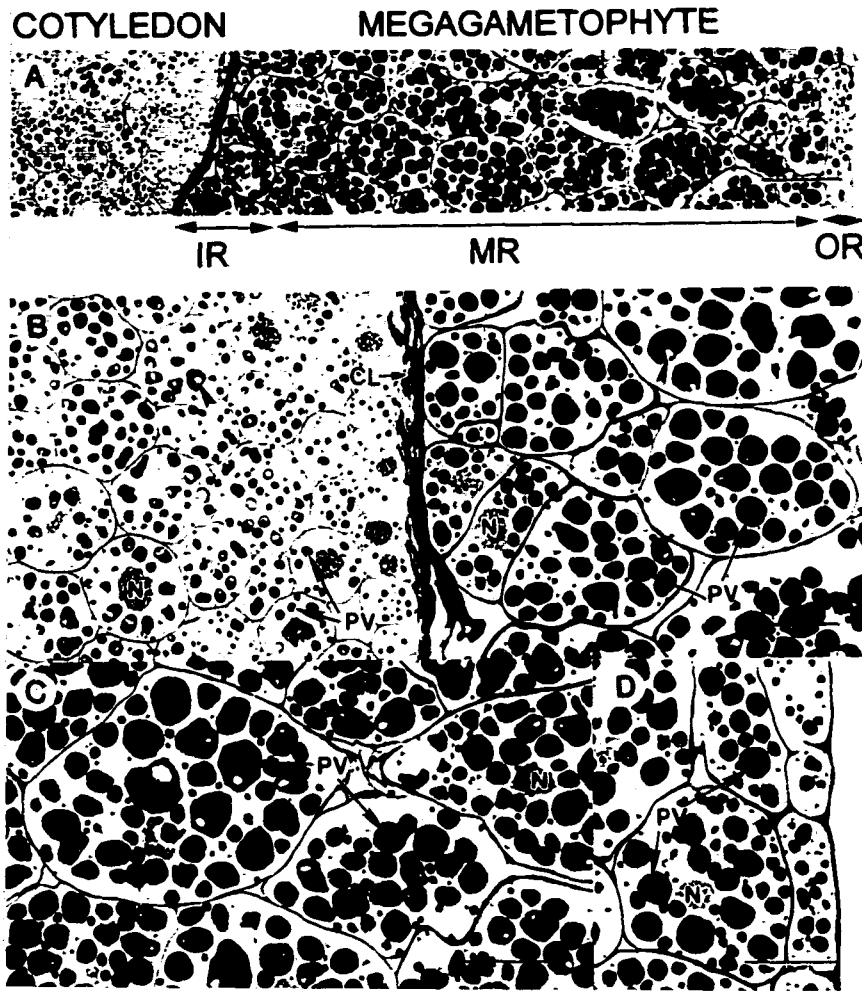


Figure 12. Light micrographs of PAS and Aniline Blue Black stained transverse sections through a plastic embedded 35 DAI₂ stratified seed, showing three different regions of the megagametophyte. Protein vacuoles (PV), globoids (arrowheads), nucleus (N).

A) Overview of the megagametophyte in relation to the cotyledons.

Bi-directional arrows indicate three different regions examined. Inner region (IR), middle region (MR), outer region (OR). Bar = 60 μ m.

B) Enlarged view of the megagametophyte inner region consisting of one to three layers of cells next to the carbohydrate-positive layer (CL). A portion of the middle region is also shown. A cotyledon is closely appressed to the carbohydrate-positive layer, so the corrosion cavity that is normally present between the cotyledon and the carbohydrate-positive layer is difficult to see. Bar = 30 μ m.

C) Enlarged view of the centre of the middle region. Cells are large and contain numerous protein vacuoles. Bar = 30 μ m.

D) Enlarged view of the outer region consisting of a single layer of epidermal-type cells, next to the middle region. Bar = 30 μ m.

megagametophyte. The middle region contained cells that were larger than those of the inner region; cells of the middle region had many intercellular spaces (Fig. 12C). The outer region was comprised of a single layer of epidermal-type cells. These were smaller than those of the inner region, were flattened, and had no intercellular spaces (Fig. 12D). The cells of the middle region comprised the majority of the megagametophyte tissue. It was in this region of the megagametophyte that the majority of protein vacuoles were located.

Megagametophyte cells from mature and stratified seeds contained irregularly shaped nuclei and angular protein vacuoles of various sizes (Figs. 12B-D). Protein vacuoles containing globoids were distributed throughout the megagametophyte, and were most often observed in the middle region (Figs. 12B, C). During germination, nuclei became smooth in shape and often took on an amoeboid appearance. Nucleoli were often observed. Apart from changes in nuclei, the appearance of the megagametophyte cells remained the same, at the light microscope level, until germination was completed at 4 DAI₃₀.

Changes in the appearance of the inner region megagametophyte cells were noted at 5 DAI₃₀, when the inner megagametophyte cells next to the carbohydrate-positive layer began to swell and the number of protein vacuoles in these cells declined (Fig. 13A). By 6 DAI₃₀, some of the innermost megagametophyte cells contained no visible protein vacuoles, while others contained only a few (Fig. 13B). Protein vacuole changes continued in the inner megagametophyte region (Fig. 13C), and large vacuoles, empty of protein, were present at 12 DAI₃₀ (Fig. 13D). The cells of the middle region of the megagametophyte at 6 DAI₃₀ (Fig. 14A) appeared very similar to the same region

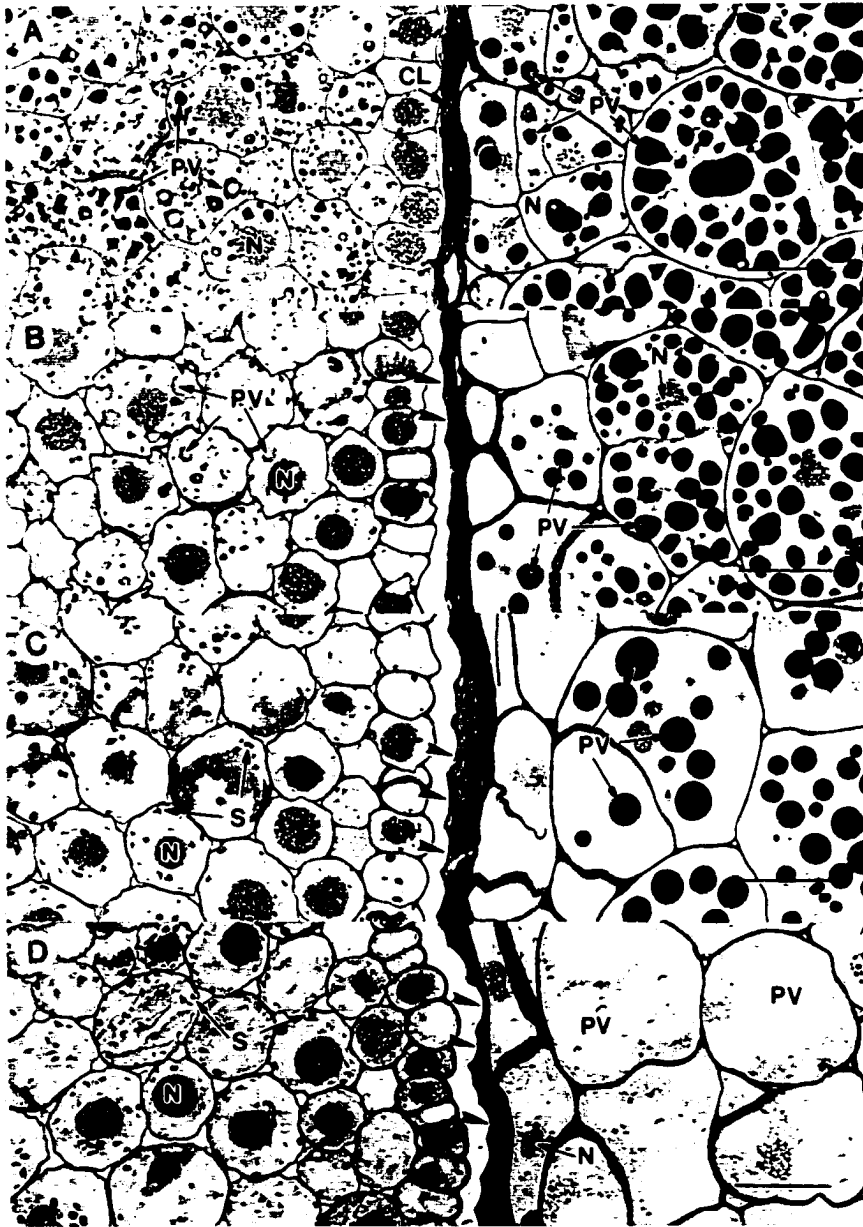
Figure 13. Light micrographs of PAS and Aniline Blue Black stained transverse sections through seeds in the area of a cotyledon (left side of the figure) and megagametophyte (right side of figure) during imbibition at 30°C. Cotyledon epidermal cell imprints (arrowheads) visible in carbohydrate-positive layer (CL). Nucleus (N), protein vacuole (PV). Bars = 30 μm.

A) Megagametophyte inner region cells 5 DAI₃₀ beginning to swell. Protein vacuoles in this region undergoing protein depletion. Protein vacuoles in the developing mesophyll of the cotyledon also are undergoing protein depletion.

B) Inner megagametophyte cells 6 DAI₃₀ swelling further. Protein vacuoles in the cotyledon are depleted of most of their protein.

C) Very few protein vacuoles left in the inner megagametophyte region 10 DAI₃₀. Starch grains (S) visible in cotyledon cells.

D) Inner region cells 12 DAI₃₀ contain protein vacuoles depleted of protein.



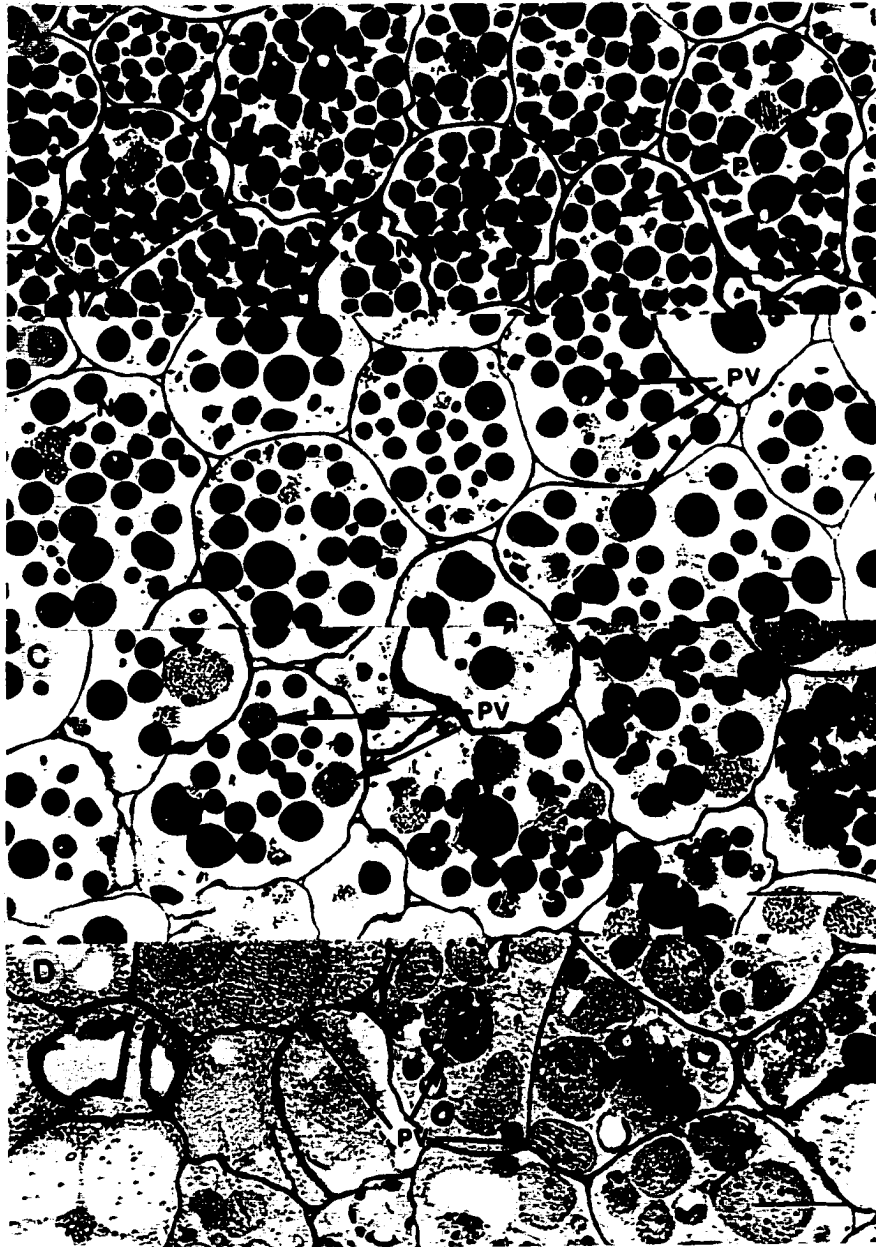


Figure 14. Light micrographs of PAS and Aniline Blue Black stained transverse sections through the centre of the megagametophyte middle region during imbibition at 30°C. Micrographs are oriented so the inner region is off to the left, and the outer layer is off to the right. Nucleus (N), protein vacuole (PV). Bars = 30 μm .

A) Middle region cells 6 DAI₃₀ contain numerous protein vacuoles.

B) Protein vacuoles 9 DAI₃₀ are larger and more variable in appearance than in the 6 DAI₃₀ cells.

C) Protein vacuoles 11 DAI₃₀ are fewer in number and variable in appearance.

D) Most of the protein vacuoles have been depleted of protein 12 DAI₃₀.

35 DAI₂ (Fig. 12A). However, by 9 DAI₃₀ changes had occurred (Fig. 14B). Protein vacuoles were less numerous, less angular, and more heterogeneous in appearance. By 11 DAI₃₀ (Fig. 14C), protein vacuole appearance was variable. By 12 DAI₃₀ the majority of the protein containing protein vacuoles were observed in the outer half of the megagametophyte middle region (Fig. 14D). Separate from the wave-like pattern of changes occurring in the inner and middle regions, which has also been described in *Picea excelsa* (De Carli *et al.*, 1987), protein vacuole changes were also noted in the megagametophyte outer region at 6 DAI₃₀ (Fig. 15A). At this time protein vacuoles were difficult to observe. The loss of protein from protein vacuoles continued through 9 DAI₃₀ (Fig. 15B) and by 12 DAI₃₀ protein in the outer region protein vacuoles was not observed (Fig. 15C).

3.2.1.4 Embryo/ seedling cotyledon and hypocotyl protein vacuole distribution and changes during germination and early seedling growth

All cells of the cotyledon and hypocotyl regions of the mature or stratified seed embryo contained protein vacuoles (Figs. 16A, B, E). However, the change in appearance of protein vacuoles within these regions varied following imbibition at 30°C. In the procambial ring and in the developing epidermis of the hypocotyl the protein vacuoles were depleted of protein by 4 DAI₃₀ (Fig. 16C). By 5 DAI₃₀, the protein vacuoles of the developing pith and cortex of the hypocotyl were also depleted of protein (Fig. 16D). In the cotyledons, protein vacuoles of the procambium and developing epidermis were depleted of protein by 4 DAI₃₀ (Fig. 16F). In contrast, a decrease in protein content of protein vacuoles of the developing mesophyll was not noticeable until



Figure 15. Light micrographs of PAS and Aniline Blue Black stained transverse sections through the megagametophyte showing the single cell layer of the outer region, and part of the middle region, during imbibition at 30°C. Nucleus (N), protein vacuole (PV). Bars = 20 μ m.

- A) Outer region protein vacuoles 6 DAI₃₀ undergoing protein depletion. No change in middle region protein vacuoles.
- B) Protein vacuoles 9 DAI₃₀ are larger and variable in appearance in the middle region cells close to the outer region.
- C) Middle region cells 12 DAI₃₀ contain very large protein vacuoles with very little protein.

Figure 16A-D. Light micrographs of PAS and Aniline Blue Black stained transverse sections through plastic-embedded hypocotyl (HYP) with surrounding megagametophyte during imbibition at 30°C. Developing epidermis (EP), developing cortex (CX), procambium (PC), developing pith (PI), protein vacuole (arrowhead). Bars = 100µm

A) Hypocotyl 35 DAI₂. Developing pith and cortex cells are relatively large and contain several protein vacuoles. Cells of the procambial ring and protoderm (PD) are relatively small and contain fewer small protein vacuoles.

B) Enlarged portion of (A). Protein vacuoles in all cells of the 35 DAI₂ hypocotyl.

C) Protein vacuoles 4 DAI₃₀ undergoing protein loss in the developing cortex, and are no longer visible in the developing epidermis and procambial ring.

D) Protein vacuoles 5 DAI₃₀ no longer visible in the hypocotyl. Imprints of hypocotyl epidermal cells in the carbohydrate-positive layer.

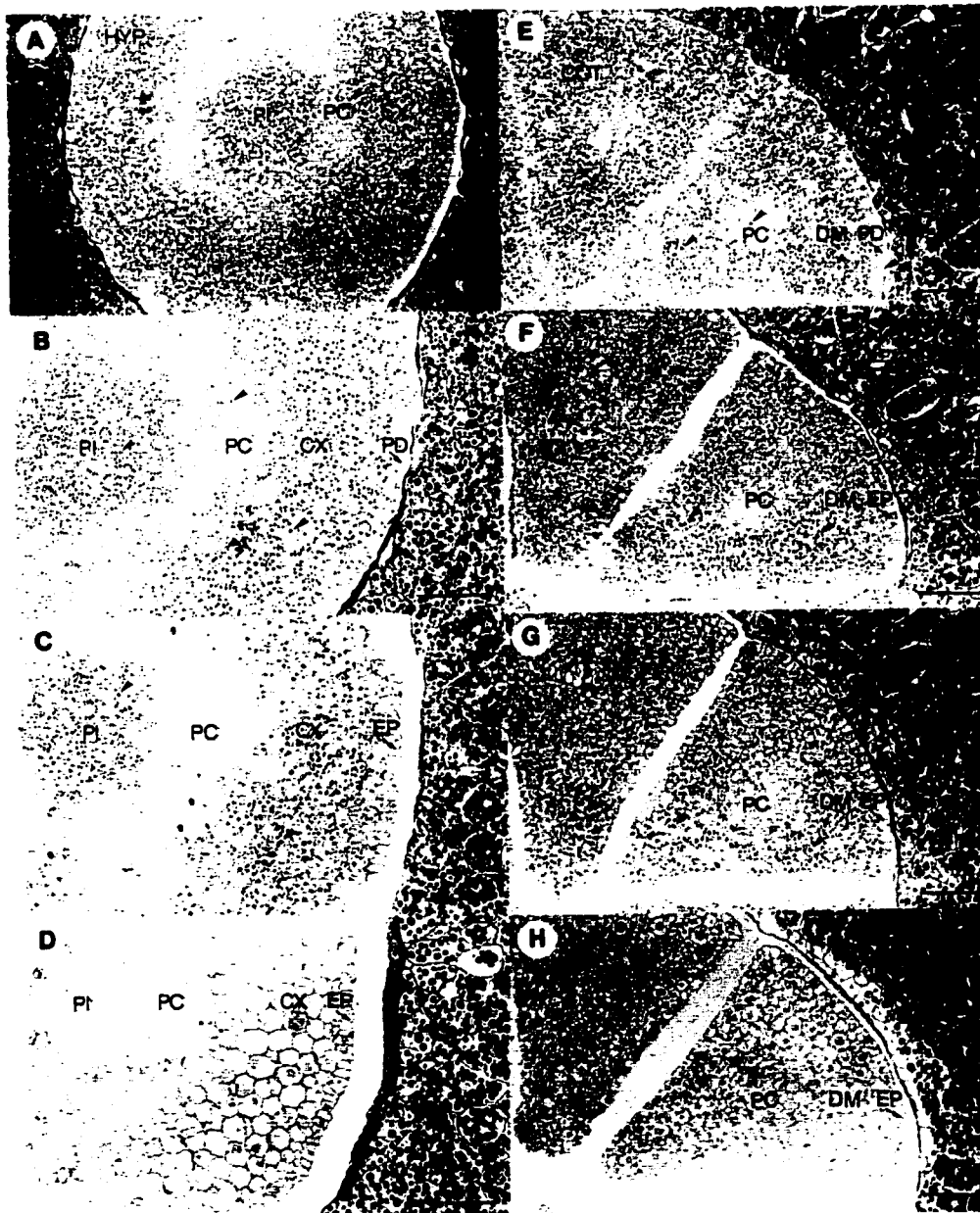
Figures 16E-H. Light micrographs of PAS and Aniline Blue Black stained transverse sections through plastic-embedded cotyledons (COT)s and surrounding megagametophyte during imbibition at 30°C. Developing epidermis (EP), procambium (PC), developing mesophyll (DM), protein vacuole (arrowhead). Bars = 100 µm.

E) Protein vacuoles are present in all the cells of 35 DAI₂ cotyledons. Developing mesophyll cells are large and contain the largest protein vacuoles of the cotyledons. Protodermal (PD) and procambial cells contain fewer and smaller protein vacuoles.

F) Protein vacuoles 4 DAI₃₀ in the developing epidermis and procambium undergoing some protein loss.

G) Protein vacuoles 5 DAI₃₀ no longer visible in most of the developing epidermis and procambium. Protein depletion occurring in the developing mesophyll.

H) Protein vacuoles 6 DAI₃₀ no longer visible in most of the cotyledon cells. Protein vacuoles in megagametophyte inner region undergoing protein hydrolysis.



5 DAI₃₀ (Fig. 16G). By 6 DAI₃₀ most of the protein had disappeared from the protein vacuoles in this region of the cotyledons (Fig. 16H).

3.2.1.5 Quantitative changes in megagametophyte and embryo/ seedling proteins

A typical mature loblolly pine seed contained 2.1 ± 0.03 mg of protein; 1.9 ± 0.03 mg of protein in the megagametophyte and 0.2 ± 0.005 mg of protein in the embryo. Expressed as a percent of seed part dry weight, the megagametophyte and embryo protein content was $20 \pm 0.3\%$ and $13.1 \pm 0.3\%$ respectively. In the megagametophyte, $81 \pm 1\%$ of the protein was phosphate buffer-insoluble. In contrast only $27 \pm 0.2\%$ of the embryo protein was buffer-insoluble. The buffer-insoluble protein of the embryo was distributed equally between the root and shoot pole regions.

In the megagametophyte, the amount of phosphate buffer-insoluble proteins remained relatively constant throughout stratification and germination (Fig. 17). After germination was completed, the quantity of insoluble proteins began to decrease. By 12 DAI₃₀, insoluble protein levels were only 10% of those found in mature seed megagametophytes. In contrast, the megagametophyte phosphate buffer-soluble protein pool increased following the completion of germination, reaching maximum levels by 10 DAI₃₀.

The phosphate buffer-insoluble protein levels in the shoot and root pole of the embryo or seedling remained constant until 2 DAI₃₀, after which a modest decrease was observed in both regions (Fig. 18B). In the root pole, the level of insoluble protein decreased to a minimum at 3 DAI₃₀, while the shoot pole level reached a minimum at 4 DAI₃₀. Insoluble protein levels then increased in both poles; the increase in the root

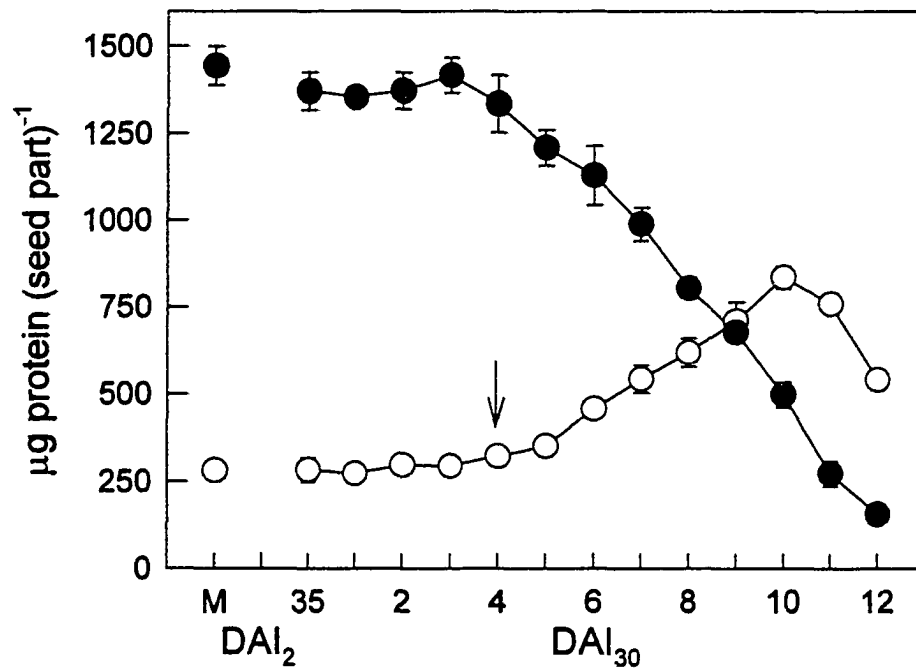


Figure 17. Quantitative changes in megagametophyte phosphate buffer-soluble (O) and -insoluble (●) proteins following imbibition. X-axis labels as described in Figure 10. Arrow indicates the completion of germination by radicle emergence from the seed coat. Each data point is the mean of three independent replicates each assayed in duplicate \pm SE of the mean.

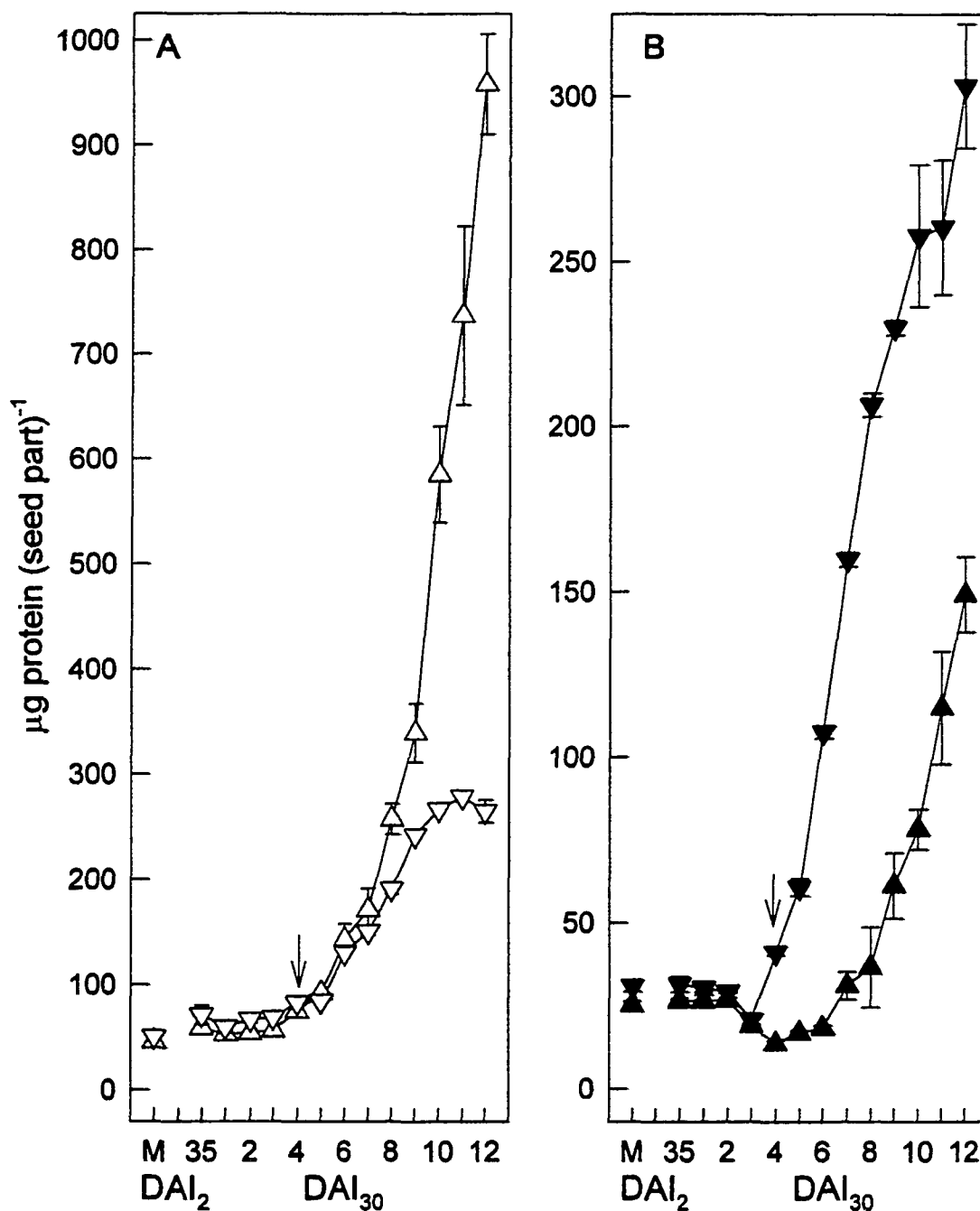


Figure 18. Quantitative embryo/ seedling protein changes during imbibition. A) Phosphate buffer-soluble protein in the shoot pole (Δ) and root pole (∇). B) Phosphate buffer-insoluble protein in the shoot pole (\blacktriangle) and root pole (\blacktriangledown). X-axis labels as described in Figure 10. Arrow indicates the completion of germination by radicle emergence from the seed coat. Each data point is the mean of three independent replicates assayed in duplicate \pm SE of the mean.

pole region was the greatest. The levels of phosphate buffer-soluble protein in the shoot and root pole regions were also relatively constant during germination and the initial stages of early seedling growth (Fig. 18A). By 6 DAI₃₀ increases in both soluble protein pools had occurred. However, by 12 DAI₃₀, the soluble protein content of the shoot pole region was significantly higher than that of the root pole region of the seedling. At this stage of seedling development, the average soluble protein content was 1.2 ± 0.06 mg per seedling of which $78 \pm 4\%$ was in the shoot pole region.

SDS-dissociated extracts of shoot and root pole regions from mature seed embryos contained two major phosphate buffer-insoluble storage proteins, a 47 kDa globulin and a 60 kDa coniferalin (Groome *et al.*, 1991). Under reducing conditions, the globulin maintained a molecular mass of 47 kDa, while the coniferalin dissociated into 37.5 and 22.5 kDa subunits (lane M in Figs. 19A, B). Breakdown of these proteins was less rapid in the shoot pole region. The depletion of the shoot pole 47 kDa protein band was complete by 8 DAI₃₀ (Fig. 19A). In contrast, the depletion of the equivalent root pole protein band was complete by 4 DAI₃₀ (Fig. 19B). The start of breakdown of the 37.5 and 22.5 kDa subunit bands were similar in both the root and shoot poles of the embryo, 4 DAI₃₀ (Figs. 19A, B), but the rates of breakdown were different. In the shoot pole these proteins, although significantly depleted, were still present by 11 DAI₃₀ (Fig. 19A), whereas the 37.5 kDa and 22.5 kDa subunit bands of the root pole were depleted by 7 DAI₃₀ (Fig. 19B).

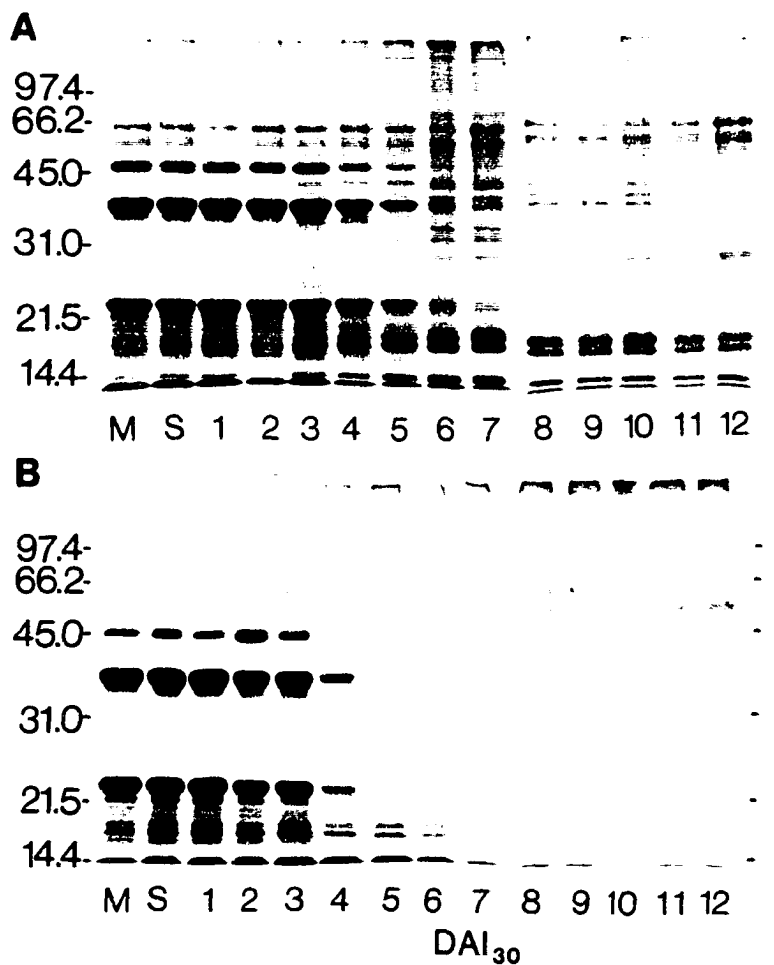


Figure 19. Coomassie blue stained SDS-PAGE profile of phosphate buffer-insoluble proteins from embryo/ seedling shoot and root poles following imbibition, run under reducing conditions in the presence of 2-mercaptoethanol. A) shoot poles; B) root poles. For each lane, 3 μ g protein was loaded in 10 μ L. Relative molecular masses of standards in kDa are shown by numerical values adjacent to the gel profiles. Lanes are mature seed (M), 35 DAI₂ seed (S), and seed imbibed up to 12 DAI₃₀.

3.2.2 The fate of stored TAG reserves during germination and early seedling growth

3.2.2.1 Quantitative changes in TAG reserves during germination and early seedling growth

Approximately 58% of the storage reserves stored in whole mature loblolly pine seeds were TAGs, based on the amounts of TAG, phosphate buffer-soluble and insoluble protein, and 80% ethanol-soluble and insoluble carbohydrate stored in the seed at this stage. The megagametophyte stored 80% of the seed's TAGs; this reserve constituted $27 \pm 0.8\%$ of the mature megagametophyte on a dry weight basis (Fig. 20A). However, TAGs were also an important reserve in the embryo since they comprised $40 \pm 0.6\%$ of the mature embryo's dry weight. These TAGs were stored in lipid bodies in the megagametophyte (Fig. 4A), cotyledon (Fig. 4B) and hypocotyl (Fig. 4C) cells. During germination and early seedling growth, TAG reserves in both the megagametophyte and seedling were depleted (Fig. 20A). Although there was some depletion of TAGs measured by 5 DAI₃₀ in the megagametophyte, the majority of TAG breakdown occurred following 6 DAI₃₀. The average TAG depletion rate between 7 and 11 DAI₃₀ was 0.34 mg triolein equivalents/ seed part/ DAI. The TAG depletion in the seedling was evident following 3 DAI₃₀ (Fig. 20B). Although the amount of TAG stored in the embryo's root and shoot pole were approximately equal on a per seed part basis in the mature seed, during imbibition at 30°C TAG levels decreased more rapidly and to a lower level in the root pole than in the shoot pole (Fig. 20B). The depletion of TAG in the root pole was close to linear between 4 and 8 DAI₃₀, with an average rate of 0.04 mg

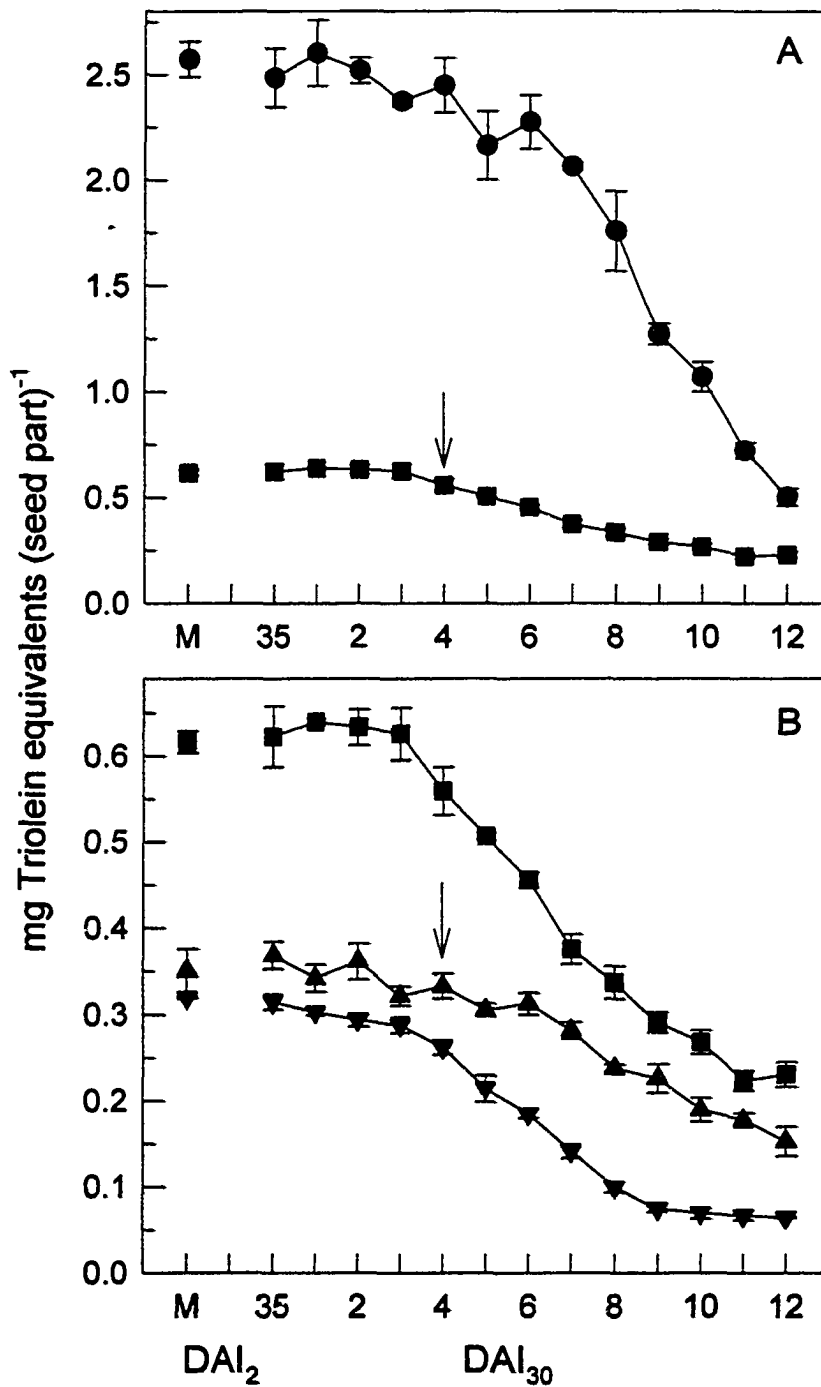


Figure 20. Quantitative changes in TAGs during imbibition. A) megagametophyte (●) and seedling (■). B) Whole seedling (■), shoot pole (▲), and root pole (▼). X-axis labels as described in Figure 10. Arrow indicates the completion of germination by radicle emergence from the seed coat. Each data point is the mean of three independent biological replicates each assayed in triplicate \pm SE of the mean.

triolein equivalents/ seed part/ DAI. The shoot pole lost an average of 0.03 mg triolein equivalents/ seed part/ DAI between 6 and 10 DAI₃₀. By 12 DAI₃₀, seedling TAG levels were 47% that of the 12 DAI₃₀ megagametophyte. Although 80% of the mature megagametophyte TAG had been depleted at 12 DAI₃₀, it still contained 0.5 mg TAG, which was approximately that stored in the mature embryo; correspondingly, lipid bodies in the megagametophyte were still numerous (Fig. 5A). However, in the seedling by 12 DAI₃₀, 56% of the shoot pole and 80% of the root pole TAG had been depleted and lipid bodies were also reduced in number (Figs. 5B, C).

3.2.3 Carbohydrates in the megagametophyte and seedling during germination and early seedling growth

3.2.3.1 Quantitative changes in carbohydrates

Seventy-one percent of the 80% ethanol-soluble carbohydrate in mature seeds was stored in the megagametophyte (Fig. 21A). During germination and into early seedling growth, megagametophyte soluble carbohydrates declined and reached minimum levels at 6 DAI₃₀, then increased until 10 DAI₃₀ after which the level remained constant. The 80% ethanol-insoluble carbohydrate levels were 3-fold lower than soluble carbohydrates in the mature megagametophyte. The insoluble carbohydrate level increased slightly, reaching a maximum at 4 DAI₃₀, then declined to levels similar to those of the mature megagametophyte.

Twenty-nine percent of the seed's 80% ethanol-soluble carbohydrates were stored in the embryo at maturity (Fig. 21B). The level of soluble carbohydrates

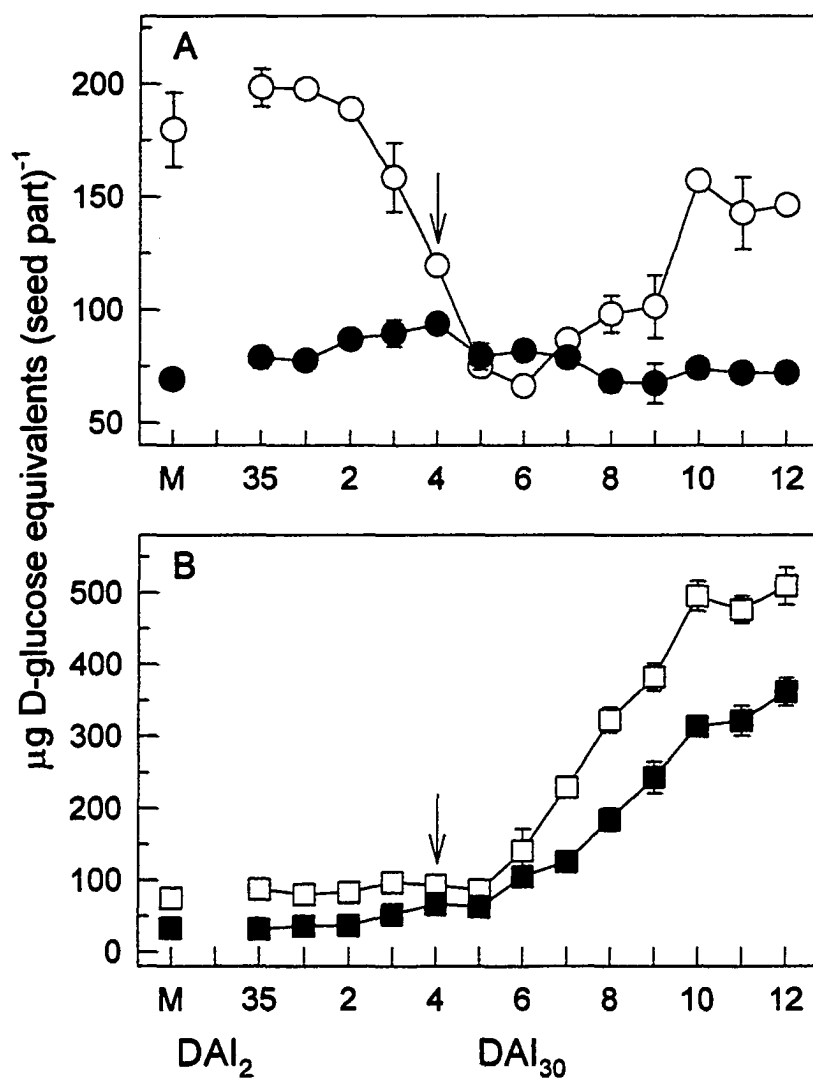


Figure 21. Quantitative changes in megagametophyte and whole embryo/ seedling 80% ethanol-soluble and insoluble carbohydrate levels during imbibition. A) Megagametophyte soluble (○) and insoluble (●) carbohydrates. B) Embryo/ seedling soluble (□) and insoluble (■) carbohydrates. X-axis labels as described in Figure 10. Arrow indicates the completion of germination by radicle emergence from the seed coat. Each data point is the mean of three independent biological replicates each assayed in triplicate \pm SE of the mean.

remained constant until 5 DAI₃₀, following which the level increased rapidly in the seedling to 10 DAI₃₀ (Fig. 21B). By 12 DAI₃₀, soluble carbohydrates in the seedling were 7-fold higher than that stored in the mature embryo. The 80% ethanol-insoluble carbohydrate levels behaved similarly to soluble levels. Most of the increase in insoluble carbohydrates occurred between 6 and 10 DAI₃₀. By 12 DAI₃₀ there was 10-fold more insoluble carbohydrate than in the mature embryo.

Within the mature embryo, the shoot and root poles contained $36 \pm 3 \mu\text{g}$ and $48 \pm 3 \mu\text{g}$ soluble carbohydrates per seed part, respectively (Figs. 22A, B). Soluble carbohydrate levels in the root pole remained steady during germination and increased following 5 DAI₃₀ (Fig. 22B). At 12 DAI₃₀, root pole soluble carbohydrates were 6-fold higher than at maturity. Unlike the root poles, shoot pole soluble carbohydrate levels declined prior to increasing during early seedling growth; this decline in soluble carbohydrate level occurred following 2 DAI₃₀ (Fig. 22A). The majority of the increase occurred between 6 and 12 DAI₃₀. By 12 DAI₃₀, soluble carbohydrate levels were equal in the root and shoot poles. The level of 80% ethanol-insoluble carbohydrate was very low at maturity in both the root and shoot poles, but began to increase following 2 DAI₃₀ in the root pole and 5 DAI₃₀ in the shoot pole. By 12 DAI₃₀, insoluble carbohydrate levels had increased 14-fold in the shoot pole and 12-fold in the root pole from mature levels.

In addition to changes in 80% ethanol-soluble and -insoluble carbohydrates, changes in sucrose, D-glucose, D-fructose and starch were also measured. At maturity, the average megagametophyte and whole embryo contained $113 \pm 0.1 \mu\text{g}$ and $63 \pm 0.5 \mu\text{g}$ sucrose, respectively (Fig. 23A). In the megagametophyte, sucrose levels increased

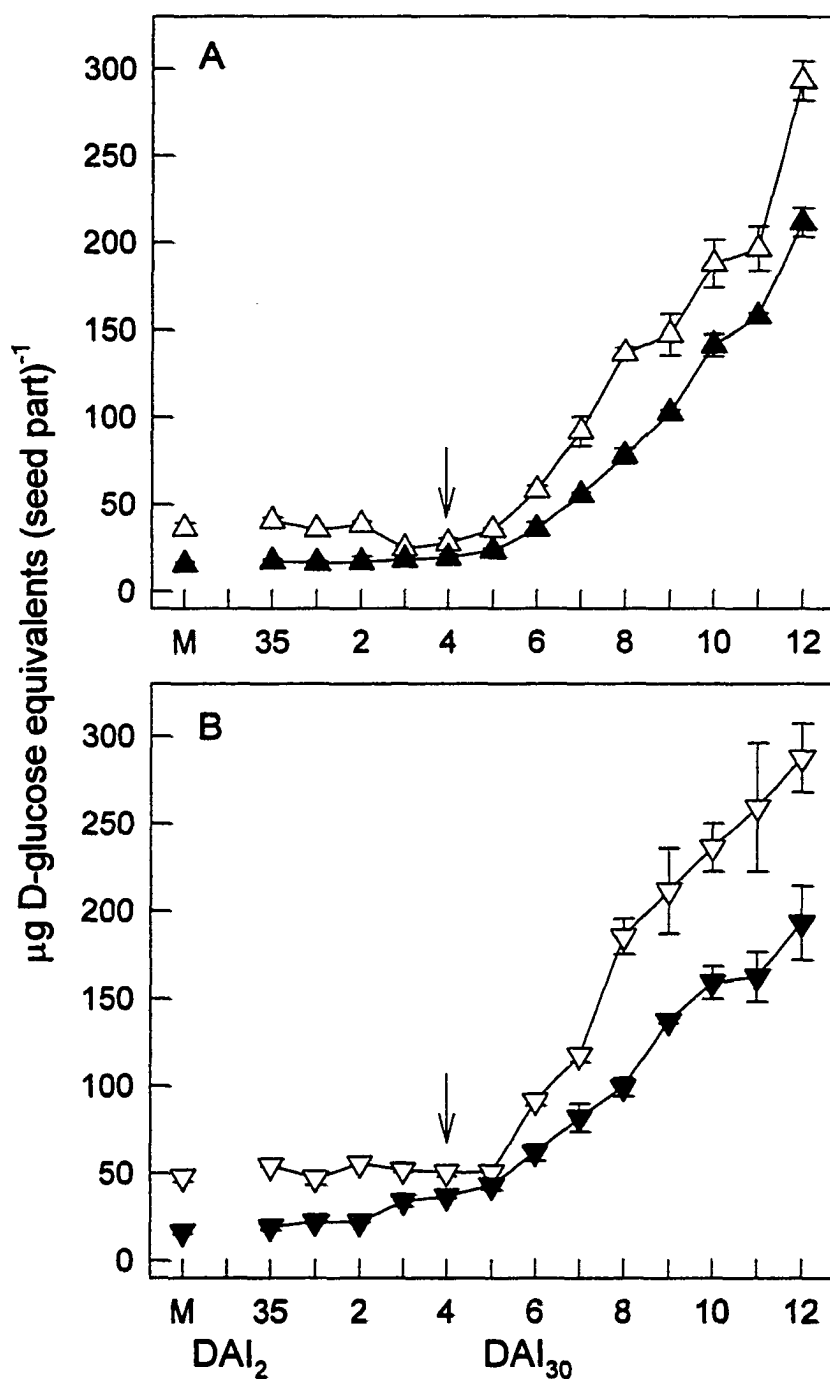


Figure 22. Quantitative changes in embryo/ seedling 80% ethanol-soluble and -insoluble carbohydrate levels during imbibition. A) Shoot pole soluble (Δ) and insoluble (\blacktriangle) carbohydrates. B) Root pole soluble (∇) and insoluble (\blacktriangledown) carbohydrates. X-axis labels as described in Figure 10. Arrow indicates the completion of germination by radicle emergence from the seed coat. Each data point is the mean of three independent biological replicates each assayed in triplicate \pm SE of the mean.

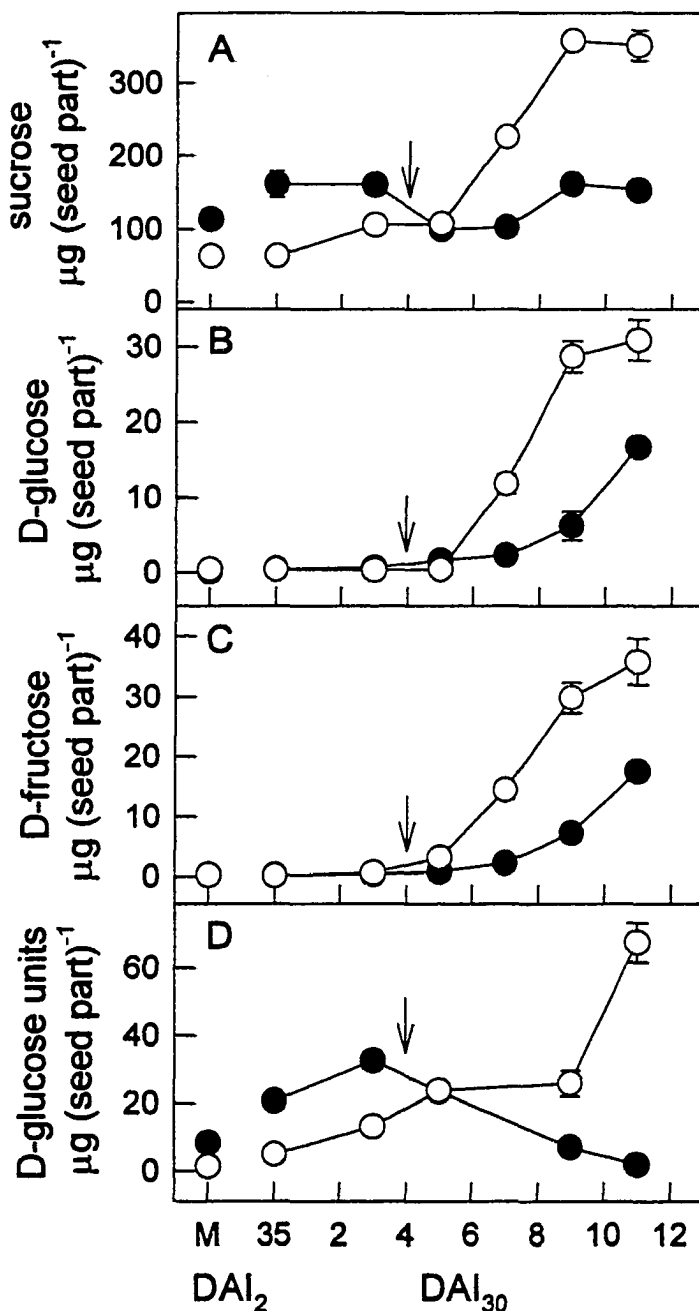


Figure 23. Quantitative changes in specific carbohydrate levels during imbibition, measured indirectly by NADPH production. Megagametophyte (●), embryo/seedling (○). A) sucrose, B) D-glucose, C) D-fructose, D) starch. X-axis labels as described in Figure 10. Arrow indicates the completion of germination by radicle emergence from the seed coat. Each data point is the mean of two independent biological replicates each assayed in duplicate \pm SD of the mean.

42% from maturity until 35 DAI₂, and remained at that level until 3 DAI₃₀. Following 3 DAI₃₀, the megagametophyte sucrose level decreased 38% where it remained constant until 7 DAI₃₀. The sucrose level rose again to that found in 35 DAI₂ megagametophytes and remained constant until 11 DAI₃₀. In the seedling, sucrose levels increased from 35 DAI₂ until 3 DAI₃₀. Following 5 DAI₃₀, sucrose levels rose rapidly to 6 times that of the mature embryo at 9 DAI₃₀. Unlike sucrose levels, D-glucose and D-fructose levels in both the mature megagametophyte and whole embryo were low. Although absolute amounts of these carbohydrates remained low until the end of early seedling growth, D-glucose and D-fructose levels increased after 5 DAI₃₀ (Figs. 23B, C).

Similar to 80% ethanol-insoluble carbohydrates, starch accumulated in the megagametophyte only transiently, peaking approximately 3 DAI₃₀ (Fig. 23D). Water-insoluble carbohydrate grains, likely starch grains due to their appearance with polarized light, were observed in the megagametophyte, usually in the corners of cells (Figs. 24A-C). The timing of starch grain appearance in localized regions of the megagametophyte varied along the longitudinal axis of the seed. Starch grains first appeared in the inner megagametophyte region 2 DAI₃₀ in the area of the root cap. The starch grains were found 3 and 4 DAI₃₀ throughout the inner (Fig. 24C), middle and outer regions of the megagametophyte in the area of the root cap. Megagametophyte starch grains in the area of the hypocotyl first appeared 3 DAI₃₀ concentrated in the inner region and were less concentrated in the middle and outer regions. Megagametophyte starch grains in the hypocotyl area maintained this distribution pattern (Fig. 24B) until 5 DAI₃₀. Starch grains were first observed in the megagametophyte tissue in the area of the cotyledons at 4 DAI₃₀, in the inner region (Fig. 24A). By 5 DAI₃₀, starch grains were present

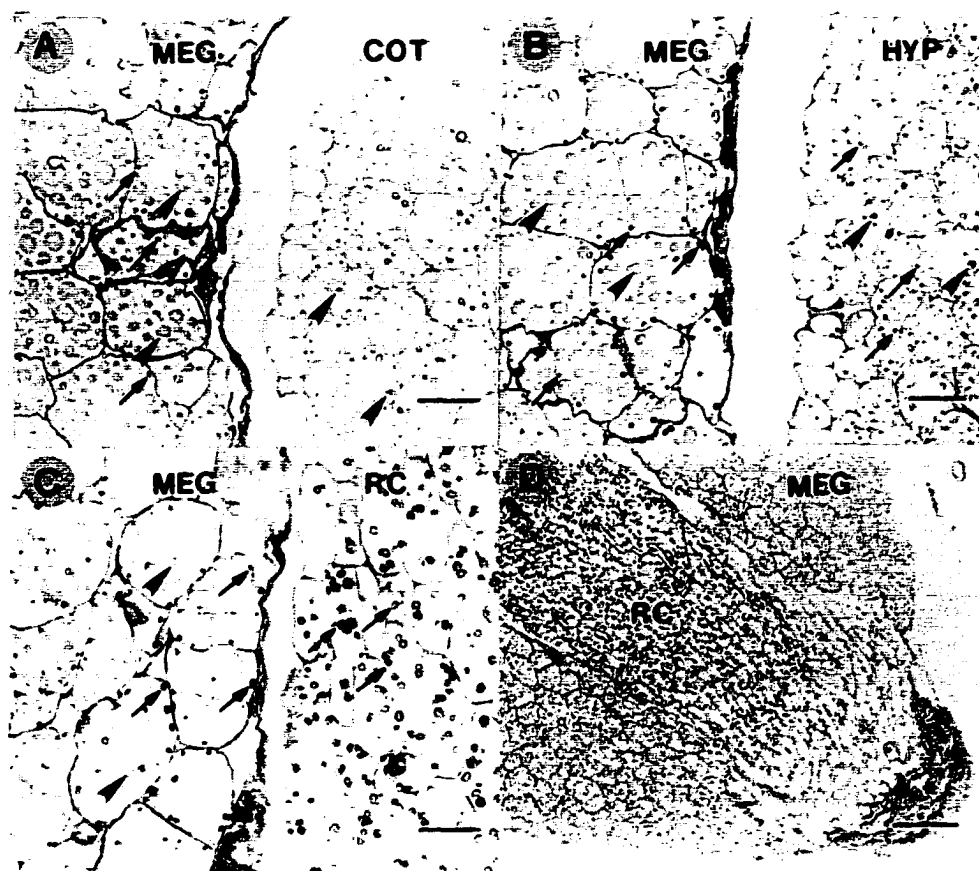


Figure 24. Light micrographs of PAS stained 4 DAI₃₀ seed material. Starch grains (arrows) and lightly stained protein vacuoles (arrowheads) were observed.

A) Transverse section through seeds at inner megagametophyte region (MEG) and cotyledon (COT). Bar = 30 μ m.

B) Transverse section through seed at inner megagametophyte region and hypocotyl (HYP). Bar = 30 μ m.

C) Longitudinal section through seed at inner megagametophyte region and root cap (RC). Bar = 30 μ m.

D) Longitudinal section through the 4 DAI₃₀ seed with integuments and nucellar cap removed showing the extensive root cap and the remnants of the embryonic suspensor (*). Bar = 140 μ m.

throughout the inner, middle and outer regions beside the cotyledons; however, at 6 DAI₃₀, grains were only found in the inner region.

The seedling starch level increased following 3 DAI₃₀, and increased rapidly following 9 DAI₃₀ (Fig. 23D). By 11 DAI₃₀, the seedling contained 48-fold more starch than at maturity. The root cap contained starch grains at maturity through until the end of early seedling growth (Fig. 24D). Starch grains were observed in the hypocotyl before they appeared in the cotyledons. At 4 DAI₃₀, starch grains were first observed in the epidermis and cortex of the hypocotyl (Fig. 24B), as well as in the pith. While the hypocotyl remained inside the megagametophyte, starch grains were observed throughout the cortex and pith tissues. However, 8 - 12 DAI₃₀, when the hypocotyl had emerged from the megagametophyte, starch grains were concentrated in cortex cells located just outside the vascular ring (Fig. 25C). A small number of starch grains were first observed at 5 DAI₃₀ in the cotyledon mesophyll cells closest to the megagametophyte. By 6 DAI₃₀, the starch grains were concentrated in the mesophyll cells closest to the megagametophyte and were easily observed (Fig. 25A). By 12 DAI₃₀, starch grains were visible throughout most of the mesophyll cells of the cotyledon (Fig. 25B).

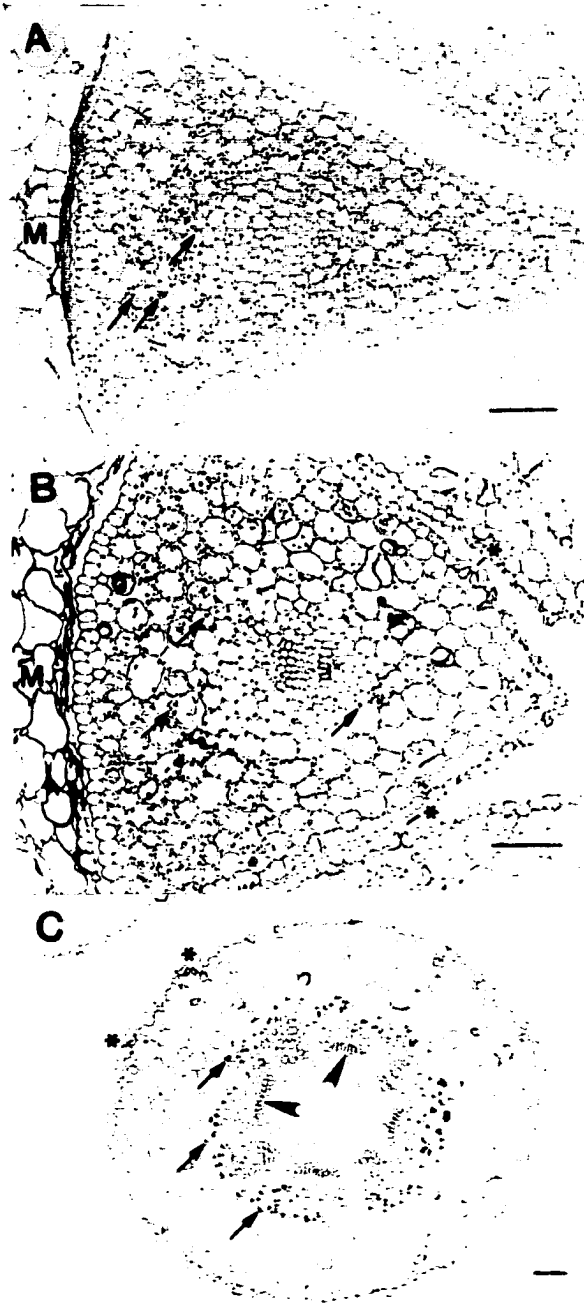
Mature seed megagametophyte and embryo/ seedling protein vacuoles (excluding the globoids) stained faintly and homogeneously for water-insoluble carbohydrate with PAS. Protein vacuoles continued to stain with PAS (Figs. 24A-C) until these organelles began to fuse during germination and early seedling growth.

Figure 25. Light micrographs of PAS stained sections through the seed transverse to the seedling. Starch grain (arrow) and stomatal complex (*). Bars = 70 μ m.

A) Cotyledon from 6 DAI₃₀ seedling. Starch grains are concentrated in the mesophyll cells closest to the megagametophyte (M).

B) Cotyledon from 12 DAI₃₀ seedling. Starch grains are found throughout most of the mesophyll.

C) Hypocotyl from 12 DAI₃₀ seedling that has emerged from the megagametophyte. Starch grains are concentrated in a ring of cortex cells to the outside of the vascular bundles (arrowhead)s.



3.2.3.2 Invertase activities

Invertases are enzymes that hydrolyze sucrose to D-glucose and D-fructose (Avigad, 1982). HEPES buffer-soluble invertase activity in 11 DAI₃₀ megagametophytes and seedlings was tested over a range of incubation buffer pHs. The seedlings had high activities over a range from pH 3.5 to 5, with peak activity at pH 4 (Fig. 26A). The megagametophytes had a peak activity at pH 4.5 (Fig. 26A). No neutral invertase activity was observed for either tissue.

Cell wall-associated invertase activity was more variable (Fig. 26B) than buffer-soluble activity, due in part to the assay of buffer-insoluble suspensions, instead of homogenous cell-free extracts. The seedling had high activities between pH 4 and 5, while the peak activity in megagametophytes was at pH 4. Similar to the soluble invertase, no neutral invertase activity was observed in cell wall-associated fractions for either tissue.

Based on the pH optima ranges found, the megagametophyte and embryo/seedling soluble acidic and cell wall-associated invertase activities were assayed using the incubation buffer at pH 4.25. The possible presence of a soluble neutral form of invertase in stages other than 11 DAI₃₀ was investigated using the incubation buffer at pH 7.5, since this was within the 7.5 - 8 pH optimum range observed for most soluble neutral invertases (Avigad, 1982).

Soluble acidic invertase activity rose in megagametophytes following 3 DAI₃₀ on both a per seed part basis (Fig. 27A) as well as a per mg protein basis (Fig. 27B). Activity per seed part peaked at 10 DAI₃₀, which was 16-fold higher than mature levels, then declined (Fig. 27A). Specific activity peaked earlier at 7 DAI₃₀ at 7-fold higher than

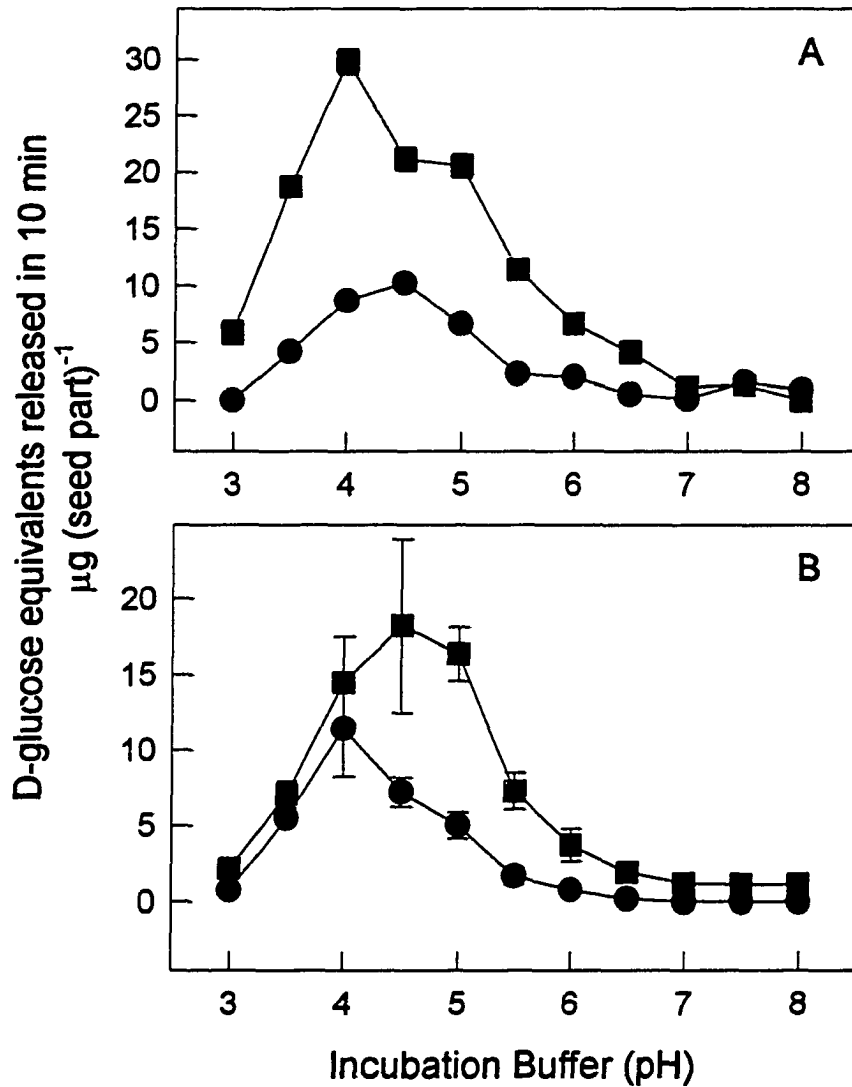


Figure 26. Invertase incubation buffer pH optima. A) soluble and B) cell wall-associated invertase forms in the megagametophyte (●) and seedling (■) of fresh 11 DAI₃₀ material. Each data point is the mean of one independent biological replicate assayed in triplicate \pm SD.

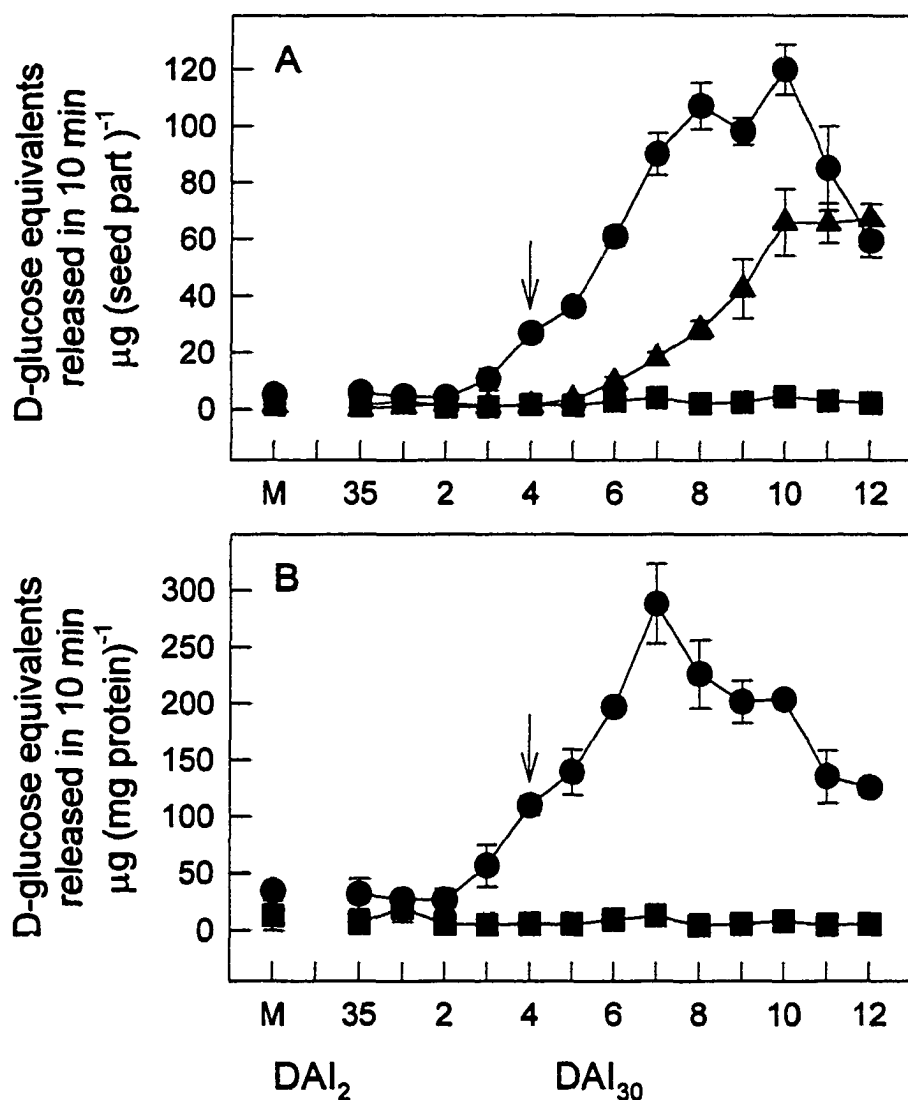


Figure 27. Megagametophyte invertase activities during imbibition, expressed A) per seed part, and as B) specific activity. Soluble acidic (●), soluble neutral (■), and cell wall-associated (▲) forms of invertase activity. X-axis labels as described in Figure 10. Arrow indicates the completion of germination by radicle emergence from the seed coat. Each data point is the mean of three independent biological replicates each assayed in triplicate \pm SE of the mean.

mature megagametophyte, then declined (Fig. 27B). Cell wall-associated invertase activity per megagametophyte increased later, following 6 DAI₃₀ (Fig. 27A). Maximum cell wall-associated activity was reached 10 DAI₃₀, then remained steady. Specific activity for cell wall-associated invertase was not calculated, since this fraction also contained the HEPES buffer-insoluble storage proteins.

Soluble acidic invertase activity also increased per seedling following 5 DAI₃₀, and increased until 11 DAI₃₀ (Fig. 28A). An increase in soluble acidic invertase specific activity occurred earlier, following 3 DAI₃₀, and increased to 7 DAI₃₀, after which it remained relatively constant (Fig. 28B). The peak specific activity of seedling soluble acidic invertase was 57-fold higher than that found in the mature embryo. Similar to the megagametophyte, seedling cell wall-associated invertase activity increased following 6 DAI₃₀ and reached a maximum at 9 DAI₃₀, after which it remained constant (Fig. 28A).

Soluble neutral invertase activity was not observed in any stage or tissue of loblolly pine during germination and early seedling growth (Figs. 27A, B; 28A, B).

3.3 The relationship between the seedling and megagametophyte

3.3.1 The composition of the carbohydrate-positive layer of the inner megagametophyte

The non-cellular layer of the megagametophyte next to the seedling stained positively for water-insoluble carbohydrates using PAS (Fig. 29A) and for cellulose using IKI-sulfuric acid (Fig. 29B). In the mature desiccated seed, this layer appeared to be composed of several flaky sheets that were not always in complete contact with the

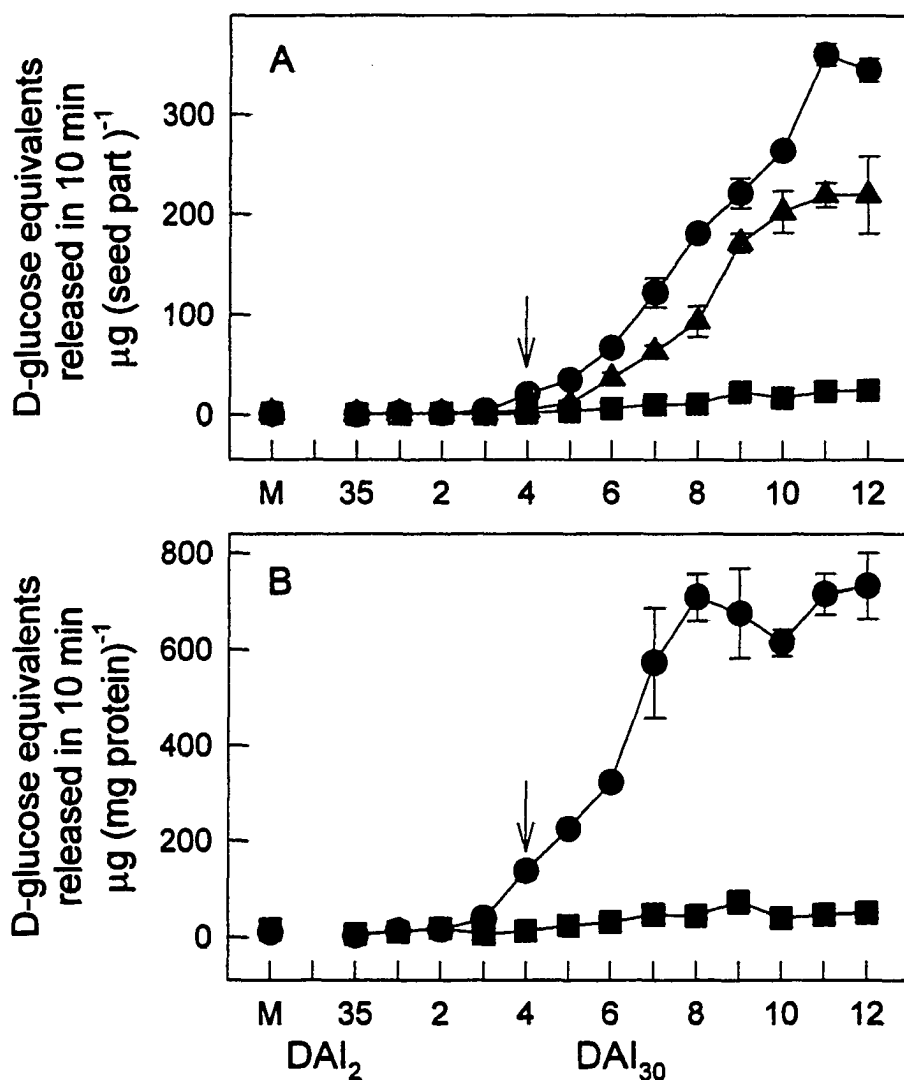


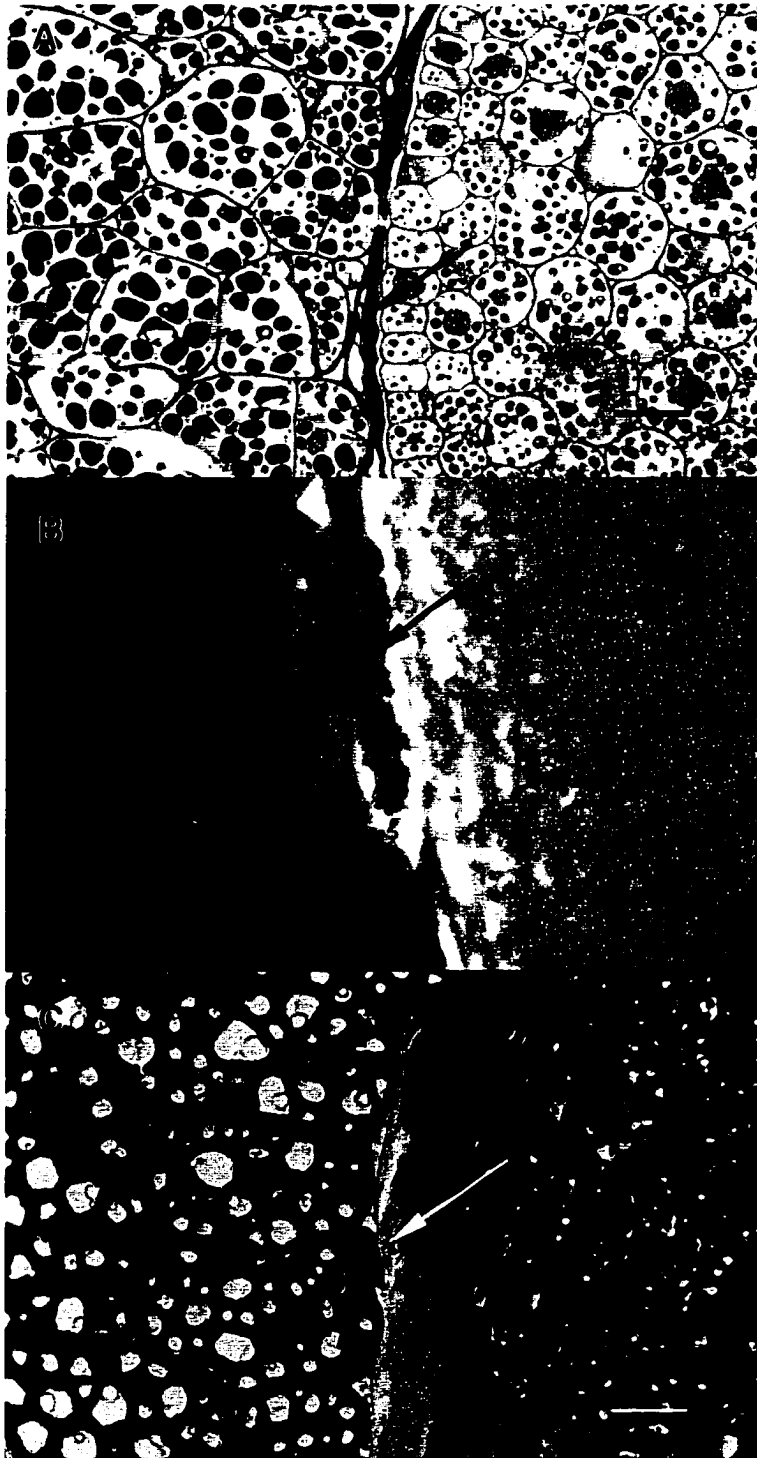
Figure 28. Embryo/ seedling invertase activities during imbibition, expressed A) per seed part, and as B) specific activity. Soluble acidic (●), soluble neutral (■), and cell wall-associated (▲) forms of invertase activity. X-axis labels as described in Figure 10. Arrow indicates the completion of germination by radicle emergence from the seed coat. Each data point is the mean of three independent biological replicates each assayed in triplicate \pm SE of the mean.

Figure 29. Light micrographs of the carbohydrate-positive layer (arrow) of the inner megagametophyte. The megagametophyte is on the left and the embryo is on the right of each figure. Bars = 30 μm .

A) Section through a 35 DAI₂ seed transverse to the megagametophyte and cotyledon stained with PAS for carbohydrate (pink) and counter-stained with Aniline Blue Black for protein (blue). Imprints of cotyledon protodermal cells are visible in the carbohydrate-positive layer.

B) Longitudinal section through a mature seed megagametophyte and hypocotyl stained with IKI-sulfuric acid for cellulose (blue).

C) Section through a 35 DAI₂ seed transverse to the megagametophyte and cotyledon stained with Sudan black B for lipid (black).



megagametophyte cell walls lining the corrosion cavity. In the stratified and 30°C imbibed seed, it was more mucilaginous and malleable. Imprints of cotyledon and hypodermal epidermal cells were often observed in 35 DAI₂ freeze-substituted material (Fig. 29A). During germination and early seedling growth, the epidermal cell imprints in the layer became more pronounced (Figs. 13A-D; 16A-H). This layer did not stain positively for protein using Aniline Blue Black (Fig. 29A) and did not stain for lipid using Sudan black B (Fig. 29C).

3.3.2 The rapid transport of substances between the megagametophyte and seedling

It has been hypothesized that megagametophyte TAGs are broken down and metabolized to produce carbohydrates that are rapidly transported to the seedling. To test this hypothesis, a number of experiments were conducted.

3.3.2.1 The effect of megagametophyte removal on seedling carbohydrate levels

Because TAG reserves were stored in both the embryo and megagametophyte, it is possible that the large pool of carbohydrate that accumulates in the seedling (Fig. 21B) during early seedling growth is due, in part, to the breakdown of embryonic TAG reserves. To test this, the effect of megagametophyte removal on seedling carbohydrate levels was measured.

When cultured with the seedling, megagametophyte 80% ethanol-soluble (Fig. 30A) and -insoluble (Fig. 30B) carbohydrate levels remained low and constant. However, after 3 days in culture in the presence of the megagametophyte, the seedling

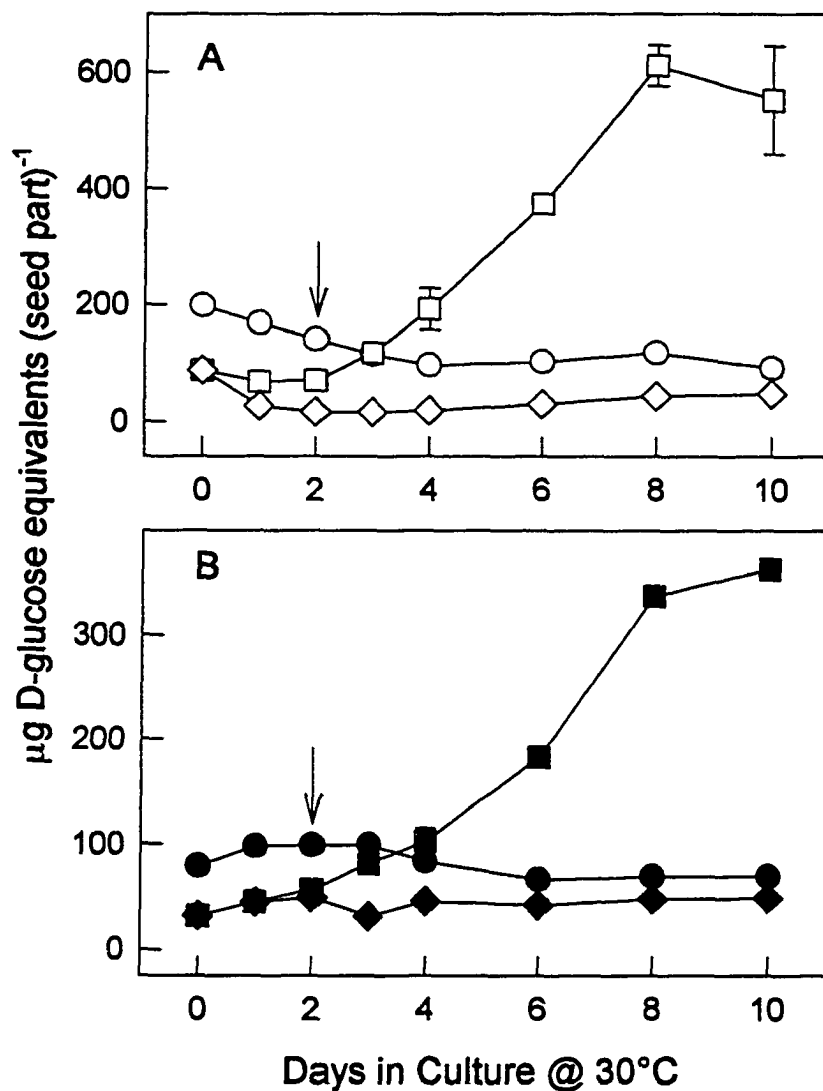


Figure 30. The effect of megagametophyte removal from 35 DAI₂ seeds, on carbohydrate levels of embryos cultured up to 10 days @ 30°C. A) 80% ethanol-soluble and B) -insoluble carbohydrate levels. Seedling levels when cultured with the megagametophyte (□, ■), seedling levels when cultured alone (◇, ◆), and megagametophyte levels when cultured with embryos (○, ●). Arrow indicates completion of germination by radicle emergence from the megagametophyte. Each data point is the mean of three independent biological replicates each assayed in triplicate ± SE of the mean.

accumulated both soluble (Fig. 30A) and insoluble carbohydrates (Fig. 30B). In contrast, when cultured in the absence of the megagametophyte, seedlings accumulated 92% and 87% less soluble (Fig. 30A) and insoluble (Fig. 30B) carbohydrate, respectively over the 10 day period. This suggests that the presence of the megagametophyte is necessary for the seedling to accumulate the large pool of carbohydrate observed *in vivo*.

3.3.2.2 The incorporation of [2-¹⁴C]sodium acetate into megagametophyte metabolic macromolecules and their subsequent movement into the seedling

To demonstrate the movement of carbohydrates from the megagametophyte to the seedling, labeling experiments with [2-¹⁴C]sodium acetate were conducted. The 80% ethanol-soluble metabolites labeled with [¹⁴C] at each time period were separated into an ether-soluble fraction, which was discarded, and a water-soluble fraction, which was further separated. If the [2-¹⁴C]sodium acetate was converted to [2-¹⁴C]acetyl CoA and entered the glyoxylate cycle followed by the gluconeogenesis pathway, it was expected that the majority of the radiolabeled metabolites would be water-soluble. It was expected that the majority of the radiolabel would be incorporated into the neutral fraction (carbohydrate) but little would be incorporated into either the acidic (organic acids and sugar phosphates) or basic (amino acids) fraction.

With seedlings attached, 10 DAI₃₀ megagametophytes were continuously labeled with [2-¹⁴C]sodium acetate for up to 120 min at 30°C. The combined uptake of 80% ethanol-soluble radioactivity in these two tissues was approximately linear over the first 90 min of radiolabeling (Fig. 31A). Throughout the 120 min of radiolabeling, the incorporation of radioactivity into the water-soluble fraction (Fig. 32A) was similar to

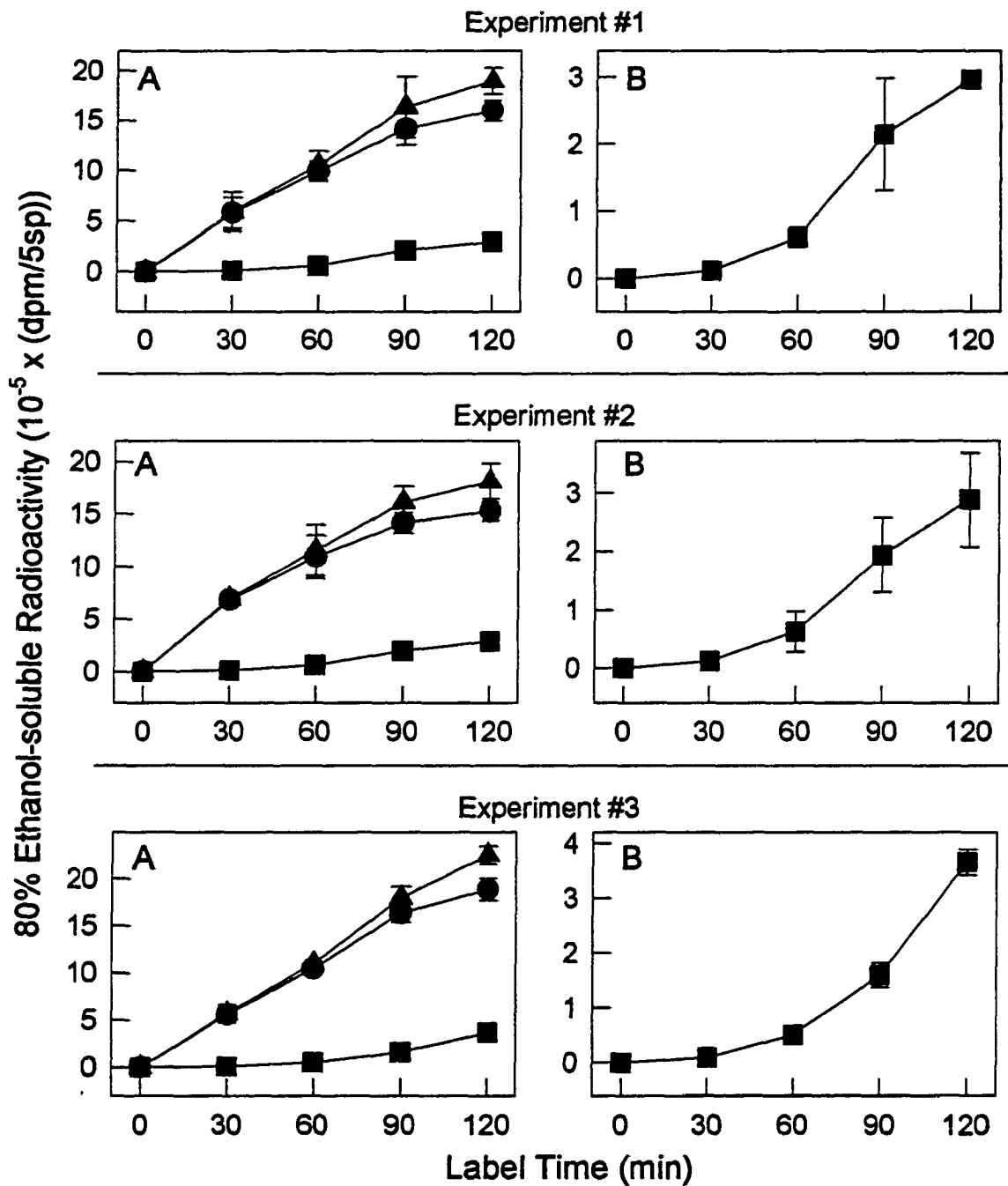


Figure 31. Radioactivity incorporated into 80% ethanol-soluble fraction from 10 DAI₃₀ seed material labeled with [2-¹⁴C]sodium acetate up to 120 min. Three separate labeling experiments show the radioactivity in A) megagametophytes (●), seedlings (■), and megagametophytes plus seedlings (▲). B) Expanded scale of seedling radioactivity (■). Each data point is the mean of two independent replicates each assayed in duplicate \pm SD of the mean.

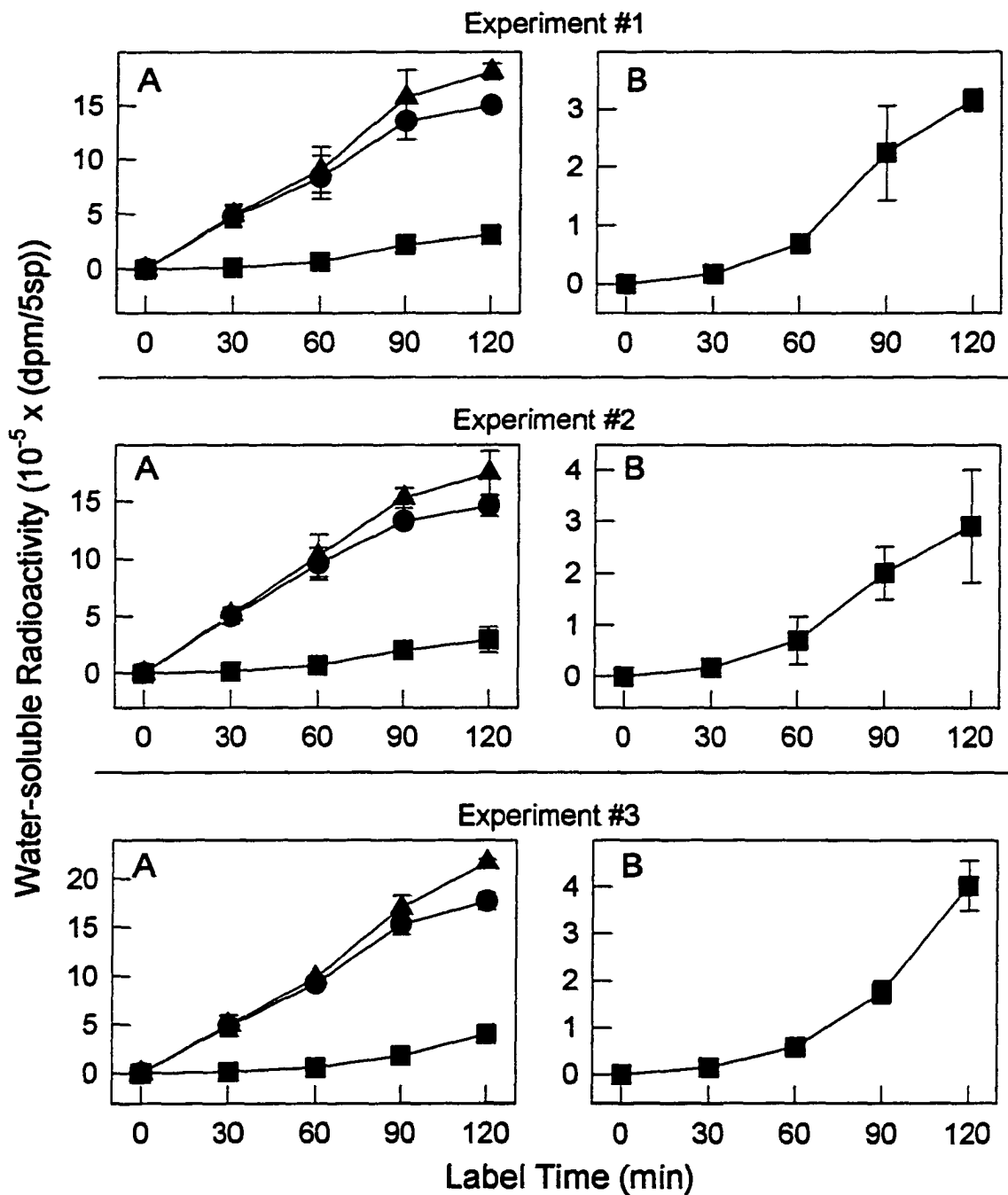


Figure 32. Water-soluble radioactivity from 10 DAI_{30} seed material labeled with $[2\text{-}^{14}\text{C}]$ sodium acetate up to 120 min. Three separate labeling experiments show the radioactivity in A) megagametophytes (●), seedlings (■), and megagametophytes plus seedlings (▲). B) Expanded scale of seedling radioactivity (■). Each data point is the mean of two independent replicates each assayed in duplicate \pm SD of the mean.

the incorporation into the 80% ethanol-soluble radioactivity pool (Fig. 31A). With increasing time of radiolabeling, the amount of radiolabeled water-soluble metabolites comprised an increasing proportion of the 80% ethanol-soluble metabolites. For example; in experiment #1, after 30 min of radiolabeling, $83 \pm 16\%$ of the 80% ethanol-soluble radioactive metabolites were water-soluble; by 120 min of radiolabeling, $96 \pm 4\%$ of the radioactive metabolites were water-soluble (Figs. 31A; 32A). Replicate experiments showed similar results (Figs. 31A; 32A). Similar to the 80% ethanol-soluble and water-soluble radioactivity levels the combined neutral fraction radioactivity of the megagametophytes and seedlings showed a similar linear increase between 30 and 90 min of radiolabeling (Fig. 33A). Although the majority of the radioactivity in these fractions was localized in the megagametophyte after 120 min of radiolabeling (Figs. 31A; 32A; 33A), between 14 and 19% of each radiolabeled fraction was localized in the seedling (Figs. 31B; 32B; 33B). The majority of the radioactive metabolites taken up from the megagametophyte by the seedling occurred following 60 min of labeling (Fig. 31B; 32B; 33B). Approximately 59,300 dpm was present in each seedling after 120 min radiolabeling, indicating that transport of metabolites from the megagametophyte had occurred (Fig. 31B, experiment #1).

After 30 min of labeling, the $[2-^{14}\text{C}]$ sodium acetate was incorporated into the neutral fraction which accounts for 28-39% of the water-soluble radioactivity in the megagametophyte (Fig. 34). The amount of radiolabel incorporated into the neutral fraction of the megagametophyte continued to increase over the 120 min radiolabeling period. At 120 min, 56-66% of the water-soluble radioactivity had been incorporated into the neutral fraction of the megagametophyte. The amount of radiolabel

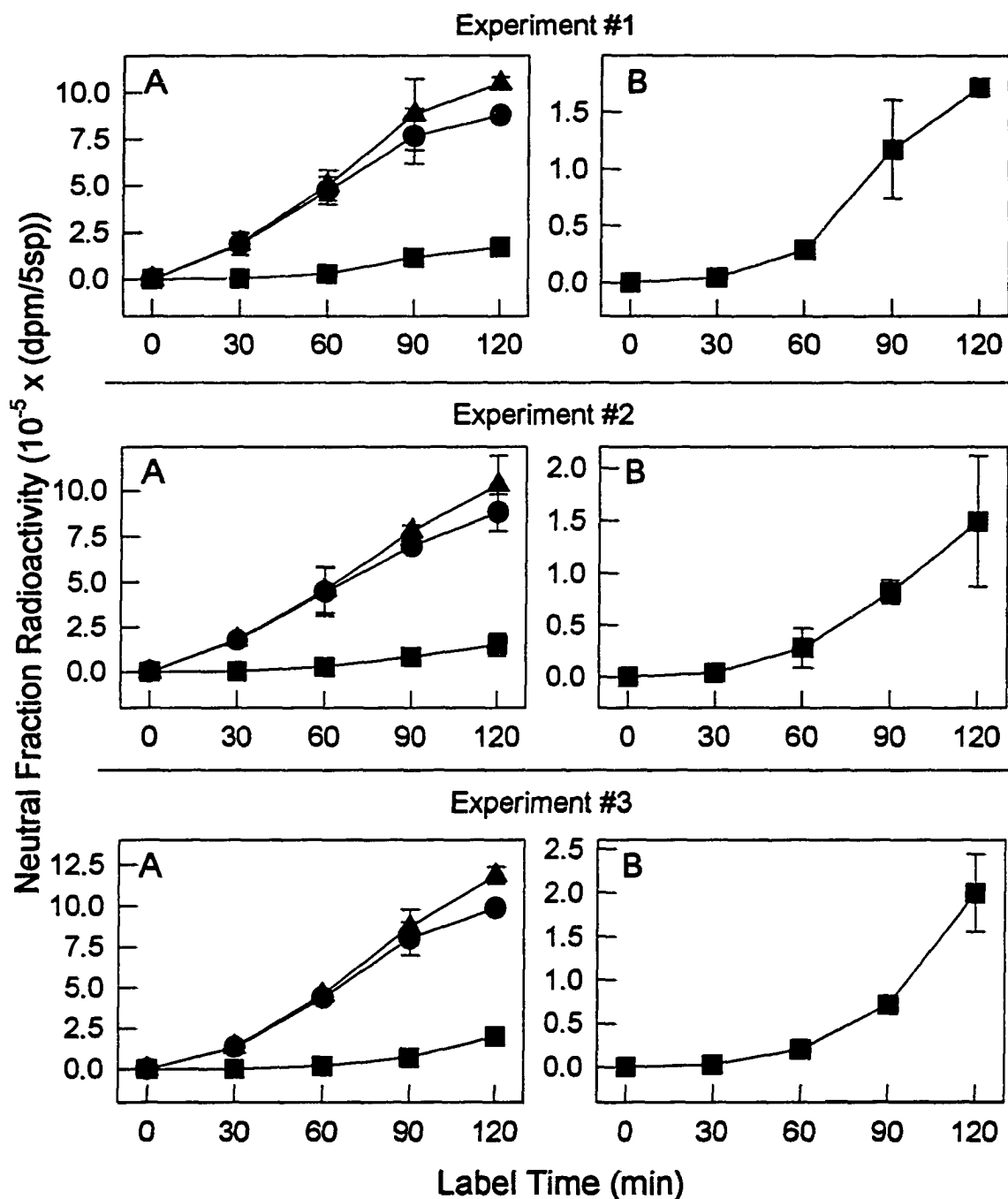


Figure 33. Neutral fraction radioactivity from 10 DAI₃₀ seed material labeled with [2-¹⁴C]sodium acetate up to 120 min. Three separate labeling experiments show the neutral fraction radioactivity in A) megagametophytes (●), seedlings (■) and megagametophytes plus seedlings (▲). B) Expanded scale of seedling radioactivity (■). Each data point is the mean of two independent replicates each assayed in duplicate \pm SD of the mean.

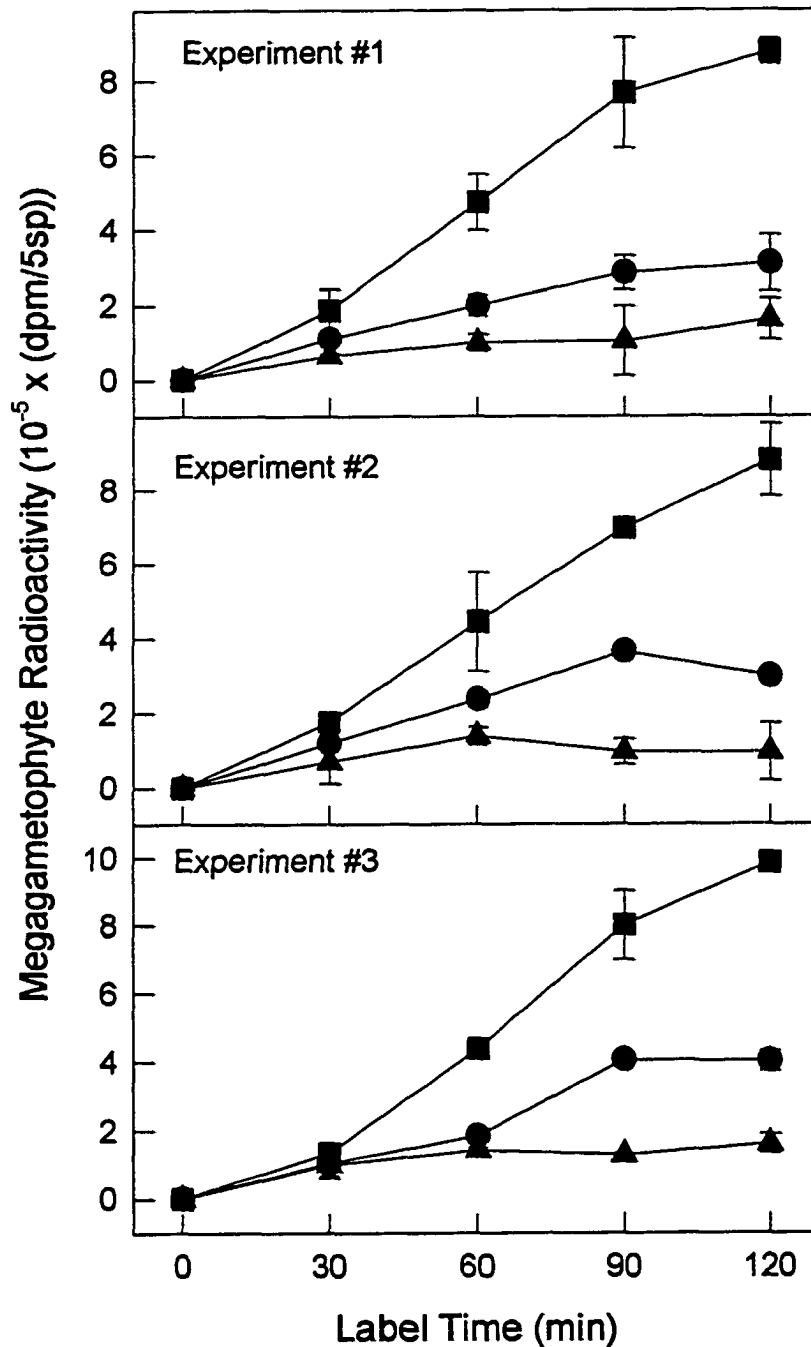


Figure 34. Radioactivity in the different water-soluble fractions of the megagametophyte from 10 DAI₃₀ seed material labeled with [2-¹⁴C]sodium acetate up to 120 min. Three separate labeling experiments show the radioactivity in basic (●), neutral (■), and acidic (▲) fractions of the megagametophyte. Each data point is the mean of two independent replicates each assayed in duplicate \pm SD of the mean.

incorporated into the basic fraction also increased with time, but at a much lower level than the neutral fraction. Relatively little radiolabel (31,993 dpm/ megagametophyte) was incorporated into the acidic fraction after 120 min of radiolabeling (Fig. 34, experiment #3).

Within the seedling, an increase in neutral and basic fraction radioactivity was observed following 60 min of radiolabeling (Fig. 35). The acidic fraction of the seedling accumulated relatively little radioactivity over the 120 min radiolabeling period, as was also observed in the megagametophyte.

The previous radiolabeling experiments indicated that the majority of radioactive compounds entered the seedling from the megagametophyte after 60 min of continuous radiolabeling. To demonstrate that radiolabel entered the seedling from the megagametophyte, a series of pulse-chase experiments were conducted.

With seedlings attached, 10 DAI₃₀ megagametophytes were labeled for 30 min with [2-¹⁴C]sodium acetate and chased with non-radioactive sodium acetate for up to 4 h at 30°C. After the first hour of chase, 22 ± 3% of the radiolabel present had been incorporated into the seedling, and 78 ± 8% was in the megagametophyte (Fig. 36, experiment #3). Experiment #1 (Fig. 36) showed a gradual decrease in megagametophyte total radioactivity with chase time. Experiments #2 and #3 demonstrated a rapid decline in the first hour of chase, followed by a more gradual decline of 80% ethanol-soluble radioactivity in the megagametophyte (Fig. 36). Radioactivity in the 80% ethanol-soluble pool continued to increase in the seedling for 2 h (experiment #3) and 3 h of chase (experiments #1 and #2) and then remained constant. After 4 h of chase, the amount of the radiolabel present in the seedling had

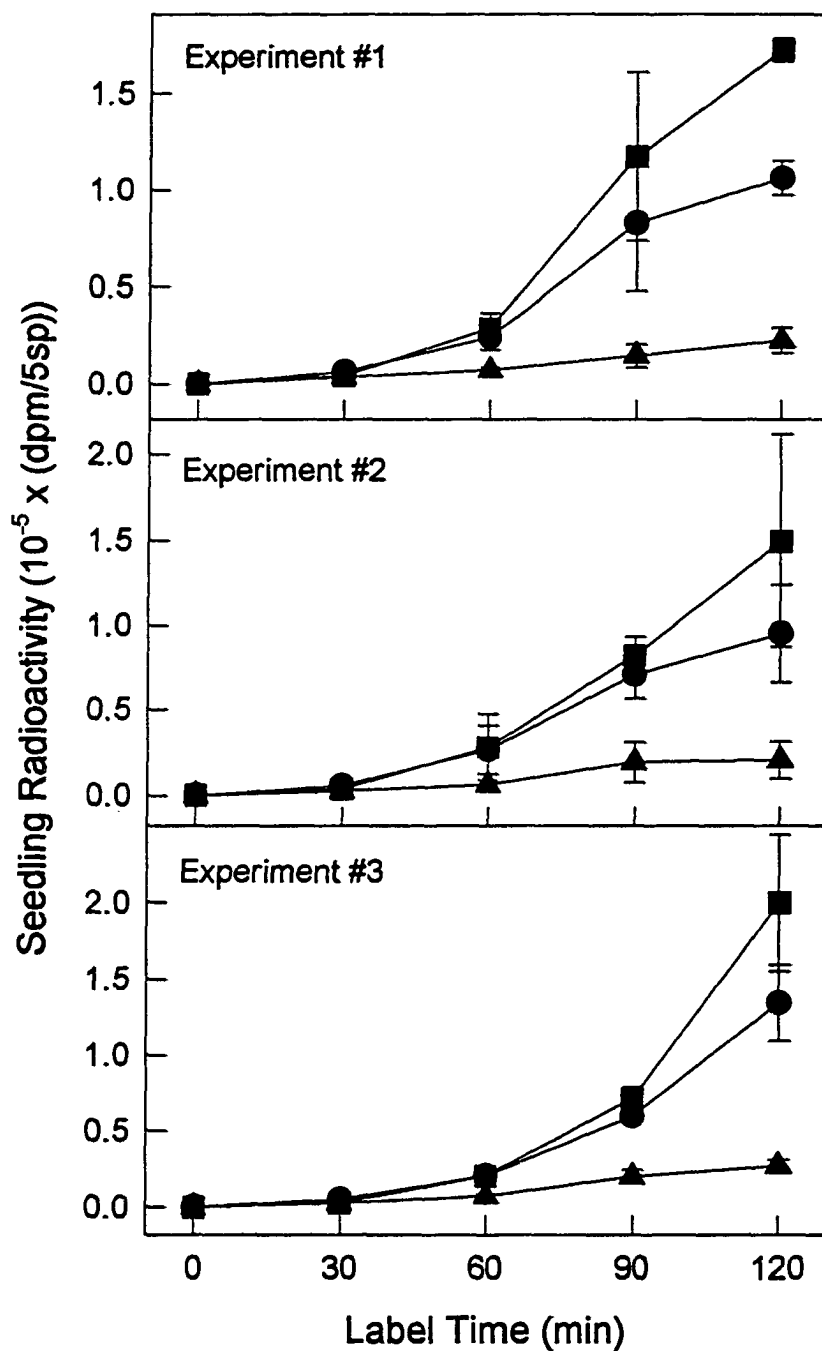


Figure 35. Radioactivity in the different water-soluble fractions of the seedling from 10 DAI₃₀ seed material labeled with [2-¹⁴C]sodium acetate up to 120 min. Three separate labeling experiments show the radioactivity in basic (●), neutral (■), and acidic (▲) fractions of the seedling. Each data point is the mean of two independent replicates each assayed in duplicate \pm SD of the mean.

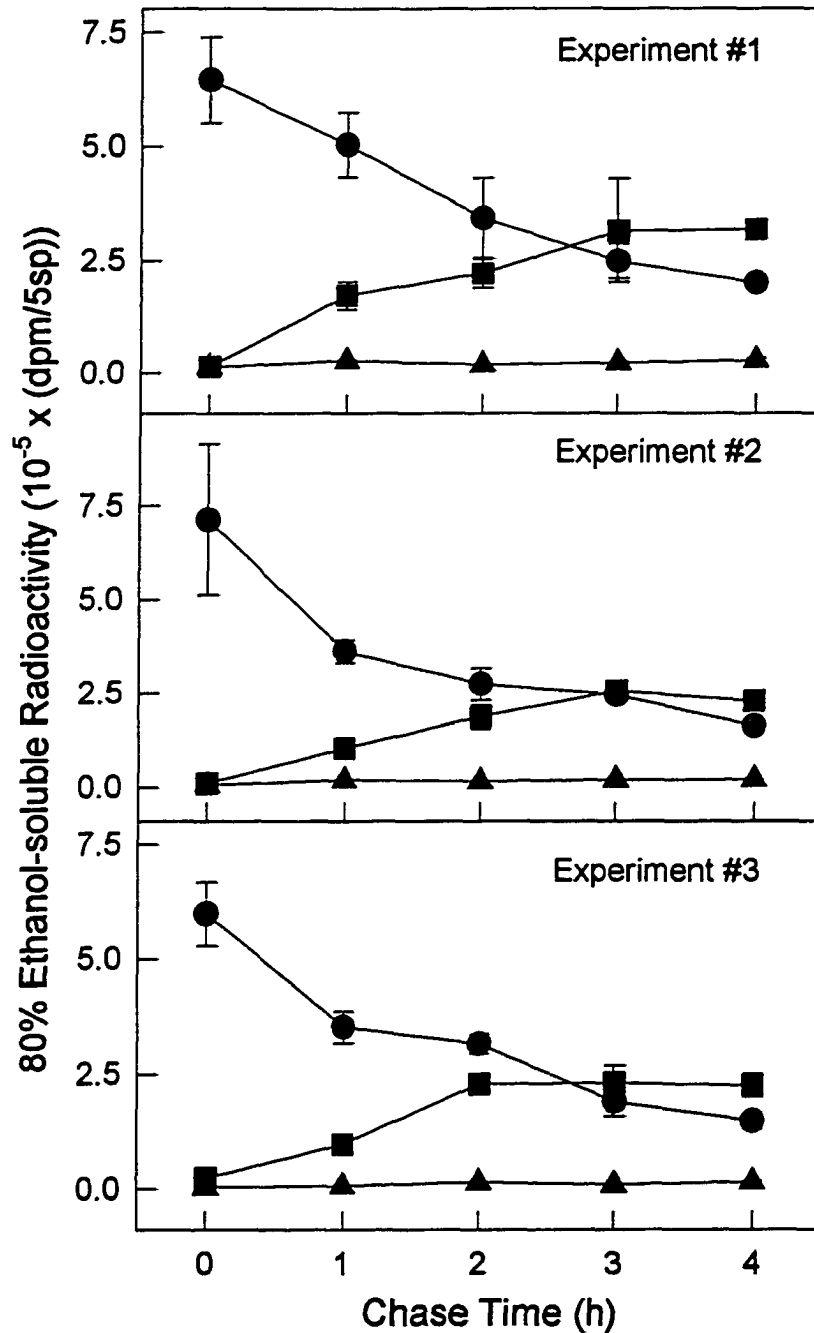


Figure 36. Radioactivity incorporated into 80% ethanol-soluble fraction from 10 DAI₃₀ seed material pulsed 30 min with [2-¹⁴C]sodium acetate and chased with non-radioactive sodium acetate up to 4 h. Three separate experiments show the radioactivity in megagametophyte (●), seedling (■), and CO₂ (▲) fractions. Each data point is the mean of two independent replicates each assayed in duplicate \pm SD of the mean.

increased to 58%, and only 38% was present in the megagametophyte (Fig. 36, experiment #3). Over the 4 h chase, only 4% of the radiolabel was incorporated into the tissue released CO₂ fraction (Fig. 36, experiment #3).

3.3.3 The role of the seedling in the regulation of megagametophyte metabolism

Because of the megagametophyte's role as a storage tissue for the embryo/seedling, it was hypothesized that in the absence of the embryo, the megagametophyte could not initiate the breakdown and metabolism of its stored reserves.

3.3.3.1 The effect of embryo removal on carbohydrate levels of 35 DAI₂ megagametophytes in culture

In the presence of the embryo, megagametophyte 80% ethanol-soluble carbohydrate levels gradually declined, reaching a minimum at 4 days in culture (Fig. 37A). Soluble carbohydrates increased slightly at 8 days, then declined again by 10 days in culture. A minor increase in the level of insoluble carbohydrate in megagametophytes cultured with embryos was observed at 1 day in culture, which declined following 3 days in culture (Fig. 37B). However, in the absence of an embryo the megagametophyte soluble carbohydrate level decreased rapidly by 1 day in culture, then increased transiently to a maximum at 3 days in culture, after which the level declined and remained steady following 6 days in culture (Fig. 37A). Between 3 and 4 days in culture without the embryo, the megagametophyte insoluble carbohydrate level increased 86%, then declined (Fig. 37B). The results of this experiment did not support the hypothesis, and indicated that the megagametophyte was capable of using stored carbohydrates in

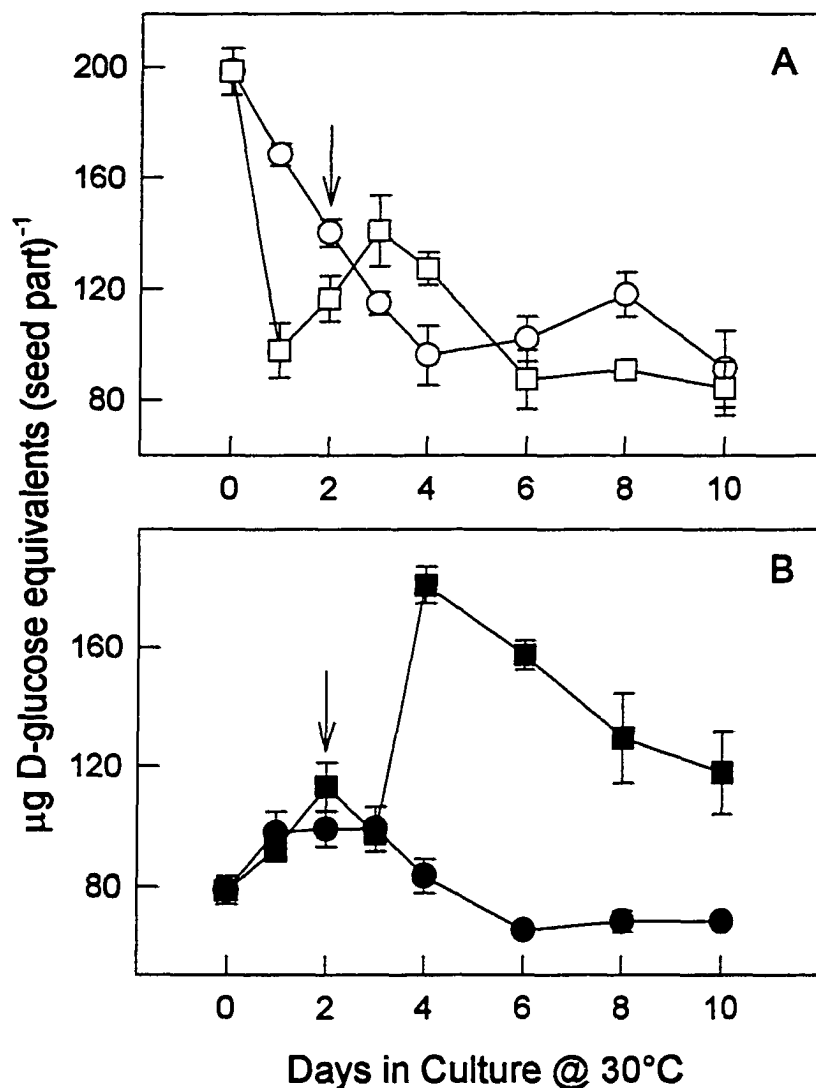


Figure 37. The effect of embryo removal from 35 DAI₂ seeds, on carbohydrate levels of megagametophytes cultured up to 10 days @ 30°C. A) 80% ethanol-soluble and B) -insoluble carbohydrate levels. Megagametophyte carbohydrate levels when cultured with the embryo (○, ●) and megagametophyte levels when cultured alone (□, ■). Arrow indicates completion of germination by radicle emergence from the megagametophyte. Each point is the mean of three independent biological experiments each assayed in triplicate \pm SE of the mean.

the absence of the seedling, but was unable to regulate its metabolism properly without the seedling.

Similar to the changes observed in the insoluble carbohydrate level, a minor increase in starch level occurred in the megagametophyte cultured 1 day with an embryo, and a decrease in starch level occurred after 3 days in culture (Fig. 38). The starch levels in megagametophytes cultured alone rose after 1 day in culture and then declined by 3 and 4 days. This was in contrast to what was observed for the insoluble carbohydrate levels which instead increased between 3 and 4 days (Fig. 37B). This experiment further indicated that the megagametophyte's metabolism was affected by the absence of the seedling.

3.3.3.2 The effect of seedling removal on 9 DAI₃₀ megagametophytes

After the removal of the hard seed coat and thin papery layer, it is possible to remove the seedling and nucellar cap remnant from a 9 DAI₃₀ seed without cutting or tearing the megagametophyte. These isolated megagametophytes will continue to export metabolites to their corrosion cavities, in the absence of a seedling. If the megagametophyte is propped with the micropylar end up, so the corrosion cavity will fill, an exudate droplet will form within 24 h at 30°C (Fig. 39).

After the 24 h period of exudate droplet formation, the isolated megagametophytes showed a significant increase in the levels of sucrose (Fig. 40A), D-glucose (Fig. 40B) and D-fructose (Fig. 40C) compared to megagametophytes cultured with seedlings. Apparently carbohydrates were exported from the isolated

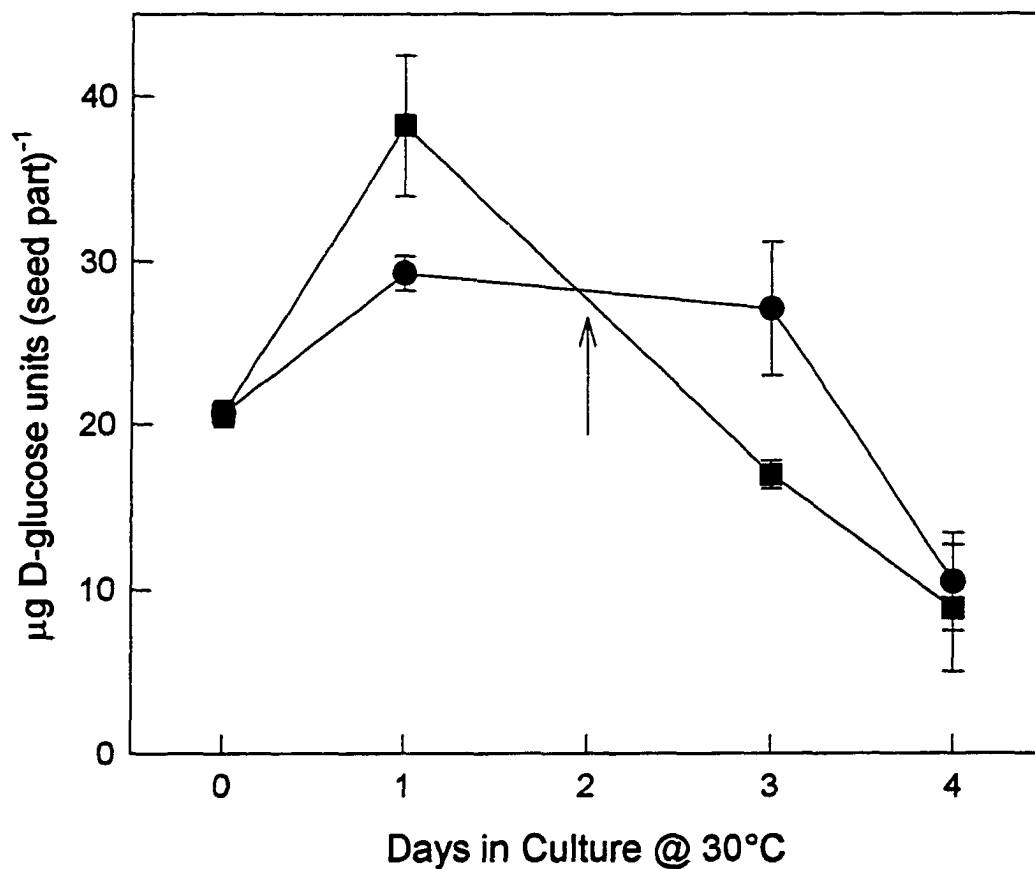


Figure 38. The effect of embryo removal from 35 DAI₂ seeds, on starch levels of megagametophytes cultured up to 4 days @ 30°C. Megagametophyte starch levels when cultured with the embryo (●) and megagametophyte levels when cultured alone (■). Arrow indicates completion of germination by radicle emergence from the megagametophyte. Each point is the mean of two independent biological experiments each assayed in duplicate \pm SD of the mean.

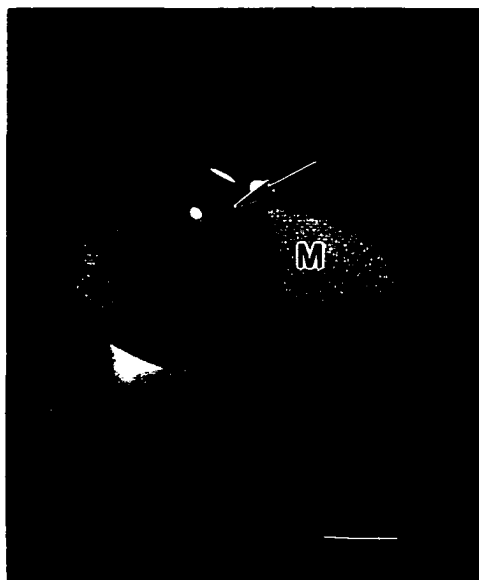


Figure 39. Isolated 9 DAI₃₀ megagametophyte (M) with exudate droplet (arrow) formed after 24 h of culture at 30°C. Bar = 700 μm.

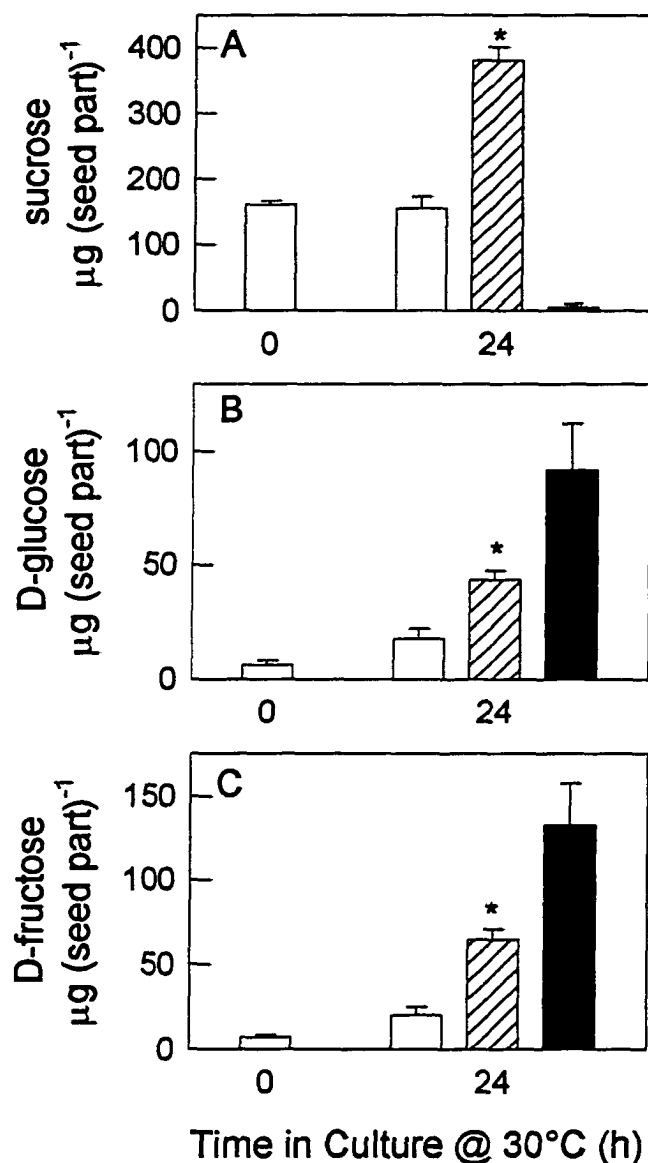


Figure 40. The effect of 9 DAI₃₀ seedling removal on megagametophyte specific carbohydrate levels after 24 h culture @ 30°C, measured indirectly by NADPH levels. A) Sucrose, B) D-glucose, and C) D-fructose levels. Megagametophyte level when cultured with the seedling (open bar), megagametophyte level when cultured alone (hatched bar), and level from exudate produced by megagametophyte cultured alone (filled bar). Each data point is the mean of three independent biological experiments assayed in duplicate \pm SE of the mean. *Statistical significance ($p < 0.05$) of differences in specific carbohydrates between the control megagametophytes cultured 24 h with seedlings and megagametophytes cultured alone was evaluated by the Student's t test.

megagametophytes during the 24 h period; high levels of D-glucose and D-fructose, but a low level of sucrose, were measured in the exudate droplet (Figs. 40A, B, C).

Because of the increase in D-glucose and D-fructose levels in isolated megagametophytes and their exudates, the invertase activity in this tissue and droplet was investigated. No significant increase in cell wall-associated (Fig. 41A) and soluble acidic (Figs. 41B, C) invertase activities were measured in megagametophytes isolated for 24 h compared to megagametophytes cultured with seedlings. However, acidic invertase activity was detected in the exudate droplet (Fig. 41B), which had a specific activity approximately half that found in the megagametophyte (Fig. 41C).

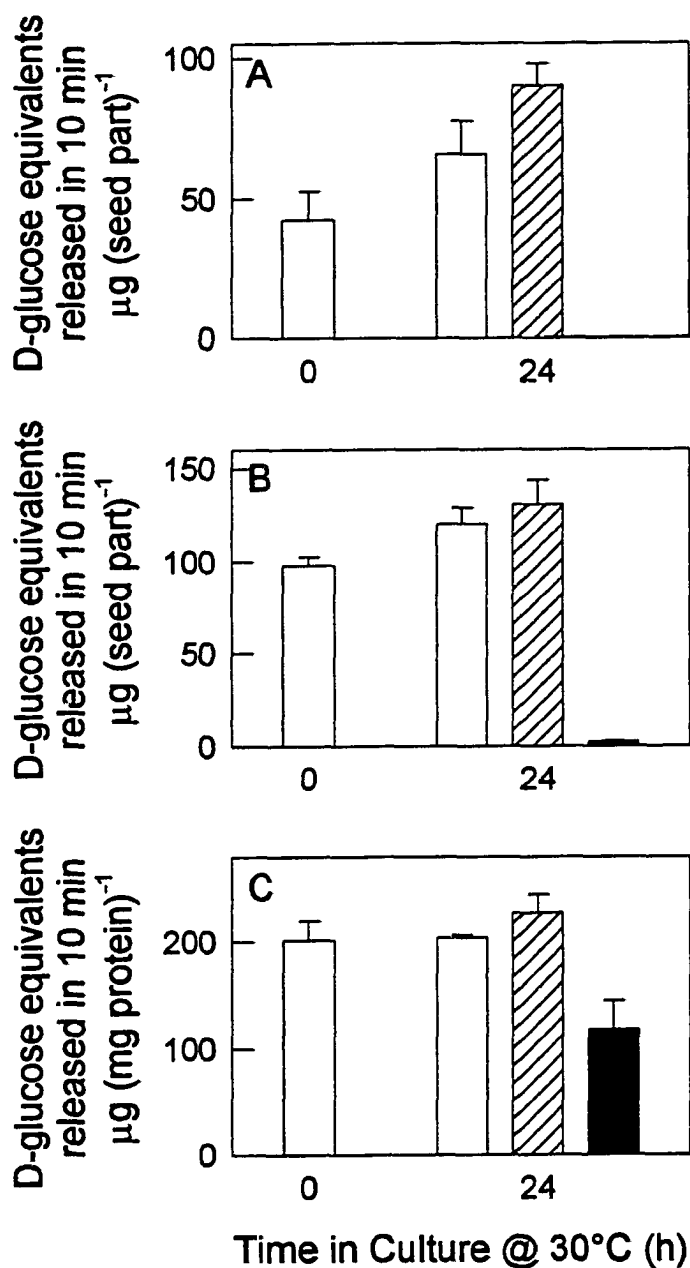


Figure 41. The effect of 9 DAI₃₀ seedling removal on megagametophyte invertase activities after 24 h culture @ 30°C. A) Cell wall-associated invertase activity per seed part, B) soluble acidic invertase activity per seed part, and C) soluble acidic invertase specific activity levels. Megagametophyte activity when cultured with the seedling (open bar), megagametophyte activity when cultured alone (hatched bar), and activity from exudate produced by megagametophyte cultured alone (filled bar). Each data point is the mean of three independent biological experiments each assayed in triplicate \pm SE of the mean. Invertase activity level differences between control megagametophytes cultured 24 h with seedlings and megagametophytes cultured alone were not statistically significant ($p > 0.05$) by evaluation with the Student's *t* test.

4. Discussion

4.1 The physical relationship between the seedling and megagametophyte

During Pinaceae seed development, the embryo develops and grows inside a fluid-filled corrosion cavity that was caused by the destruction of megagametophytic cells. It has been hypothesized that the cell walls remaining from this cellular degradation were pressed against the remaining megagametophyte tissue by the embryo as it completed its development, producing a carbohydrate-positive layer of material (De Carli *et al.*, 1987; JN Owens, personal communication). Alternatively, it is possible that this layer may have arisen by the secretion of substances from megagametophyte cells. In mature, desiccated seeds, the presence of cellulose and the multiple sheet-like appearance of the layer that was not completely attached to the megagametophyte cells lends support to its production from the pressed remains of megagametophyte cells. It is quite likely that during imbibition of the mature seed, other components are secreted into the layer, such as pectins that would increase the layer's malleability. Further histochemical staining is necessary to identify any additional components of the carbohydrate-positive layer.

During stratification, the cotyledons become fully hydrated and are closely pressed against one another, as well as to the carbohydrate-positive layer; thus the corrosion cavity is eliminated. As the cotyledons expand and grow during imbibition at 30°C, they spread out from one another, pressing further against the layer, leaving clear imprints of their epidermal cells. The hypocotyl is also in close contact with the layer while still inside the megagametophyte, as imprints of its epidermal cells are also present.

The limited space between the seedling and megagametophyte is not fluid filled; the megagametophyte and seedling are moist where they contact each other, but no extra liquid is present. This is in stark contrast to the corrosion cavity, which is fluid filled during the development of the seed.

After the completion of germination, loblolly pine seedlings develop in an epigeal growth pattern. Growth of the seedling is initially by the expansion and division of the radicle and hypocotyl cells, while the cotyledons remain inside the megagametophyte. After the radicle had penetrated the Kimpak support, the hypocotyl hook began to straighten and grow towards the light. In doing so, the cotyledons, still inside the megagametophyte, were lifted off the Kimpak support. As this occurred, the majority of stored TAG and protein reserves had not yet been broken down in the megagametophyte. Thus, it is extremely important for the seedling to not lose the megagametophyte prematurely, since the megagametophyte is the source of most of its nutrients. The role of the carbohydrate-positive layer is not fully understood at this time. Because this layer is both firm, due to the presence of cellulose, as well as malleable, possibly due to the presence of pectins, it may provide a substrate into which the cotyledons can spread and anchor in order to lift the megagametophyte. The malleability also allows the seedling to grow out of the megagametophyte without causing any damage to its epidermis. In addition, the carbohydrate-positive layer may also play a role in increasing the surface area of the megagametophyte in contact with the cotyledons. Since the carbohydrate-positive layer covers the entire corrosion cavity surface of the megagametophyte, the amino acids and carbohydrates resulting from

megagametophyte reserve breakdown must also move through the layer before they can be taken up by the seedling.

4.2 The transport of metabolites within the seedling

At around 6 DAI₃₀, loblolly pine seedlings have a complete xylem connection, and are capable of water uptake and transport to the cotyledons. The presence of helical thickenings on the cell walls of all the tracheids observed in the seedlings allowed for the large amount of cellular expansion that occurred during early seedling growth. Not only is the xylem important for water transport, but it has also been demonstrated that xylem can transport amino acids to a limited extent (Salisbury and Ross, 1992). Thus some of the amino acids produced in or imported by the seedling during early seedling growth could be transported throughout the seedling via the xylem. The tracheids differentiated first in the cotyledons and upper portion of the hypocotyl; the delay of lignification in the bottom half of the hypocotyl may be due to the tissue's rapid elongation. However, in stained paraffin sectioned *Pinus resinosa* seedlings, tracheids were observed in the hypocotyl before being seen in the cotyledons; no mention was made as to whether the tracheids were found throughout the hypocotyl, or in just one area (Sasaki and Kozlowski, 1969). While the xylem may play a role in amino acid transport, the majority of amino acids and carbohydrates are transported in the phloem. In *Pinus resinosa* seedlings, phloem differentiates earlier than xylem (Sasaki and Kozlowski, 1969). If that holds true for loblolly pine, then phloem must differentiate prior to 5 DAI₃₀, which would provide a means for amino acid and carbohydrate transport within the seedling during germination. Aniline blue staining of seedling sections or cleared whole seedlings

needs to be done to verify this. Unlike the seedling, the megagametophyte does not have a vascular system for the transport of amino acids and carbohydrates. It is unknown whether the transport of metabolites within the megagametophyte tissue occurs primarily through a symplastic or apoplastic route.

4.3 The breakdown and catabolism of stored TAG reserves

The majority of TAG reserve breakdown in loblolly pine occurred during early seedling growth, as was also observed in *Pinus edulis* (Hammer and Murphy, 1994). Fatty acids released from Pinaceae megagametophytic TAGs via lipase activity (Ching, 1968; Kovac and Wrischer, 1984; Hammer and Murphy, 1994) are oxidized by the β -oxidation spiral followed by the glyoxylate cycle (Firenzuoli *et al.*, 1968; Ching, 1970; Lopez-Perez *et al.*, 1974; Noland and Murphy, 1984; Pinzauti *et al.*, 1986; Mullen and Gifford, 1995a, 1995b, 1997). In relation to this, the maximum rate of TAG breakdown correlates well with the rate of activities of key enzymes involved in this process: isocitrate lyase (Mullen and Gifford, 1997), malate synthase (Mullen and Gifford, 1995b) and acyl CoA oxidase (Gifford, unpublished data).

Following germination, loblolly pine embryonic TAG reserves were also broken down, however the rate was approximately 10% of that measured in the megagametophyte; *Pinus edulis* was similar in this regard (Hammer and Murphy, 1994). Interestingly it is not at all certain how TAGs are broken down in the seedling. For example, in *P. edulis*, lipase activity was less than 10% of that in the megagametophyte (Hammer and Murphy, 1994). Also, very low isocitrate lyase and malate synthase activities were observed in loblolly pine seedlings (Mullen, 1995; Mullen and Gifford,

1995b), as well as seedlings of *Pinus pinea* (Firenzuoli *et al.*, 1968), *P. ponderosa* (Ching, 1970), *P. lambertiana* (Noland and Murphy, 1984) and *Abies alba* (Kovac and Wrischer, 1984). It is possible that loblolly pine seedlings do not possess an active glyoxylate cycle linked to gluconeogenesis. Instead, TAG breakdown may occur through the glyoxysomal β -oxidation spiral, releasing energy through the mitochondrial Krebs's cycle. Glyoxysomal β -oxidation followed by Krebs's cycle is thought to occur in non-lipid storing tissues. For example, glyoxysomes isolated from germinating barley embryos contained β -oxidation enzyme activity but no glyoxylate cycle enzyme activity (Holtman *et al.*, 1994), while in the aleurone layer, which contained relatively more lipid, both β -oxidation spiral and glyoxylate cycle enzyme activities were detected.

A number of loblolly pine seedling stages during germination and early seedling growth have recently been examined for acyl CoA oxidase activity. In contrast to the high activity measured in the megagametophyte during early seedling growth, no cell-free extract acyl CoA oxidase activity was detected in the seedling (Gifford, unpublished data). However, it has recently been demonstrated by Western blotting that 9 DAI₃₀ loblolly pine shoot poles do contain very low levels of acyl CoA oxidase enzyme (Gifford, unpublished data). The low activity and/ or protein levels of both the key β -oxidation and glyoxylate cycle enzymes (Mullen, 1995; Mullen and Gifford, 1995b) does not support the hypothesis that embryonic TAGs are catabolized through the β -oxidation spiral followed by the Krebs's cycle. The low activities/ protein levels of lipase, β -oxidation enzymes and glyoxylate cycle enzymes, and the relatively slow rate of TAG breakdown measured, may all be due to the fact that there is a relatively low amount of TAG stored in the Pinaceae embryo, compared to the megagametophyte. In

order to study the metabolism of embryonic TAGs further, a more sensitive approach is necessary. Pulse-chase experiments may provide that approach. Embryonic TAG reserve depletion occurred primarily 4 - 10 DAI₃₀, so seedlings in these seeds should have a relatively active glyoxylate cycle and gluconeogenesis pathway if their metabolism is similar to megagametophytes. The cotyledons of seedlings removed from their megagametophytes during these stages could be pulse-chased with [2-¹⁴C]sodium acetate, and the radiolabeled metabolites could be identified. The production of radiolabeled carbohydrate would be an indication that the glyoxylate cycle and gluconeogenic pathway are active, albeit in low levels, in the seedlings during early seedling growth.

4.4 The dynamics of reserve breakdown in the seedling

The rapid and early breakdown of protein and TAG reserves in the root poles of loblolly pine may have been due to the large amount of energy and building materials the radicle required for the rapid growth and elongation that occurs during and after germination. Similar observations of rapid breakdown of protein vacuoles and lipid bodies in hypocotyl/ radicles have been made in *Picea abies* (Simola, 1974b, 1976), *P. excelsa* (De Carli *et al.*, 1987) and *Pinus sylvestris* (Simola, 1974a).

Conversely, the slow and incomplete breakdown of TAG in the shoot pole may be due to the constant import of metabolites from the megagametophyte. During early seedling growth, when the majority of TAG breakdown occurred in the megagametophyte, only the cotyledons of the seedling were in contact with the megagametophyte. The constant flow of carbohydrates, amino acids (King and Gifford,

1997) and other metabolites from the megagametophyte into the seedling may inhibit key enzymes of TAG catabolism. For instance, gene expression of acyl CoA oxidase, the key β -oxidation spiral enzyme, was repressed by D-glucose, but not sucrose, in yeast (Wang *et al.* 1992). However sucrose, as well as glucose, fructose and raffinose repressed the expression of isocitrate lyase and malate synthase genes in cucumber cell cultures (Graham *et al.*, 1994). It is unknown whether specific carbohydrates similarly repress the TAG catabolism genes, or inhibit their enzyme activity in loblolly pine. The level of soluble carbohydrates was approximately equal in both the shoot and root poles of the seedling; however the specific carbohydrates in each pole have not been determined. It is possible that the carbohydrates are present in different proportions in the shoot and root poles.

Because the cotyledons became green and had GO activity during early seedling growth, the slow rate of reserve depletion in the shoot pole could also be due to a redistribution of energy. In the presence of an adequate flow of metabolites from the megagametophyte, the cotyledons may expend less energy on maintaining enzymes involved in reserve metabolism, and expend more energy on the creation and maintenance of photosynthetic machinery. The pool of TAGs remaining in the cotyledons at 12 DAI₃₀ may be due to the lack of TAG catabolizing enzymes or it may be a basal level required for the synthesis of new membrane components by the cotyledons.

4.5 The movement of carbohydrates from the megagametophyte to the seedling

The breakdown and metabolism of TAG reserves is often accompanied by an increase in the carbohydrate pool size in the storage organ, as in castor bean endosperm (Huang and Beevers, 1974). However, as TAGs decreased in loblolly pine megagametophytes, there was only a minor increase in the megagametophyte carbohydrate pool; a rather major increase in the carbohydrate pool of the seedling was observed. The same trend also occurred in *Pseudotsuga menziesii* (Ching, 1966), *Pinus taiwanensis* (Kao, 1973), and *Cunninghamia lanceolata* (Kao, 1973). The lack of significant carbohydrate accumulation in the megagametophyte may be due to their rapid export from the megagametophyte at a rate that paralleled the rate of TAG breakdown. A similar lack of accumulation of free amino acids also occurred in megagametophytes of loblolly pine (King and Gifford, 1997), *Pinus banksiana* (Ramaiah *et al.*, 1971) and *Pseudotsuga menziesii* (Ching, 1966); this indicates that rapid export of amino acids also occurs. Evidence that the large carbohydrate pool in the seedling was due to import from the megagametophyte, was provided by the fact that in the absence of the megagametophyte the seedling was not capable of generating these large carbohydrate pools from its own TAG reserves. Loblolly pine seedlings were similarly unable to accumulate a large pool of amino acids in the absence of megagametophytes (King and Gifford, 1997).

The rapid export of carbohydrates from the megagametophyte was further supported by [2-¹⁴C]sodium acetate radiolabeling and pulse-chase experiments. In both the labeling as well as the pulse-chase experiments, radioactively labeled metabolites were exported from the loblolly pine megagametophyte to the seedling; the majority of

seedling import occurred after 60 minutes. Because of the large amount of carbohydrate labeled in the megagametophyte, it is likely that the carbohydrates are exported to the seedling. To verify this, the pulse-chase products need to be fractionated to see if the carbohydrates labeled in the megagametophyte are exported to the seedling during the chase period.

Sucrose is generally considered to be the carbohydrate that is transported to the seedling during the germination of oilseeds (Bewley and Black, 1994), such as castor bean (Kriedemann and Beevers, 1967). It has long been speculated that the end-product of gluconeogenesis in the germinated conifer megagametophyte is also sucrose (Ching, 1972; Kao, 1973; Murphy and Hammer, 1994). Due to the relatively large amount of sucrose present in the megagametophyte during early seedling growth, it also appears that sucrose was the primary product of TAG breakdown in loblolly pine megagametophytes.

In some developing seed systems in which the carbohydrates are transported across an apoplastic space, sucrose is hydrolyzed to maintain an appropriate metabolite gradient for export. Since the export of carbohydrates from the megagametophyte to seedling also involves crossing the apoplast, the possible involvement of a sucrose cleaving enzyme was investigated. In faba bean, carbohydrates are exported from the maternal seed coat, across an apoplastic space to the developing embryo. During early embryonic development when the embryo is an inefficient sink, a cell-wall associated invertase cleaves sucrose as it leaves the seed coat, resulting in a high D-glucose and D-fructose to sucrose ratio in the apoplast bathing the embryo (Weber *et al.*, 1995). During this time, a hexose transporter gene is expressed in the developing cotyledons

(Weber *et al.*, 1997). Later, after the cotyledons have developed fully and are in contact with the seed coat, the expression of the hexose transporter gene declines and the seed coat invertase activity declines. At the time of this switch, the cotyledons develop transfer cell morphology and express a sucrose transporter gene in the cotyledon protoderm. Correlated with the sucrose transporter gene expression was a low D-glucose and D-fructose to sucrose ratio in the embryo (Weber *et al.*, 1997).

In loblolly pine, soluble acidic invertase activity began to increase during germination in both megagametophytes and seedlings. This enzyme is often associated with tissues that are undergoing rapid growth and development (as reviewed by Avigad, 1982) and may play a similar role in the rapidly growing seedling of loblolly pine. Enzymes involved in TAG reserve breakdown in loblolly pine megagametophytes, such as acyl CoA oxidase, isocitrate lyase and malate synthase, each showed a peak in activity during early seedling growth, followed by a decline (Mullen, 1995; Mullen and Gifford, 1995b; Gifford, unpublished data). The cell wall-associated invertase activity in both the megagametophyte and seedling increased during early seedling growth, but did not decline. The cell wall-associated activity levels were also lower than that found for the soluble acidic invertase in both tissues. If the seedling was receiving D-glucose and D-fructose, or receiving sucrose that was immediately cleaved to D-glucose and D-fructose, the levels of these two carbohydrates should be relatively high in the seedling during early seedling growth. Since they were not, and sucrose levels were high and increased during this time period, it seems likely that a sucrose cleaving enzyme, such as invertase, was not involved in the transport of carbohydrate to the seedling. Sucrose would seem to be the most likely carbohydrate imported by loblolly pine seedlings.

Sucrose also accumulated during early seedling growth in *Pinus lambertiana* (Murphy and Hammer, 1988), *P. edulis* (Murphy, *et al.*, 1992) and castor bean (Kriedemann and Beevers 1967) seedlings. A similar sucrose increase was also noted in *P. thunbergii* (Hattori and Shiroya, 1951), although it was unclear whether the seedling alone, or the seedling with its megagametophyte, was analyzed. In castor bean, the level of sucrose remained high in the seedling because the sucrose transported from the endosperm to the cotyledons of the seedling was maintained as sucrose when transported to the radicle (Kriedemann and Beevers, 1967), but it is unknown whether this is also the case for seedlings of loblolly pine, or other conifer seedlings.

Despite its probable importance in conifer seed germination, sucrose transport to the conifer seedling has received limited attention. Murphy and Hammer (1994) delivered ^{14}C -sucrose to the corrosion cavity of 10 day incubated *Pinus edulis* seeds, and demonstrated that both the seedling and megagametophyte tissues were capable of sucrose uptake. However, they did not provide any evidence that sucrose was the carbohydrate normally exported from the megagametophyte to the seedling *in vivo*. Carrier and co-workers (1997) also showed that sucrose was a requirement for the germination of excised zygotic and somatic embryos of interior spruce. However, the lack of a megagametophyte made it difficult to assess the importance of sucrose delivery to the germinating seedling *in vivo*. To ascertain the carbohydrates that are exported from the megagametophyte to the developing seedling, pulse-chase experiments with radiolabeled substrates applied to the outside of intact megagametophytes with seedlings must be conducted, and the specific carbohydrates made and exported identified.

4.6 Starch storage

Starch in the megagametophyte is transient; the localization of starch in the megagametophyte next to the radicle may either be an indication that TAG breakdown is initiated in that area, or carbohydrates are reallocated to that area to be exported to the energy requiring radicle. At this time the seedling's metabolism of imported carbohydrates may be relatively slow, which may lead to a temporary and minor build up of carbohydrates in the megagametophyte. The metabolism of imported carbohydrates in the seedling is likely occurring at a higher rate during the rest of early seedling growth, since the megagametophyte carbohydrate levels decline and seedlings accumulate starch. Starch also accumulated in seedlings of *Abies alba* (Kovac and Kregar, 1989), *Pseudotsuga menziesii* (Ching, 1966), *Picea excelsa* (De Carli *et al.*, 1987) and *Pinus edulis* (Murphy and Hammer, 1994). In loblolly pine the starch grain tissue distribution in the hypocotyl varied depending on whether it was still inside or was outside the megagametophyte. The hypocotyl tissue next to the megagametophyte probably received metabolites directly from the megagametophyte and may convert the carbohydrates to starch in the outer portion of the cortex in order to maintain an appropriate metabolite gradient for import. Once the hypocotyl tissue has emerged from the megagametophyte, it is no longer receiving metabolites directly from the megagametophyte, but is receiving them from the cotyledons via the phloem. The production of starch in the cells surrounding the vascular bundles is likely necessary to maintain a proper soluble carbohydrate gradient for phloem unloading (Zamski, 1996). Loblolly pine seedlings accumulated starch during early seedling growth that was approximately 10% of the level accumulated in *Pinus edulis* seedlings during early

seedling growth (Murphy and Hammer, 1994). *P. edulis* seedlings were grown in a dark chamber with only periodic exposures to light for watering (Murphy and Hammer, 1994, personal communication); thus the starch that accumulated in these seedlings was due to heterotrophic metabolism. In contrast, the loblolly pine seedlings in this study were grown under continuous low light levels and may have accumulated some starch due to low level photosynthesis. Under these growth conditions, one would expect the seedling grown in the light to accumulate more starch than the seedling grown in the dark, not vice versa. It is unlikely that the different growth conditions account for the difference in starch accumulation noted here. It is more likely that the extra starch accumulated in *P. edulis* seedlings is due to the amount of TAG originally stored in the megagametophyte. *P. edulis* seeds were much larger than loblolly pine, and thus also contained a larger megagametophyte. Each *P. edulis* mature megagametophyte stored approximately 105 mg of TAG (Hammer and Murphy, 1994), compared to 2.5 mg stored in loblolly pine. Thus *P. edulis* seedlings may receive approximately 40-fold more carbohydrates due to megagametophyte TAG reserve metabolism. This exemplifies just one inherent difference between *Pinus* species that has yet to be explored further.

4.7 Are Pinaceae seed storage proteins glycosylated?

Storage proteins are often glycosylated (Shewry *et al.*, 1995); this has led to the speculation that some of the Pinaceae storage proteins may also be glycosylated. The PAS staining of protein vacuoles in *Picea abies* (Simola, 1974b, 1976) has previously been considered as evidence supporting the glycosylation of storage proteins. This staining of protein vacuoles is not isolated to *P. abies*, but also occurs in *P. glauca*

(Krasowski and Owens, 1993), as well as in loblolly pine. Conversely, Durzan *et al.* (1971) observed that the protein vacuoles in *Pinus banksiana* did not stain with PAS. It seems unlikely that the protein vacuole staining is an indication of storage protein glycosylation since it has more recently been shown that none of the proteins stored in mature seeds of nine species of *Pinus* and *Picea glauca* are glycosylated when separated using SDS-PAGE and stained with PAS (Gifford, 1988; Gifford and Tolley, 1989; Misra and Green, 1990). So what is causing the carbohydrate staining of protein vacuoles? They don't appear to contain starch, since they did not stain with potassium iodide in *Picea abies* (Simola, 1976). It was noticed in loblolly pine (this study) that protein vacuoles stained relatively more intensely for carbohydrate 35 DAI₂, compared to mature seeds. Similar observations have not been made for other Pinaceae seeds. During this stratification period in loblolly pine, soluble carbohydrate levels increased in both the megagametophyte and embryo (Gifford, unpublished data). It is possible that these soluble carbohydrates are stored inside protein vacuoles. The protein vacuoles density may provide some protection to the carbohydrates, during the tissue fixation and processing, as well as the PAS staining procedure, that usually removes the water-soluble carbohydrates.

4.8 The development of photosynthetic competence in the seedling

The timing of photosynthetic competence in Pinaceae seedlings has interested many researchers, because of the observation that seedling tissues begin to green, and thus may be capable of photosynthesis, while still inside the megagametophyte (Bogorad, 1950; Sasaki and Kozłowski, 1969). The early greening, presence of stomata, and

increase in shoot pole GO activity during its early growth, all lend support to the hypothesis that the seedling is capable of supplementing the metabolites it is receiving from the megagametophyte with photosynthate produced by the cotyledons as they emerge. Oxygen release due to photosynthesis was measured from cotyledons midway through early seedling growth in *Picea excelsa*. At this stage, the cotyledons were green and were about to emerge from the megagametophyte (De Carli *et al.*, 1987).

Photosynthesis and photorespiration require light to occur (Goodwin and Mercer, 1983). However, light is not a requirement in *Pinus* and *Picea* seedlings for chloroplast development, chlorophyll accumulation, light harvesting complex production, RuBisCO accumulation, as well as other factors involved in photosynthesis (Wieckowski and Goodwin, 1966; Lewandowska and Öquist, 1980; Selstam and Widell, 1986; Mariani *et al.*, 1990; Canovas *et al.*, 1991, 1993; Jansson *et al.*, 1992; Garcia-Gutierrez *et al.*, 1995). This implies that the seedling can produce its photosynthetic machinery prior to emergence from the megagametophyte, and may be prepared to photosynthesize when irradiated with light. The question as to when photosynthesis begins during seedling development has yet to be answered. To address this, GO activity was measured as an indicator of the earliest possible time of photosynthetic competence. GO was chosen because photorespiration is directly linked to photosynthesis through the oxygenase activity of RuBisCO. The initiation of greening, emergence from the megagametophyte, and the formation of stomatal complexes all occurred in the hypocotyl before it occurred in the cotyledons. Correlated with this trend was the specific activity of GO, which increased in the root pole before it increased in the shoot pole. However, due to the low level of phosphate buffer-soluble protein in the root pole, GO activity per seed part only

increased in the shoot pole during early seedling growth. This indicated that photosynthesis could only be occurring in the cotyledons as they emerged from the megagametophyte.

Supporting the rapid onset of photosynthesis as the cotyledons emerge from the megagametophyte is the presence of stomatal complexes on tissues inside the megagametophyte. Each of these stomatal complexes contained a stomatal aperture with guard cell wall thickenings around that aperture as well as a substomatal chamber. Stomatal complexes were also observed on *Pinus resinosa* hypocotyls (Sasaki and Kozlowski, 1969) and *P. radiata* cotyledons (Riding and Aitken, 1982) prior to the emergence of the tissue from the megagametophyte. The functionality of the stomatal complexes in emerging seedling tissues is further supported by the presence of guard cell walls that contain lignin thickenings around the stomatal aperture, and the presence of subsidiary cells arched over the guard cells. It has been hypothesized that the lignin thickenings of guard cells function in opening and closing the stoma aperture (Kaufman, 1927 as described in Fahn, 1990). Guard cells containing lignin have been reported in other conifers, as well as other gymnosperms, vascular cryptogams, and some species of angiosperms ((Kaufman, 1927; Florin, 1931, 1933) as described in Fahn, 1990; Fuchs, 1963; Boulter, 1970).

Photosynthesis may be initiated during early seedling growth, but it is likely that this process plays a minor role in seedling nutrition. During this period, the majority of seedling nutrition is provided by the breakdown of seed reserves, primarily in the megagametophyte. In relation to seedling nutrition, the premature removal of the megagametophyte near the end of early seedling growth, affected the elongation of the

hypocotyl-radicle and cotyledons of *Pinus resinosa* (Sasaki and Kozlowski, 1969) and *P. strobus* (Tabor and Barnett, 1987), as well as the primary needles of *P. resinosa* (Sasaki and Kozlowski, 1969). By 12 DAI₃₀, near the end of the early seedling growth, the seedling must be nearly or completely photosynthetically independent. Certainly chloroplasts, mitochondria and microbodies (presumably leaf-type peroxisomes) were present in both the hypocotyl and cotyledons by this time. The cotyledons of many conifer species, including loblolly pine, remain green and attached to the seedling often for several months (Durzan *et al.*, 1971; De Carli *et al.*, 1987). Their contribution to photosynthetic production by the seedling relative to needles has yet to be determined.

4.9 The role of the seedling in the maintenance of megagametophyte metabolism

The embryonic axis controls the initiation of storage reserve breakdown in most angiosperm seeds, such as castor bean (Gifford *et al.*, 1984), mung bean (Kern and Chrispeels, 1978) and cucumber (Davies and Chapman, 1979). However, loblolly pine embryos do not exert a similar control over the megagametophyte, since mature and 35 DAI₂ megagametophytes have the ability to initiate the breakdown of their protein (King and Gifford, 1997; King, 1998) and TAG (Gifford, unpublished data) reserves without an embryo.

Mature loblolly pine megagametophytes cultured without embryos initiated TAG breakdown; however after 3 days in culture TAG breakdown stopped and the level then remained constant (Gifford, unpublished data). This may be due to feedback inhibition, since in the present study isolated 35 DAI₂ megagametophytes accumulated 80% ethanol-soluble carbohydrate between 1 and 3 days. The buildup of soluble

carbohydrates in the megagametophyte without an efficient sink to remove them also caused a shift in metabolism resulting in the accumulation of an insoluble carbohydrate between 3 and 4 days in culture. Interestingly, this insoluble carbohydrate was not starch. Possibly this carbohydrate was a non-native form of starch, such as an oxidized or phosphorylated form, since the enzymatic starch assay used would only produce NADPH from D-glucose, and not from phosphorylated glucose. However, to my knowledge, no non-native forms of starch has been identified in plants. The 80% ethanol-insoluble storage form could be “pure” mannan or glucomannan deposits in the cell walls, since these have been described as cellulose-like and are water-insoluble (Meier and Reid, 1982). The “pure” mannans are linear (1 → 4)-β linked chains composed of >90% D-mannose residues, while the glucomannans form similar chains in which some of the D-mannose residues are replaced by D-glucose (Meier and Reid, 1982). Although neither mannan type has been identified in conifer megagametophytes, mannose residues have been measured in hydrolyzed hemicellulose fractions from mature megagametophyte cell walls of *Picea glauca* (Downie *et al.*, 1997). Furthermore, the activity of endo-β-mannanase, an enzyme that hydrolyzes mannans, is present during germination and early seedling growth in megagametophytes of *P. glauca*, as well as six other Pinaceae species (Dirk *et al.*, 1995). Thus during the development of the megagametophyte, mannose-containing polysaccharides were deposited into cell walls; perhaps under the artificial conditions of culture the isolated megagametophytes shift their metabolism to add similar deposits to their cell walls. Additional studies are necessary for the identification of this insoluble carbohydrate.

Over a 24 h period, 9 DAI₃₀ megagametophytes cultured without seedlings continued to produce and export amino acids (King, 1998) and carbohydrates. When propped so that the corrosion cavity would fill, the exported amino acids and carbohydrates collected in an exudate droplet. Surprisingly the exudate droplet contained predominantly more D-glucose and D-fructose than sucrose. This was likely due to invertase activity since soluble acidic invertase activity was measured in the exudate. King (1998) showed that a small quantity of protein was also found in this exudate droplet in loblolly pine.

4.10 Senescence of the megagametophyte

TAG and phosphate buffer-insoluble protein comprise $27 \pm 0.8\%$ and $15 \pm 0.2\%$ of the mature loblolly pine megagametophyte's dry weight, respectively. By 10 DAI₃₀, approximately two-thirds of the megagametophyte TAG and insoluble protein reserves had been broken down and the tissue was beginning to senesce. Following 10 DAI₃₀, isocitrate lyase, malate synthase and catalase activities declined (Mullen, 1995; Mullen and Gifford, 1995b). At 12 DAI₃₀, electron-dense non-membrane bound clumps of amorphous material were observed in the megagametophyte cells, but not in the seedling cells. These clumps varied between 1.5 - 5 μm in size and may be the remainder of organelles broken down due to senescence of the megagametophyte. Lipid bodies were still present in the megagametophyte cells, and were often in close contact with microbodies. The microbodies often contained cytoplasmic inclusions. These cytoplasmic inclusions were probably not related to senescence, as the microbodies containing these have also been observed during the initial stages of early seedling

growth in megagametophytes of *Pinus ponderosa* (Ching, 1970), *P. sylvestris* (Simola, 1974a) and *P. pinea* (Lopez-Perez *et al.*, 1974), and cotyledons of tomato (Newcomb, 1982), cucumber and sunflower (Gruber *et al.*, 1970).

GO is a key enzyme of photorespiration and is usually present in high levels in the leaf-type peroxisome (Huang, *et al.*, 1983). However, GO is not limited to using glycolic acid as a substrate, but can also use several other α -hydroxyacids, such as L-lactic acid and oxalate (Masters and Crane, 1995). Perhaps because of its multiple substrates, GO is found in low levels in all types of peroxisomes, not just leaf-type peroxisomes involved in photorespiration (Vigil, 1970; Thomas and Trelease, 1981). GO activity has been observed previously in other non-photosynthetic plant tissues such as castor bean endosperm during early seedling growth, castor bean root during germination, potato tuber and carrot root (Huang and Beevers, 1971; Huang and Beevers, 1973). It has also been found in senescing green cotyledons of cucumber (Kim and Smith, 1994) and *Brassica napus* (Vincentini and Matile, 1993), although GO activity levels were lower than that found in the cotyledons during their photosynthetic stages. During the late stages of early seedling growth GO specific activity in loblolly pine megagametophyte began to rapidly increase. GO may play an important role in senescent tissue, as a scavenger of α -hydroxyacids. The increasing specific activity of this enzyme is an indication that GO is an important component of the megagametophyte enzyme complement during the later stages of early seedling growth. Other enzymes are thought to be important in the process of senescence. Isocitrate lyase and malate synthase protein levels and enzyme activities were shown to increase during senescence of cotyledons of pumpkin (De Bellis and Nishimura, 1991; Nishimura *et al.*, 1993),

cucumber (McLaughlin and Smith, 1995) and *B. napus* (Vincentini and Matile, 1993). It is thought that these glyoxylate cycle enzymes are involved in membrane lipid catabolism (Olsen, 1998). Carboxypeptidases have also been shown to increase in activity during late stages of early seedling growth and are thought to act as protein scavengers during senescence of megagametophytes of *Pinus contorta* (Gifford *et al.*, 1989) and *P. sylvestris* (Salmia and Mikola, 1976b).

4.11 Future directions

In this study, it has been demonstrated that seedlings breakdown their TAG reserves, but there still remains the question of how those TAGs are broken down. Why is the rate of TAG breakdown slower in the seedling than in the megagametophyte? Why doesn't the seedling completely deplete its TAG reserves?

It has also been demonstrated that metabolites are rapidly exported to the seedling. Does the carbohydrate-positive layer of the megagametophyte play any role in the trapping of metabolites, or is it simply a supportive layer that acts as a conduit for metabolite transport? By using tissue printing throughout a pulse-chase radiolabel experiment, it may be possible to observe any build up of radioactivity in this layer. Conversely this may also be done by pulse-chasing with a fluorescently tagged metabolite (as long as the fluorescent tag is relatively small) and observing the outcome with confocal laser microscopy. How does carbohydrate uptake occur in the seedling? Does it involve sucrose and hexose transporters? Does it require an enzymatic hydrolysis step? Is the mechanism of uptake the same throughout early seedling growth?

It has also been shown that the seedlings may be capable of photosynthesis throughout early seedling growth. What is the relationship between the loss of heterotrophy and the onset of autotrophy in the seedling? When does photosynthesis begin in the seedling? How much does the photosynthate contribute to the seedling's nutrition?

There are many interesting questions that require further investigation. It is clear that we have only scratched the surface of understanding the complex and interrelated activities occurring during germination and early seedling growth in loblolly pine.

5. Literature Cited

- Allona I, R Casado, C Aragoncillo 1992 Seed storage proteins from *Pinus pinaster* Ait.: homology of major components with 11S proteins from angiosperms. *Plant Science* 87: 9-18.
- Allona I, R Casado, C Aragoncillo 1994a Biochemical genetics of a 7S globulin-like protein from *Pinus pinaster* seeds. *Theor Appl Genet* 88: 454-459.
- Allona I, C Collada, R Casado, C Aragoncillo 1994b 2S arginine-rich proteins from *Pinus pinaster* seeds. *Tree Physiol* 14: 211-218.
- Allona I, C Collada, R Casado, C Aragoncillo 1994c Electrophoretic analysis of seed storage proteins from gymnosperms. *Electrophoresis* 15: 1062-1067.
- Arahira M, C Fukazawa 1994 *Ginkgo* 11S seed storage protein family mRNA: unusual Asn-Asn linkage as post-translational cleavage site. *Plant Mol Biol* 25: 597-605.
- Attree SM, MK Pomeroy, LC Fowke 1992 Manipulation of conditions for the culture of somatic embryos of white spruce for improved triacylglycerol biosynthesis and desiccation tolerance. *Planta* 187: 395-404.
- Avigad G 1982 Sucrose and other disaccharides. Pages 217-347 in FA Loewus, W Tanner, eds. *Encyclopedia of Plant Physiology*. Vol 13A. *Plant Carbohydrates I: Intracellular Carbohydrates*. Springer-Verlag, New York.
- Baker SS, CL Rugh, FW Whitmore, JC Kamalay 1996 Genes encoding 11S-globulin-like proteins are expressed in the megagametophyte soon after fertilization in eastern white pine (*Pinus strobus* L.). *Int J Plant Sci* 157: 453-461.
- Baldan B, A Bonaldo, N Rascio, A Vitale, F Meggio, P Profumo, P Mariani 1995 *Cercis siliquastrum* L.: a comparative study of endosperm and embryo development and reserve accumulation. *Int J Plant Sci* 156: 181-187.
- Baron FJ 1978 Moisture and temperature in relation to seed structure and germination of sugar pine (*Pinus lambertiana* Dougl.). *Amer J Bot* 65: 804-810.
- Bergfeld R, Y-N Hong, T Kühnl, P Schopfer 1978 Formation of oleosomes (storage lipid bodies) during embryogenesis and their breakdown during seedling development in cotyledons of *Sinapis alba* L. *Planta* 143: 297-307.
- Bewley JD, M Black 1994 *Seeds: physiology of development and germination*. 2nd edition. Plenum Press, New York.

- Bianco J, G Garello, MTL Page-Degivry 1997 *De novo* ABA synthesis and expression of seed dormancy in a gymnosperm: *Pseudotsuga menziesii*. *Plant Growth Regul* 21: 115-119.
- Bogorad L 1950 Factors associated with the synthesis of chlorophyll in the dark in seedlings of *Pinus jeffreyi*. *Bot Gaz* 111: 221-241.
- Boulter MC 1970 Lignified guard cell thickenings in the leaves of some modern and fossil species of Taxodiaceae (Gymnospermae). *Biol J Linn Soc* 2: 41-46.
- Bradford MM 1976 A rapid and sensitive method for the quantification of microgram quantities of protein utilizing the principle of protein-dye binding. *Anal Biochem* 72: 248-254.
- Briggs C 1993 Endosperm development in *Solanum nigrum* L. Formation and distribution of lipid bodies. *Ann Bot* 72: 295-301.
- Bronner R 1975 Simultaneous demonstration of lipids and starch in plant tissues. *Stain Technol* 50: 1-4.
- Brown MJ, JS Greenwood 1990 Involvement of the golgi apparatus in crystalloid protein deposition in *Ricinus communis* cv Hale seeds. *Can J Bot* 68: 2353-2360.
- Burk RR, M Eschenbruch, P Leuthard, G Steck 1983 Sensitive detection of proteins and peptides in polyacrylamide gels after formaldehyde fixation. *Methods Enzymol* 91: 247-254.
- Cánovas FM, FR Cantón, F Gallardo, A García-Gutiérrez, A de Vicente 1991 Accumulation of glutamine synthetase during early development of maritime pine (*Pinus pinaster*) seedlings. *Planta* 185: 372-378.
- Cánovas FM, FR Cantón, A García-Gutiérrez, F Gallardo, R Crespillo 1998 Molecular physiology of glutamine and glutamate biosynthesis in developing seedlings of conifers. *Physiol Plant* 103: 287-294.
- Canovas F, B McLarney, J Silverthorne 1993 Light-independent synthesis of LHC IIb polypeptides and assembly of the major pigmented complexes during the initial stages of *Pinus palustris* seedling development. *Photosynth Res* 38: 89-97.
- Cao YZ, AHC Huang 1986 Diacylglycerol acyltransferase in maturing oil seeds of maize and other species. *Plant Physiol* 82: 813-820.
- Cardemil L, A Reiner 1982 Changes of *Araucaria araucana* seed reserves during germination and early seedling growth. *Can J Bot* 60:1629-1638.

- Carpita NC, A Skaria, JP Barnett, JR Dunlap 1983 Cold stratification and growth of radicles of loblolly pine (*Pinus taeda*) embryos. *Physiol Plant* 59: 601-606.
- Carrier DJ, JE Cunningham, DC Taylor, DI Dunstan 1997 Sucrose requirements and lipid utilization during germination of interior spruce (*Picea glauca engelmannii* complex) somatic embryos. *Plant Cell Rep* 16: 550-554.
- Casey R, C Domoney, N Ellis 1986 Legume storage proteins and their genes. Pages 1-95 in *Oxford surveys of plant molecular and cell biology*. Vol 3. Oxford University Press, Oxford.
- Chamberlain CJ 1957 *Gymnosperms: structure and evolution*. University of Chicago Press. Chicago, IL, USA. 484 pp.
- Chatthai M, S Misra 1998 Sequence and expression of embryogenesis-specific cDNAs encoding 2S seed storage proteins in *Pseudotsuga menziesii* [Mirb.] Franco. *Planta* 206: 138-145.
- Ching TM 1966 Compositional changes of Douglas fir seeds during germination. *Plant Physiol* 41: 1313-1319.
- Ching TM 1968 Intracellular distribution of lipolytic activity in the female gametophyte of germinating Douglas fir seeds. *Lipids* 3: 482-488.
- Ching TM 1970 Glyoxysomes in megagametophytes of germinating ponderosa pine seeds. *Plant Physiol* 46: 475-482.
- Ching TM 1972 Metabolism of germinating seeds. Pages 103-218 in TT Kozlowski, ed. *Seed Biology*. Vol 2. Germination control, metabolism, and pathology. Academic Press, New York.
- Chou K-H, WE Splittstoesser 1972 Changes in amino acid content and the metabolism of γ -aminobutyrate in *Cucurbita moschata* seedlings. *Physiol Plant* 26: 110-114.
- Chrispeels MJ 1980 The endoplasmic reticulum. Pages 389 - 412 in NE Tolbert, ed. *The Biochemistry of Plants*. Vol 1. Academic Press, Toronto.
- Chrispeels MJ, TJL Higgins, S Craig, D Spencer 1982a Role of the endoplasmic reticulum in the synthesis of reserve proteins and the kinetics of their transport to protein bodies in developing pea cotyledons. *J Cell Biol* 93: 5-14.
- Chrispeels MJ, TJL Higgins, S Craig, D Spencer 1982b Assembly of storage protein oligomers in the endoplasmic reticulum and processing of the polypeptides in the protein bodies of developing pea cotyledons. *J Cell Biol* 93: 306-313.

- Collada C, I Allona, P Aragoncillo, C Aragoncillo 1993 Development of protein bodies in cotyledons of *Fagus sylvatica*. *Physiol Plant* 89: 354-359.
- Craig S 1988 Structural aspects of protein accumulation in developing legume seeds. *Biochemie und Physiologie der Pflanzen* 183: 159-171.
- Cummins I, MJ Hills, JHE Ross, DH Hobbs, MD Watson, DJ Murphy 1993 Differential, temporal and spatial expression of genes involved in storage oil and oleosin accumulation in developing rapeseed embryos: implications for the roll of the oleosins and the mechanisms of oil-body formation. *Plant Mol Biol* 23: 1015-1027.
- Davies HV, JM Chapman 1979 The control of food mobilization in seeds of *Cucumis sativus* L. I. The influence of embryonic axis and testa on protein and lipid degradation. *Planta* 146: 579-84.
- De Bellis L, M Nishimura 1991 Development of enzymes of the glyoxylate cycle during senescence of pumpkin cotyledons. *Plant Cell Physiol* 32: 555-561.
- De Carli ME, B Baldan, P Mariani, N Rascio 1987 Subcellular and physiological changes in *Picea excelsa* seeds during germination. *Cytobios* 50: 29-39.
- Derbyshire E, DJ Wright, D Boulter 1976 Legumin and vicilin, storage proteins of legume seeds. *Phytochem* 15: 3-24.
- Dirk LM, AM Griffen, B Downie, JD Bewley 1995 Multiple isozymes of endo- β -D-mannanase in dry and imbibed seeds. *Phytochem* 40: 1045-1056.
- Downie B, JD Bewley 1996 Dormancy in white spruce (*Picea glauca* [Moench.] Voss.) seeds is imposed by tissues surrounding the embryo. *Seed Science Research* 6: 9-15.
- Downie B, HWM Hilhorst, JD Bewley 1997 Endo- β -mannanase activity during dormancy alleviation and germination of white spruce (*Picea glauca*) seeds. *Physiol Plant* 101: 405-415.
- Dubois M, KA Billes, JK Hamilton 1956 Colorimetric method for determination of sugars and related substances. *Anal Chem* 28: 350-356.
- Durzan DJ, V Chalupa 1968 Free sugars, amino acids, and soluble proteins in the embryo and female gametophyte of jack pine as related to climate at the seed source. *Can J Bot* 46: 417-428.

- Durzan DJ, AJ Mia, PK Ramaiah 1971 The metabolism and subcellular organization of the jack pine embryo (*Pinus banksiana*) during germination. *Can J Bot* 49: 927-938.
- Fahn A 1990 *Plant Anatomy* 4th edition. Pergamon Press Canada Ltd, Toronto. 588 pp.
- Feirer RP 1995 The biochemistry of conifer embryo development: amino acids, polyamines and storage proteins. Pages 317-336 in S Jain, P Gupta, R Newton, eds. *Somatic embryogenesis in woody plants*. Vol 1. Kluwer Academic, Dordrecht.
- Feirer RP, JH Conkey, SA Verhagen 1989 Triglycerides in embryogenic conifer calli: a comparison with zygotic embryos. *Plant Cell Rep* 8: 207-209.
- Fernandez DE, LA Staehelin 1987 Does gibberellic acid induce the transfer of lipase from protein bodies to lipid bodies in barley aleurone cells? *Plant Physiol* 85: 487-496.
- Firenzuoli AM, P Vanni, E Mastronuzzi, A Zanobini, V Baccari 1968 Participation of the glyoxylate cycle in the metabolism of germinating seed of *Pinus pinea*. *Life Sci* 7: 1251-1258.
- Flinn BS, DR Roberts, DT Webb, BCS Sutton 1991 Storage protein changes during zygotic embryogenesis in interior spruce. *Tree Physiol* 8: 71-81.
- Flinn BS, DR Roberts, CH Newton, DR Cyr, FB Webster, IEP Taylor 1993 Storage protein gene expression in zygotic and somatic embryos of interior spruce. *Physiol Plant* 89: 719-730.
- Florin R 1931 Untersuchungen zur Stammesgeschichte der Coniferales und Cordaitales. *Svenska Vetensk Akad Handl Ser 5* 10: 1-588.
- Florin R 1933 Studien über die Cycadales des Mesozoikums nebst Erörterungen über die Spaltöffnungsapparate der Bennettiales. *K svenska Vetensk Akad Handl, ser 3* 12: 1-134.
- Florin R 1951 Evolution in Cordaites and Conifers. *Acta Horti Bergiana* 15: 285-282.
- Frey-Wyssling A, E Grieshaber, K Mühlethaler 1963 Origin of spherosomes in plant cells. *J Ultrastructure Research* 8: 506-516.
- Foster AS, EM Gifford 1959 *Comparative Morphology of Vascular Plants*. WH Freeman and Company, San Fransisco. 555 pp.

- Fowells HA 1965 Silvics of forest trees of the United States. United States Forest Service, Division of Timber Management Research, U.S. Department of Agriculture, Washington, D.C. U.S.D.A. Agricultural Handbook No. 271: 360-372.
- Fuchs CH 1963 Fuchsin staining with NaOH clearing for lignified elements of whole plants or plants organs. *Stain Technol* 38: 141-144.
- García-Gutiérrez A, FR Cantón, F Gallardo, F Sánchez-Jiménez, FM Cánovas 1995 Expression of ferredoxin-dependent glutamate synthase in dark-grown pine seedlings. *Plant Mol Biol* 27: 115-128.
- Gifford EM 1950 Softening refractory plant material embedded in paraffin. *Stain Technol* 25:161-162.
- Gifford DJ 1988 An electrophoretic analysis of the seed proteins from *Pinus monticola* and eight other species of pine. *Can J Bot* 66: 1808-1812.
- Gifford DJ, JD Bewley 1983 An analysis of the subunit structure of the crystalloid protein complex from castor bean endosperm. *Plant Physiol* 72: 376-381.
- Gifford DJ, JD Bewley 1984 Interactions between subunit polypeptides of the crystalloid protein complex of castor bean endosperm. *Plant Sci Lett* 36: 37-42.
- Gifford DJ, MC Tolley 1989 The seed proteins of white spruce and their mobilization following germination. *Physiol Plant* 77: 254-261.
- Gifford DJ, JS Greenwood, JD Bewley 1982 Deposition of matrix and crystalloid storage proteins during protein body development in the endosperm of *Ricinus communis* L. cv. Hale seeds. *Plant Physiol* 69:1471-1478.
- Gifford DJ, E Thakore, JD Bewley 1984 Control by the embryo axis of the breakdown of storage proteins in the endosperm of germinated castor bean seed: a role for gibberellic acid. *J Exp Bot* 35: 669-677.
- Gifford DJ, KA Wenzel, DL Lammer 1989 Lodgepole pine seed germination. I. Changes in peptidase activity in the megagametophyte and embryonic axis. *Can J Bot* 67: 2539-2543.
- Goodwin TW, EI Mercer 1983 Introduction to Plant Biochemistry. 2nd edition. Pergamon Press, Toronto.
- Gori P 1979 An ultrastructural investigation of protein and lipid reserves in the endosperm of *Pinus pinea* L. *Ann Bot* 43: 101-105.

- Graham IA, KJ Denby, CJ Leaver 1994 Carbon catabolite repression regulates glyoxylate cycle gene expression in cucumber. *Plant Cell* 6: 761-772.
- Green MJ, JK McLeod, S Misra 1991 Characterization of Douglas fir protein body composition by SDS-PAGE and electron microscopy. *Plant Physiol Biochem* 29: 49-55.
- Groome MC, SR Axler, DJ Gifford 1991 Hydrolysis of lipid and protein reserves in loblolly pine seeds in relation to protein electrophoretic patterns following imbibition. *Physiol Plant* 83: 99-106.
- Gruber PJ, RN Trelease, WM Becker, EH Newcomb 1970 A correlative ultrastructural and enzymatic study of cotyledonary microbodies following germination of fat-storing seeds. *Planta* 93: 269-288.
- Guitton Y 1964 Métabolisme de l'arginine dans les premiers stades du développement de *Pinus pinea* L. *Physiol Veg* 2: 95-156.
- Gunning ES, MW Steer 1975 Ultrastructure and the biology of plant cells. Edward Arnold (Publishers) Ltd, London. 312 pp.
- Gurr MI 1980 Biosynthesis of triacylglycerols. Pages 205-248 in PK Stumpf, ed. *The Biochemistry of Plants*. Vol 4. Academic Press, Toronto.
- Gurr MI, JL Harwood 1991 *Lipid biochemistry: an introduction*. 4th edition. Chapman and Hall, New York. 406 pp.
- Häger K-P, N Dank 1996 Seed storage proteins of Cupressaceae are homologous to legumins from angiosperms: molecular characterization of cDNAs from incense cedar (*Calocedrus decurrens* [Torr.] Florin). *Plant Science* 116: 85-96.
- Häger K-P, H Braun, A Czihal, B Müller, H Bäumlein 1995 Evolution of seed storage protein genes: legumin genes of *Ginkgo biloba*. *J Mol Evol* 41: 457-466.
- Häger K-P, U Jensen, J Gilroy, M Richardson 1992 The N-terminal amino acid sequence of the β -subunit of the legumin-like protein from seeds of *Ginkgo biloba*. *Phytochem* 31: 523-525.
- Hakman I 1993a Embryology in norway spruce (*Picea abies*). An analysis of the composition of seed storage proteins and deposition of storage reserves during seed development and somatic embryogenesis. *Physiol Plant* 87: 148-159.
- Hakman I 1993b Embryology in norway spruce (*Picea abies*). Immunochemical studies on transport of a seed storage protein. *Physiol Plant* 88: 427-433.

- Hakman I, P Stabel, P Engström, T Eriksson 1990 Storage protein accumulation during zygotic and somatic embryo development in *Picea abies* (norway spruce). *Physiol Plant* 80: 441-445.
- Hammer MF, JB Murphy 1994 Lipase activity and *in vivo* triacylglycerol utilization during *Pinus edulis* seed germination. *Plant Physiol Biochem* 32: 861-867.
- Harris N, D Boulter 1976 Protein body formation in cotyledons of developing cowpea (*Vigna unguiculata*) seeds. *Ann Bot* 40: 739-744.
- Harwood JL, A Sodja, PK Stumpf, AK Spurr 1971 On the origin of oil droplets in maturing castor bean seeds, *Ricinus communis*. *Lipids* 6: 851-854.
- Hattori S, T Shiroya 1951 The sugars in the seeds and seedlings of *Pinus thunbergii*. *Arch Biochem Biophys* 34: 121-134.
- Higgins CF, JW Payne 1977 Peptide transport by germinating barley embryos. *Planta* 34: 205-206.
- Higgins TJV 1984 Synthesis and regulation of major proteins in seeds. *Ann Rev Plant Physiol* 35: 191-221.
- Hoff RJ 1987 Dormancy in *Pinus monticola* seed related to stratification time, seed coat and genetics. *Can J For Res* 17:294-298.
- Holtman WL, JC Heistek, KA Mattern, R Bakhuizen, AC Douma 1994 β -oxidation of fatty acids is linked to the glyoxylate cycle in the aleurone but not in the embryo of germinating barley. *Plant Science* 99: 43-53.
- Huang AHC 1992 Oil bodies and oleosins in seeds. *Annu Rev Plant Physiol Plant Mol Biol* 43: 177-200.
- Huang AHC, H Beevers 1971 Isolation of microbodies from plant tissues. *Plant Physiol*. 48: 637-641.
- Huang AHC, and H Beevers 1973 Localization of enzymes within microbodies. *J Cell Biol* 58: 379-389.
- Huang AHC, H Beevers 1974 Developmental changes in endosperm of germinating castor bean independent of embryonic axis. *Plant Physiol* 54: 277-279.
- Huang AHC, RN Trelease, TS Moore 1983 *Plant Peroxisomes*. Academic Press, New York. 252 pp.

- Imbs AB, LQ Pham 1996 Fatty acids and triacylglycerols in seeds of Pinaceae species. *Phytochem* 42: 1051-1053.
- Janick J, CC Velho, A Whipkey 1991 Developmental changes in seeds of loblolly pine. *J Amer Soc Hort Sci* 116: 297-301.
- Jansson S, I Virgin, P Gustafsson, B Andersson, G Öquist 1992 Light-induced changes of photosystem II activity in dark-grown Scots pine seedlings. *Physiol Plant* 84: 6-12.
- Jensen U, H Berthold 1989 Legumin-like proteins in gymnosperms. *Phytochem* 28: 1389-1394.
- Jensen U, C Lixue 1991 *Abies* seed protein profile divergent from other Pinaceae. *Taxon* 40: 435-440.
- Jensen WA 1962 *Botanical histochemistry: principles and practice*. W.H. Freeman and Company, San Francisco. 408 pp.
- Johansen DA 1940 *Plant Microtechnique*. McGraw-Hill, Inc., New York. 523 pp.
- Joy (IV) RW, EC Yeung, L Kong, TA Thorpe 1991 Development of white spruce somatic embryos: I. Storage product deposition. *In Vitro Cell Dev Biol* 27P: 32-41.
- Kao C 1973 Biochemical changes in seeds of Taiwan red pine and Chinese fir during germination. *Forest Sci* 19: 297-302.
- Kao C, KS Rowan 1970 Biochemical changes in seed of *Pinus radiata* D. Don during stratification. *J Exp Bot* 21: 869-873.
- Kaufman K 1927 Anatomie und Physiologie der Spaltöffnungsapparate mit verholzten Schliesszellmembranen. *Planta* 3: 27-59.
- Kern R, Chrispeels MJ 1978 Influence of the axis on the enzymes of protein and amide metabolism in the cotyledons of mung bean seedlings. *Plant Physiol* 62: 815-819.
- Kim D-J, SM Smith 1994 Expression of a single gene encoding microbody NAD-malate dehydrogenase during glyoxysome and peroxisome development in cucumber. *Plant Mol Biol* 26: 1833-1841.
- Kim WT, VR Franceschi, HB Krishnan, TW Okita 1988 Formation of wheat protein bodies: involvement of the Golgi apparatus in gliadin transport. *Planta* 176: 173-182.

- King JE 1998 The role of arginine and arginase in *Pinus taeda* L. early seedling growth. PhD diss. University of Alberta, Edmonton, AB.
- King JE, DJ Gifford 1997 Amino acid utilization in seeds of loblolly pine during germination and early seedling growth. *Plant Physiol* 113: 1125-1135.
- Koie B, G Nielsen 1977 Techniques for the separation of barley and maize proteins. Pages 25-35 in BJ Mifflin, PR Shewry, eds. Commission of the European Communities, Luxembourg.
- Kovac M, I Kregar 1989 Protein metabolism in silver fir seeds during germination. *Plant Physiol Biochem* 27: 35-41.
- Kovac M, M Vardjan 1981 Metabolism of lipids in fir seeds (*Abies alba* Mill.). *Acta Bot Croat* 40: 95-109.
- Kovac M, M Wrischer 1984 The activity of some enzymes of lipid metabolism in silver fir seeds (*Abies alba* Mill.) during germination. *Acta Bot Croat* 43: 31-42.
- Krasowski MJ and JN Owens 1993 Ultrastructural and histochemical post-fertilization megagametophyte and zygotic embryo development of white spruce (*Picea glauca*) emphasizing the deposition of seed storage products. *Can J Bot* 71: 98-112.
- Kriedemann P, H Beevers 1967 Sugar uptake and translocation in the castor bean seedling I. Characteristics of transfer in intact and excised seedlings. *Plant Physiol* 42: 161-173.
- Krishnan HB, VR Franceschi, TW Okita 1986 Immunochemical studies on the role of the Golgi complex in protein body formation in rice seeds. *Planta* 169: 471-481.
- Kyle DJ, ED Styles 1977 Development of aleurone and sub-aleurone layers in maize. *Planta* 137: 185-193.
- Laemmli UK 1970 Cleavage of structural proteins during the assembly of the head of bacteriophage T4. *Nature* 227:680-685.
- Lammer D, DJ Gifford 1989 Lodgepole pine seed germination. II. The seed proteins and their mobilization in the megagametophyte and embryonic axis. *Can J Bot* 67: 2544-2551.
- Larkins BA, WJ Hurkman 1978 Synthesis and deposition of protein bodies of maize endosperm. *Plant Physiol* 62: 256-263.

- Lea PJ, KW Joy 1983 Amino acid interconversion in germinating seeds. Pages 77-109 in *Recent Advances in Phytochem.* Plenum Press, New York.
- Lea PJ, BJ Mifflin 1980 Nitrogen transport within the plant. Pages 569-607 in BJ Mifflin, ed. *The Biochemistry of Plants. Vol 5.* Academic Press, New York.
- Leal I, S Misra 1993a Developmental gene expression in conifer embryogenesis and germination. III. Analysis of crystalloid protein mRNAs and desiccation protein mRNAs in the developing embryo and megagametophyte of white spruce (*Picea glauca* (Moench) Voss). *Plant Science* 88: 25-37.
- Leal I, S Misra 1993b Molecular cloning and characterization of a legumin-like storage protein cDNA of Douglas fir seeds. *Plant Mol Biol* 21: 709-715.
- Leal I, S Misra, SM Attree, LC Fowke 1995 Effect of abscisic acid, osmoticum and desiccation on 11S storage protein gene expression in somatic embryos of white spruce. *Plant Science* 106: 121-128.
- Lee K, FY Bih, GH Learn, JTL Ting, C Sellers, AHC Huang 1994 Oleosins in the gametophytes of *Pinus* and *Brassica* and their phylogenetic relationship with those in the sporophytes of various species. *Planta* 193: 461-469.
- Leprince O, AC van Aelst, HW Pritchard, DJ Murphy 1998 Oleosins prevent oil-body coalescence during seed imbibition as suggested by a low-temperature scanning electron microscope study of desiccation-tolerant and -sensitive oil seeds. *Planta* 204: 109-119.
- Lewandowska M, G Öquist 1980 Development of photosynthetic electron transport in *Pinus silvestris*. *Physiol Plant* 48: 134-138.
- Lopez-Perez MJ, A Gimenez-Solves, FD Calonge, A Santos-Ruiz 1974 Evidence of glyoxysomes in germinating pine seeds. *Plant Sci Lett* 2: 377-386.
- Lott JNA 1980 Protein bodies. Pages 589-623 in NE Tolbert, ed. *The Biochemistry of Plants Vol 1.* Academic Press, Toronto.
- Lott JNA, MS Buttrose 1978 Globoids in protein bodies of legume seed cotyledons. *Aust J Plant Physiol* 5: 89-111.
- Lowry OH, NJ Rosebrough, AL Farr, RJ Randall 1951 Protein measurement with the Folin phenol reagent. *J Biol Chem* 193:265-275.
- Mariani P, ME De Carli, N Rascio, B Baldan, G Casadoro, G Gennari, M Bodner, W Larcher 1990 Synthesis of chlorophyll and photosynthetic competence in

- etiolated and greening seedlings of *Larix decidua* as compared with *Picea abies*. *J Plant Physiol* 137: 5-14.
- Masters C, D Crane 1995 The peroxisome: a vital organelle. Cambridge University Press, New York. 286 pp.
- Mazelis M 1980 Amino acid catabolism. Pages 541-567 in BJ Mifflin, ed. The Biochemistry of Plants. Vol 5. Academic Press, New York.
- McLaughlin JC, SM Smith 1995 Glyoxylate cycle enzyme synthesis during the irreversible phase of senescence of cucumber cotyledons. *J Plant Physiol* 146: 133-138.
- Meier H, JSG Reid 1982 Reserve polysaccharides other than starch in higher plants. Pages 418-471 in FA Loewus, W Tanner, eds. Plant Carbohydrates I. Springer-Verlag, New York.
- Migabo T 1995 Characterization of enzymes involved in storage protein hydrolysis in castor bean endosperm. MSc thesis. University of Alberta, Edmonton, AB.
- Misra S 1994 Conifer zygotic embryogenesis, somatic embryogenesis, and seed germination: biochemical and molecular advances. *Seed Science Research* 4: 357-384.
- Misra S, MJ Green 1990 Developmental gene expression in conifer embryogenesis and germination. I. Seed proteins and protein body composition of mature embryo and the megagametophyte of white spruce (*Picea glauca* [Moench] Voss.). *Plant Science* 68: 163-173.
- Misra S, MJ Green 1991 Developmental gene expression in conifer embryogenesis and germination. II. Crystalloid protein synthesis in the developing embryo and megagametophyte of white spruce (*Picea glauca* [Moench] Voss.). *Plant Science* 78: 61-71.
- Misra S, MJ Green 1994 Legumin-like storage polypeptides of conifer seeds and their antigenic cross-reactivity with 11S globulins from angiosperms. *J of Exp Bot* 45: 269-274.
- Mollenhauer HH, DJ Morr e 1980 The Golgi apparatus. Pages 437-488 in NE Tolbert, ed. The Biochemistry of Plants Vol 5. Academic Press, Toronto.
- Mullen RT 1995 Regulation of glyoxysomal enzyme gene expression in loblolly pine (*Pinus taeda* L.) seeds following imbibition. PhD diss. University of Alberta, Edmonton, AB.

- Mullen RT, DJ Gifford 1995a Isocitrate lyase from germinated loblolly pine megagametophytes: enzyme purification and immunocharacterization. *Plant Physiol Biochem* 33(1): 87-95.
- Mullen RT, DJ Gifford 1995b Purification and characterization of the glyoxysomal enzyme malate synthase following seed germination in *Pinus taeda*. *Plant Physiol Biochem* 33: 639-648.
- Mullen RT, DJ Gifford 1997 Regulation of two loblolly pine (*Pinus taeda* L.) isocitrate lyase genes in megagametophytes of mature and stratified seeds and during postgerminative growth. *Plant Mol Biol* 33: 593-604.
- Mullen RT, JE King, DJ Gifford 1996 Changes in mRNA populations during loblolly pine (*Pinus taeda*) seed stratification, germination and post-germinative growth. *Physiol Plant* 97: 545-553.
- Murphy DJ 1993 Structure, function and biogenesis of storage lipid bodies and oleosins in plants. *Prog Lipid Res* 32: 247-280.
- Murphy DJ, I Cummins 1989 Biosynthesis of seed storage products during embryogenesis in rapeseed, *Brassica napus*. *J Plant Physiol* 135: 63-69.
- Murphy JB, MF Hammer 1988 Respiration and soluble sugar metabolism in sugar pine embryos. *Physiol Plant* 74: 95-100.
- Murphy JB, MF Hammer 1994 Starch synthesis and localization in post-germination *Pinus edulis* seedlings. *Can J For Res* 24: 1457-1463.
- Murphy JB, MR Rutter, MF Hammer 1992 Activity of sucrose synthase and soluble acid invertase following germination of pinyon (*Pinus edulis*) seeds. *Can For Res* 22: 442-446.
- Murray DR, O Wara-Aswapati, HMM Ireland, JW Bradbeer. 1973. The development of activities of some enzymes concerned with glycollate metabolism in greening bean leaves. *J Exp Bot* 24: 175-184.
- Nelson N 1944 A photometric adaptation of the Somogyi method for the determination of glucose. *J Biol Chem* 153: 375-380.
- Newcomb EH 1982 Ultrastructure and cytochemistry of plant peroxisomes and glyoxysomes. Pages 228-241 in H Kindl, PB Lazarow, eds. *Peroxisomes and glyoxysomes*. Vol 386. *Annals of the New York Academy of Sciences*, New York.

- Newton CH, BS Flinn, BCS Sutton 1992 Vicilin-like seed storage proteins in the gymnosperm interior spruce (*Picea glauca/engelmannii*). *Plant Mol Biol* 20: 315-322.
- Nishimura M, Y Takeuchi, L De Bellis, I Hara-Nishimura 1993 Leaf peroxisomes are directly transformed to glyoxysomes during senescence of pumpkin cotyledons. *Protoplasma* 175: 131-137.
- Noland TL, JB Murphy 1984 Changes in isocitrate lyase activity and ATP content during stratification and germination of sugar pine seeds. *Seed Sci & Technol* 12: 777-787.
- O'Brien TP, ME McCully 1981 The study of plant structure: principles and selected methods. Termarcaphi Pty Ltd., Melbourne, Australia.
- Olsen LJ 1998 The surprising complexity of peroxisome biogenesis. *Plant Mol Biol* 38: 163-189.
- Osborne TB 1918 The vegetable proteins. Monographs on Biochemistry. RHA Plimmer, FG Hopkins, eds. Longmans, Green and Co., New York. 125 pp.
- Owens JN, M Molder 1977 Seed-cone differentiation and sexual reproduction in western white pine (*Pinus monticola*). *Can J Bot* 55: 2574-2590.
- Owens JN, SJ Morris, S Misra 1993 The ultrastructural, histochemical, and biochemical development of the post-fertilization megagametophyte and the zygotic embryo of *Pseudotsuga menziesii*. *Can J For Res* 23: 816 - 827.
- Owens JN, SJ Simpson, M Molder 1982 Sexual reproduction of *Pinus contorta*. II. Postdormancy ovule, embryo, and seed development. *Can J Bot* 60: 2071-2083.
- Peng CC, JTC Tzen 1998 Analysis of the three essential constituents of oil bodies in developing sesame seeds. *Plant Cell Physiol* 39: 35-42.
- Pinzauti G, E Giachetti, G Camici, G Manao, G Cappugi, P Vanni 1986 An isocitrate lyase of higher plants: analysis and comparison of some molecular properties. *Arch Biochem Biophys* 244: 85-93.
- Pitel JA, WM Cheliak 1988 Metabolism of enzymes with imbibition and germination of seeds of jack pine (*Pinus banksiana*). *Can J Bot* 66: 542-547.
- Pitel JA, WM Cheliak, BSP Wang 1984 Changes in isoenzyme patterns during imbibition and germination of lodgepole pine (*Pinus contorta* var. *latifolia*). *Can J For Res* 14: 743-746.

- Qu R, SM Wang, YH Lin, VB Vance, AHC Huang 1986 Characteristics and biosynthesis of membrane proteins of lipid bodies in the scutella of maize (*Zea mays* L.). *Biochem J* 234: 57-65.
- Ramaiah PK, DJ Durzan, AJ Mia 1971 Amino acids, soluble proteins, and isoenzyme patterns of peroxidase during the germination of jack pine. *Can J Bot* 49: 2151-2161.
- Rest JA, JG Vaughan 1972 The development of protein and oil bodies in the seed of *Sinapis alba* L. *Planta* 105: 245-262.
- Reynolds ES 1963 The use of lead citrate at high pH as an electron-opaque stain in electron microscopy. *JCB* 17: 208-212.
- Riding RT, J Aitken 1982 Needle structure and development of the stomatal complex in cotyledons, primary needles, and secondary needles of *Pinus radiata* D. Don. *Bot Gaz* 143: 52-62.
- Robert LS, C Nozzolillo, I Altosaar 1985 Homology between rice glutelin and oat 12 S globulin. *Biochimica et Biophysica Acta* 829: 19-26.
- Salisbury FB, CW Ross 1992 *Plant Physiology*. 4th ed. Wadsworth Publishing Co., Belmont, CA. 682 pp.
- Salmia MA 1981 Proteinase activities in resting and germinating seeds of Scots pine, *Pinus sylvestris*. *Physiol Plant* 53: 39-47.
- Salmia MA, JJ Mikola 1975 Activities of two peptidases in resting and germinating seeds of Scots pine, *Pinus sylvestris*. *Physiol Plant* 33: 261-265.
- Salmia MA, JJ Mikola 1976a Localization and activity of naphthylamidases in germinating seeds of Scots pine, *Pinus sylvestris*. *Physiol Plant* 38: 73-77.
- Salmia MA, JJ Mikola 1976b Localization and activity of a carboxypeptidase in germinating seeds of Scots pine, *Pinus sylvestris*. *Physiol Plant* 36: 388-392.
- Salmia MA, SA Nyman, JJ Mikola 1978 Characterization of the proteinases present in germinating seeds of Scots pine, *Pinus sylvestris*. *Physiol Plant* 42: 252-256.
- Saponen T 1979 Development of peptide transport activity in barley scutellum during germination. *Plant Physiol* 64: 570-574.
- Sasaki S, TT Kozłowski 1969 Utilization of seed reserves and currently produced photosynthates by embryonic tissues of pine seedlings. *Ann Bot* 33: 473-82.

- Schneider WL 1993 Biochemical changes during the breaking of dormancy in loblolly pine seeds, *Pinus taeda* L. MSc thesis. University of Alberta, Edmonton, AB.
- Schneider WL, GJ Gifford 1994 Loblolly pine seed dormancy. I. The relationship between protein synthesis and the loss of dormancy. *Physiol Plant* 90: 246-252.
- Selstam E, A Widell 1986 Characterization of prolamellar bodies, from dark-grown seedlings of Scots pine, containing light- and NADPH-dependent protochlorophyllide oxidoreductase. *Physiol Plant* 67: 345-352.
- Shewry PR, JA Napier, AS Tatham 1995 Seed storage proteins: structures and biosynthesis. *Plant Cell* 7: 945-956.
- Simola LK 1974a The ultrastructure of dry and germinating seeds of *Pinus sylvestris* L. *Acta Bot Fenn* 103: 1-31.
- Simola LK 1974b Subcellular organization of cotyledons of *Picea abies* during germination. *Portug Acta Biol* 14: 413-428.
- Simola LK 1976 Changes in the subcellular organization of endosperm and radicle cells of *Picea abies* during germination. *Z Pflanzenphysiol Bd* 78 S: 41-51.
- Singh, H and BM Johri 1972 Development of gymnosperm seeds. Pages 21-75 in TT Kozlowski, ed. *Seed Biology*. Vol 1. Academic Press, New York.
- Smith CG 1974 The ultrastructural development of spherosomes and oil bodies in the developing embryo of *Crambe abyssinica*. *Planta* 119: 125-142.
- Spurr AR 1969 A low-viscosity epoxy resin embedding medium for electron microscopy. *J Ultrastruct Res* 26:31-43.
- Stenram U, WK Heneen, JH Skerritt 1991 Immunochemical localization of wheat storage proteins in endosperm cells 30 days after anthesis. *J Exp Bot* 42: 1347-1355.
- Stewart CR, H Beevers 1967 Gluconeogenesis from amino acids in germinating castor bean endosperm and its role in transport to the embryo. *Plant Physiol* 42: 1587-1595.
- Stumpf PK 1980 Biosynthesis of saturated and unsaturated fatty acids. Pages 177-204 in Stumpf PK, ed. *The Biochemistry of Plants*. Vol 4. Academic Press, Toronto.

- Tabor CA, NM Barnett 1987 An experimental system for studying interrelationships between the embryo and megagametophyte of *Pinus strobus* during seed germination. *Can J Bot* 65: 1212-1217.
- Taikawa F, K Oono, D Wing, A Kato 1991 Sequence of three members and expression of a new major subfamily of glutelin genes from rice. *Plant Mol Biol* 17: 875-885.
- Taylor JRN, L Schussler, NvdW Liebonberg 1985 Protein body formation in the starch endosperm of developing *Sorghum bicolor* (L.) Moench seeds. *S Afr J Bot* 51: 35-40.
- Thomas J, RN Trelease 1981 Cytochemical localization of glycolate oxidase in microbodies (glyoxysomes and peroxisomes) of higher plant tissues with the $CeCl_3$ technique. *Protoplasma* 108: 39.
- Thompson JF 1980 Arginine and proline synthesis. Pages 375-402 in BJ Miflin, ed. *The Biochemistry of Plants*. Vol 5. Academic Press, Toronto.
- Tillman-Sutela E and A Kauppi 1995 The morphological background to imbibition in seeds of *Pinus sylvestris* L. of different provenances. *Trees* 9:123-133.
- Trenin VV 1985 Development of the endosperm in some conifers. *Biologicheskii-Nauki* 3: 75-79.
- Tzen JTC, YZ Cao, P Laurent, C Ratnayake, AHC Huang 1993 Lipids, proteins, and structure of seed oil bodies from diverse species. *Plant Physiol* 101: 267-276.
- van Rooijen GJH, MM Moloney 1995 Structural requirements of oleosin domains for subcellular targeting to the oil body. *Plant Physiol* 109: 1353-1361.
- Vigil EL 1970 Cytochemical and developmental changes in microbodies (glyoxysomes) and related organelles of castor bean endosperm. *J Cell Biol* 46: 435-454.
- Vincentini F, P Matile 1993 Gerontosomes, a multifunctional type of peroxisome in senescent leaves. *J Plant Physiol* 142: 50-56.
- Wang TW, AS Lewin, GM Small 1992 A negative regulating element controlling transcription of the gene encoding acyl-CoA oxidase in *Saccharomyces cerevisiae*. *Nucleic Acids Res* 20: 3495-3500.
- Wanner G, RR Theimer 1978 Membranous appendices of spherosomes (oleosomes). *Planta* 140: 163-169.

- Wanner G, H Formanek, RR Theimer 1981 The ontogeny of lipid bodies (spherosomes) in plant cells. *Planta* 151: 109-123.
- Weber H, L Borisjuk, U Heim, P Buchner, U Wobus 1995 Seed coat-associated invertases of fava bean control both unloading and storage functions: cloning of cDNAs and cell type-specific expression. *Plant Cell* 7: 1835-1846.
- Weber H, L Borisjuk, U Heim, N Sauer, U Wobus 1997 A role for sugar transporters during seed development: molecular characterization of a hexose and a sucrose carrier in fava bean seeds. *Plant Cell* 9: 895-908.
- Wieckowski S, TW Goodwin 1966 Assimilatory pigments in cotyledons of four species of pine seedlings grown in darkness and in light. *Phytochem* 5: 1345-1348.
- Wolff RL 1997 New tools to explore lipid metabolism. *INFORM* 8: 116-119.
- Wolff RL, B Comps, LG Deluc, AM Marpeau 1998 Fatty acids of the seeds from pine species of the *Ponderosa-Banksiana* and *Halepensis* sections. The peculiar taxonomic position of *Pinus pinaster*. *Journal of the American Oil Chemists' Society* 75: 45-50.
- Wolff RL, B Comps, AM Marpeau, LG Deluc 1997a Taxonomy of *Pinus* species based on the seed oil fatty acid compositions. *Trees* 12: 113-118.
- Wolff RL, E Dareville, JC Martin 1997b Positional distribution of Δ^5 -olefinic acids in triacylglycerols from conifer seed oils: general and specific enrichment in the sn-3 position. *JAOC* 74: 515-523.
- Wolff RL, LG Deluc, AM Marpeau 1996 Conifer seeds: oil content and fatty acid composition. *JAOC* 73: 765-771.
- Wolff RL, LG Deluc, AM Marpeau, B Comps 1997c Chemotaxonomic differentiation of conifer families and genera based on the seed oil fatty acid compositions: multivariate analyses. *Trees* 12: 57-65.
- Zamski E 1996 Anatomical and physiological characteristics of sink cells. Pages 283-310 in E Zamski, AA Schaffer, eds. *Photoassimilate distribution in plants and crops: source-sink relationships*. Marcel Dekker, New York.